

**Basin Evaluation of Turonian Deposits in the Lower Congo Basin  
using outcrops, cores, well-logs and seismic**

By

**NTOUADI KIBINI Neil Jessy Joyce**

**3371226**

**Master thesis 2017**



Supervisor: **Mimonitu OPUWARI**

Co- supervisor: **Jacques DURAND**

**University of Western Cape, Department of Applied Geology**

**Declaration**

I declare that **‘Basin evaluation of Turonian deposits in the Lower Congo Basin using outcrops, cores, well-logs and seismic data’** is my own work, that it has never been submitted for any degree or examination in any other university and that all the sources i have or quoted have been indicated by complete references.

Full Name: NTOUADI KIBINI Neil Jessy Joyce

Signature:.....

Date:.....



UNIVERSITY *of the*  
WESTERN CAPE

## **Dedication**

To God almighty,

The depth of the riches of both wisdom and knowledge, how unsearchable are his judgements, and his ways past finding out. Romans 11:33



UNIVERSITY *of the*  
WESTERN CAPE

## Acknowledgements

I would like to thank Total E&P Congo for funding my studies.

As author, I would like to express my profound sense of reverence to my supervisor and mentor, Prof. Jacques–Pierre DURAND (Total E&P), for his constant guidance, support, motivation and untiring help during the course of my masters and for providing me with insights into sedimentology, stratigraphy and methodology that will be useful throughout my career.

I am deeply indebted to my supervisor Dr. Mimonitu OPUWARI (University of the Western Cape) for the unfailing trust and opportunity of his sustained supervision, for many useful discussions.

I am also indebted to Vincent DELHAYE-PRAT who with my Co-supervisor suggested the research topic.

I am very grateful to Dr. Cédric MABILLE (Total E&P engineer) for his guidance on the field, his input and support, his extremely useful discussions, and suggestions on the manuscript, to Prof. Ireneusz WALASZCZYK and to Dr. Herbert KLINGER for his great contributions in the identification of the ammonites. I am deeply grateful to Prof. CHATTERJEE for fruitful discussions and his contribution in the determination of the foraminifera and to Dr. Nicoletta BURATTI in the identification of microfossils.

I wish to thank Laurent SCHULBAUM (Total E&P Congo's geology head of department) and Dr. Antoine MASSALA (Total E&P Congo geosciences' tutor) for the opportunity they gave to use their data and their assistance during my stay in Congo.

I am also thankful to Albin MANONGHO PANDI for his assistance on the field, to Jacques NTSAKALA (Total E&P Congo engineer) for the insight to sismage, to Charly MINGUERI for useful insight to Petrel software (engineer) to all Total E&P Congo geosciences department engineers for their sense of being and their multiform assistance.

My gratitude goes to my father Mr. Arthur NTOUADI, my mother Me Claire Alphonsine NTOUADI, to my siblings Dr. Clive Hedley Prince NTOUADI OPOUCKOU and Lesly Stein Hettner NTOUADI; your continued support was a springboard for this research in time most needed. Special thanks Ruth Corinne Ganongo Po for her support and prayers, to Rod Distel Ganongo Po for his prayers, to Rigobert Axel ENGO MBA and Archange KEYE for their camaraderie; it was a good support during this research.

## Contents

Chapter1: Introduction .....	12
1.1. Study area .....	12
1.2. Geological setting summary.....	14
1.2.1. Tectonic setting:.....	14
1.2.2. Stratigraphy and sedimentary environment .....	16
1.2.3. Previous works on Turonian series:.....	19
Chapter2: Material and method .....	24
2.1. Data.....	24
2.1.1. Outcrops.....	24
2.1.2. Offshore Data.....	24
2.2. Methodology .....	26
Chapter 3: Results and Discussions .....	28
3.1. Biostratigraphy.....	28
3.1.1. Outcrops.....	28
3.1.2. Wells .....	37
3.2. Facies model .....	53
3.2.1. Outcrops.....	53
3.2.2. Wells .....	74
3.3. Basin framework correlation.....	112
3.4. Diagenetic environment, processes and relationship with sedimentological evolution.....	122
3.5. Petrophysic properties.....	126
Chapter 4: Conclusions and recommendations.....	130
Chapter 5: References .....	133
Appendix.....	142

## List of Figures

Figure 1: Congolese Coastal Basin oilfields (red blocks represent oilfield of interest wells, Grey blocks represent oilfields probable Turonian reservoirs, black line represent oilfileds boundaries, purple line represent onshore-offshore boundary) .....	13
Figure 2:Paleogeographic map of the Cretaceous break up of Africa and South America (modified from Brownfield and Charpentier, 2006) .....	15
Figure 3: Generalized stratigraphic column of the Congo Basin (from Brownfield & Legorjus, 2006) ....	18

Figure 4: Studied wells and outcrops locations( green lines represent seismic lines, green dots represent well with available cores, red dots represent wells without core) (the names of the seismic lines were not provided due to confidentiality).....	25
Figure 5: Distribution of palynomorphs at Pointe Mvassa .....	29
Figure 6: Stratigraphical distribution of palynomorphs, foraminifera and ammonites at Pointe Mvassa...	32
Figure 7: Distribution of palynomorphs at Djeno. ....	34
Figure 8: Stratigraphic distribution of palynomorphs, foraminifera and ammonite at Djeno.....	36
Figure 9: Palynological biozonation correlation in North and West Africa and Northern America (from Deaf <i>et al.</i> , 2014, modified after Schrank, 1992).....	37
Figure 10: Correlation cross section from Mvassa to TCDM3 (Wells Turonian interval and outcrops)....	40
Figure 11: Correlation cross section from Pointe Indienne to SUEM2 .....	42
Figure 12: Correlation cross section from Sea Port towell SUEM2–offshore Turonian .....	44
Figure 13: Correlation cross section from wellDSM1 to LKFM1 (Turonian correlation). ....	46
Figure 14: Correlation cross section from well DSM 1 to EMM103 Wells(Turonian correlation).....	48
Figure 15: Correlation cross section from TBEM106 to TCDM3 Wells.....	50
Figure 16a: Upper Cretaceous paleogeographic map and Turonian geographical extension (Massamba, 1985) .....	52
Figure 17: Outcrops locations .....	53
Figure 18: Bed of densely packed epifaunal bivalves.....	57
Figure 19: Bay facies (modified from Mangano & Buatois, 2011) ( <i>RHizocarallium</i> : Rz, <i>Teichichnus</i> : Te, <i>Paleophycus</i> : Pa).....	63
Figure 20: Bay facies (modified from Mangano & Buatois, 2011) .....	70
Figure 21: Mvassa sedimentological log .....	72
Figure 22: Djeno sedimentological log.....	73
Figure 23: Locations of reference wells.....	74
Figure 24: Debris flow facies.....	76
Figure 25: a. Sandstone with both anhedral;b. hedral dolomitic cement (note both cements in right pictures) .....	77
Figure 26: Sandstone with dolomitic sparry equant cement (anhedral dolomitic cement), note formation of dolomitic cement prior to formation of calcite. ....	77
Figure 27:Planar cross bedded facies.....	79
Figure 28: Internal architecture of tidally influenced point bar, McMurray formation (Musial <i>et al.</i> , 2011). ....	80
Figure 29: Soil facies (TBEM 2 from 614, 80 – 615m).....	81
Figure 30: TBEM-106 at 606.85m) .....	81
Figure 31: Note roots, vacuolar porosity (left picture, TBEM2 at 621.45m), and intercrystal porosity and root remnant in filled vacuole or clast (right picture TBEM2 at 614.94) .....	82
Figure 32: Hedral dolomite recrystallization from original calcite (TBEM2 at 621.77m) .....	82
Figure 33: Argillaceous dolomitic siltstone facies, note flame structure at the base. (A.TBEM-2 between 616.5 and 616m; B.TBEM-106 between 605 and 605m) .....	84
Figure 34: Argillaceous dolomitic facies (TBEM-106), note non-erosive contact.....	85
Figure 35: Micrite to microsparry cement; note replacement of former calcite (in red) by dolomite. ....	85

Figure 36: Dolomitic siltstone with anhydrite nodules .....	87
Figure 37: Dolomitization of former calcite (a), vacuole filled with Anhydrite, well TBEM-106 at 578.72m (An: anhydrite) (b) .....	87
Figure 38: Bay facies (from Mangano & Buatois, 2011).....	89
Figure 39: Argillaceous dolomitic siltstone, arrow shows <i>teichichnus</i> .....	90
Figure 40: Cylindrical horizontal laminated facies: a. massive or thinly laminated, b. with <i>Ophiomorpha</i> .....	92
Figure 41: Facies silty matrix under microscope .....	93
Figure 42: microcrystalline to dolomitic cement. ....	93
Figure 43: Bioclastic silty dolomudstone.....	95
Figure 44: Micro-sparry cement with translucent aureole around the dolomite rhombs .....	96
Figure 45: Silty dolo-mudstone facies; note calcite replacement by dolomite .....	96
Figure 46: Note formation of calcite prior to replacement by dolomite (TBEM-2 at 562.70m) .....	98
Figure 47: Note both moldic and interparticle porosity (TBEM-2 5 at 61.58m) .....	98
Figure 48: Wackestone silty calcareous dolomite.....	100
Figure 49: Intercrystal porosity.....	100
Figure 50: Silty bioclastic peloidal limestone (TBEM2 between 557 and 557.50m).....	102
Figure 51: A. silty bioclastic peloidal limestone, B. note hedral dolomite in molds. ....	103
Figure 52: Silty bioclastic peloidal limestone; note dolomite in moldic space.....	103
Figure 53: Silty bioclastic packstone (note hardground at 571.80m).....	105
Figure 54: Silty bioclastic dolo-packstone, moldic space filled with calcite .....	106
Figure 55: Silty bioclastic dolo-packstone.....	106
Figure 56: Bioclastic calcareous siltstone (TBEM2 from 549, 50 to 549,77m). ....	108
Figure 57: facies thin sections showing echinoids and dolomite rhombs .....	109
Figure 58: Turonian facies model .....	111
Figure 59: Well TBEM-2 sequential stratigraphy (based on vertical superposition of the environments) .....	114
Figure 60: Well TCDM3 sequential stratigraphy (Based on vertical superposition of the environments) .....	115
Figure 61: Basin correlation; cross section from TBEM106 to TCDM3 through TBEM2. ....	117
Figure 62: Basin correlation, cross section from DSM1 to EMM103 .....	118
Figure 63: Basin correlation; cross section from DSM to LKFM1 .....	119
Figure 64: Hydrologic settings of meteoric diagenetic environments as a function of sea level and depositional settings (isolated platform vs. land-tied shelf). (A) During sea-level high stand; (B) during sea-level low stand (Moore, 1989).....	123
Figure 65: Conceptual model of the major diagenetic environments and hydrologic conditions present in the meteoric realm (From Moore, 1989).....	124
Figure 66: Geologic setting for the dolomitization–dedolomitization of Jurassic ooid packstones from the Paris Basin. Final porosity consists of cement-reduced dolomite crystal-moldic porosity. Used with permission of Springer-Verlag, New York (From Purser, 1985).....	125
Figure 67: Petrophysical property – sedimentologic logs tied (well TBEM2).....	128
Figure 68: Petrophysical property – sedimentologic logs tied (well TCDM3) .....	129

## List of plates

Plate 1: Figure 1 and 2 -sample showing pod facies (note whole shells trapped between pod and surrounding rocks; figure 3- pod on outcrop; figure 4-microscopic view of the facies showing silt size grains in calcareous matrix .....	55
Plate 2: Figure 1: bioclastic sandy facies with scoured base (note scored base), figure 2: note upward grading of shells size from samples, figure 3-4: thin section of the facies. ....	59
Plate 3: Figure 1: note trough cross bedding within the facies, figure 2: sample, figures 3- 4: sparry cement and moldic porosity (note silt within the matrix).....	61
Plate 4: Te: <i>Teichichnus</i> , Ar: <i>Arenicolites</i> , Th: <i>Thalassinoides</i> , Pa: <i>Paleophycus</i> , Rh: <i>Rhynchocorallium</i> , Sc: <i>Scolicia</i> .....	64
Plate 5: 1, 3, 4 bioclastic calcareous very fine to silty sandstone, 2 note replacement of calcite by dolomite .....	65
Plate 6: Figures 1-3: nested facies on outcrop (note scours at the base of the nests), Figure 4: microscopic view displaying silt in argillaceous matrix and figure 5: note sparry cement.....	68
Plate 7: Figures 1-3: very fine bioclastic calcareous sandstone, Figures 4-5: formation of secondary dolomite in moldic space. ....	71

## Appendix

Appendix 1: Figures 1,2,4: <i>Texanites venustus</i> Collignon, figure 3: <i>Prototexanites</i> sp., figures 5-6: <i>Texanites soutoni</i> , figures 7-8: <i>Menuites</i> sp, .....	143
Appendix 2: Figures 9-11: <i>Lopha aucapitanei</i> (COQUAND), figures 12-13: <i>Lopha Lombardi</i> nov. Sp, figures 14-16: <i>Plicatula hirsuta</i> , .....	144
Appendix 3: 18-20 <i>Plicatula ferryi</i> Coquand, 21 <i>Fusus</i> sp., <i>Anchura</i> ( <i>Dicroloma</i> ) Sp., <i>Tibia</i> ( <i>Calyptophorus</i> ) <i>palhata</i> (forbes). ....	145
Appendix 4: Figures 24 and 27: <i>Trigonarca curvadonta</i> ; figure 25: <i>Anofia aro</i> Reyment, figure 26: <i>Agelasina pledonta</i> ; figures: 28-29: <i>Enchodus crenulatus</i> , figure 30: <i>Anacorax kaupi</i> , figures 31-34: fishbones. ....	146
Appendix 5: Mvassa section .....	147
Appendix 6: A selection of CXIVb palynomorph index species is shown in this table. The material comes from both the Pointe M'Vassa and Djeno outcrops. The scale bar is 30µ long, except where otherwise stated. Figs. 1,2,4) <i>Dinogymnium</i> spp.; Fig. 3) <i>Oligosphaeridium</i> sp.; Figs. 5-7) <i>Isabelidium</i> spp.; Fig. 8) <i>Cribroperidinium</i> sp. ; Fig. 9) <i>Odontochitina costata</i> ; Figs. 10-12) <i>Senegalinium</i> spp. ; Fig. 13) <i>Ephedripites jansonii</i> ; Figs. 14,18) <i>Hexaporotricolpites emelianovi</i> ; Figs. 15-17) <i>Constantinisporites</i> spp.; Fig. 19) <i>Myrtacidites</i> sp.; Fig. 20) <i>Cretacaeiporites</i> cf. <i>infrabaculatus</i> ; Fig. 21) <i>Tricolporites</i> sp. 164. ....	148
Appendix 7: <i>Puzosia</i> Sp, 2 <i>Trigonarca curvadonta</i> , 3 <i>Plicatula ferryi</i> COQUAND, 4 <i>Trigonarca curvadonta</i> .....	149
Appendix 8: Djeno section.....	150

Appendix 9: similarity between sequence within well TBEM2 and carbonate ramp by Nichols (2009). 151  
Appendix 10: Depth versus porosity graph (well TCDM3)..... 152  
Appendix 11: Porosity versus Depth graph (well TBEM 106)..... 153  
Appendix 12: porosity versus depth (well TBEM2)..... 154



UNIVERSITY *of the*  
WESTERN CAPE

## Abstract

This manuscript presents a review of the Turonian series of the Congolese Coastal Basin using outcrop, core, well-logs and seismic data in order to provide a comprehensive model for the series and increase the oil recovery. The objectives of this study were: a) to define the age assignment of the stratal units, b) to define geographical extension of the series, c) to characterize lithologically Turonian series and define a facies model for the series, d) to determine petrophysical properties of the Turonian series.

The study mainly included age assignment study of two main outcrops (Djeno and Pointe Mvassa) where 13 samples were collected and age assignment review of for six wells from palynological data from Total E&P Congo database. The two main outcrops (Pointe Mvassa and Djeno) have been measured bed by bed and sampled (58 samples) to study the stratigraphy, describe and interpret the facies and characterize the depositional environment along with three wells (eight metres of sediments each) also described in great detail. The study of the outcrops at Djeno and Mvassa showed ammonites (at Mvassa particularly) *Prototexanites*, *Texanites venustus*, *Texanites soutoni* and palynomorph assemblage containing *Cystsandacritarchs*, *Hexaporotricolpites emelianovi*, *Ephedripites spp.*, *Constantinisorites spp.*, *Myrtacidites spp.*, *Tricolporites spp.*, *Cleistosphaeridium spp.*, *Cribroperidinium spp.*, *Spiniferites spp.* and *Cyclonephelium spp.*; peridionoid cysts such as *Dinogymnium spp.*, *Senegalinium spp.*, *Isabelidium spp.* and rare *Alisogymnium spp.* smooth cysts, referred to the genus *Leiosphaeridia* a relative higher frequency of the pollen *Constantinisorites sp.* at Djeno.

The findings of this work include association of species with Coniacian to Campanian (Maastrichtian) distribution even if some Albian to Senonian palynomorph such as *Hexaporotricolpites emelianovi* were found along the outcrop. Coniacian to Santonian (Campanian) age was suggested for these outcrops what is younger than the Turonian age previously suggested by previous authors. Offshore of the basin Turonian intervals were determined on the basis of palynomorphs assemblage containing *Sp. 36 Multipropollenites Sp.*, *Sp 28 Perotroletes Sp.*, *Sp 168 Dissaccates*, *C3P6E*, *Ephedrales*, *P3 Sp 101*, *PP Sp 36*, *Hedbergella Sp.*, *Dinogymnium acuminatum*.

The correlation from offshore wells with defined Turonian intervals to outcrops such as Pointe Indienne and Seaport allowed assigning a Turonian age to these outcrops.

The geographical extension of the Turonian series was determined through correlation from wells with well defined Turonian interval to Turonian outcrops onshore; this allowed refining the paleogeographical map proposed for Turonian.

A detailed study of Turonian series of the basin has led to recognition of twelve lithofacies grouped into: fluvial (estuary), bay (proximal and distal bay), and shallow ramp (or Chenier), middle ramp, deep ramp and offshore facies associations. The same facies associations were also identified at the Coniacian (Santonian) to Campanian outcrops; hence showing diachronism in the series.

The vertical facies associations demonstrated an overall transgressive sequence. Four major transgressive-regressive cycles were distinguished in Turonian series of the Congolese Coastal Basin marked by dissolution and dolomitisation during regressive episodes.

Turonian series of the Congolese Coastal Basin present petrophysical properties highly dependent on the primary nature of the rock and the type of dissolution-dolomitization process to which the facies has been exposed.



UNIVERSITY *of the*  
WESTERN CAPE

## Chapter1: Introduction

The Cretaceous series of the lower Congo Basin present great economic potential as the reservoirs contain high oil accumulations offshore of the basin. Since the discovery Loango oilfield oil has been Tapped from Turonian reservoirs offshore of the Congo Basin; however, the previous work carried on Turonian series of the lower Congo Basin yielded different facies model which made the understanding of the series hydrocarbon potential, facies model, geographic extent difficult. This project aims at providing a comprehensive model for the series in order to increase the oil recovery by integrating in one study the outcrops, cores, well-logs and seismic data.

To achieve the above aims, the objectives for this project are:

- ❖ To define the age assignement of the stratal units
- ❖ To define extension of the series
- ❖ To characterize lithologically the Turonian series and defines a facies model
- ❖ To determinethe petrophysical properties from the facies distribution of the Turonian series.

### 1.1. Study area

The Turonian series of the Congo Basin belong to the post-salt formations of the lower Congo Basin. The Congolese coastal basin is an onshore-offshore passive margin basin, located on the West African continental margin between longitude 13° and 11° E and latitude 4° and 5° S (Mbani, 2008). The basin extends 150km in North-South direction and between Angola and Congo. It is surrounded eastward by Precambrian Mayombe massif and east-westward onshore and offshore presently known by drilling extends 110 km (Massala, 1993).

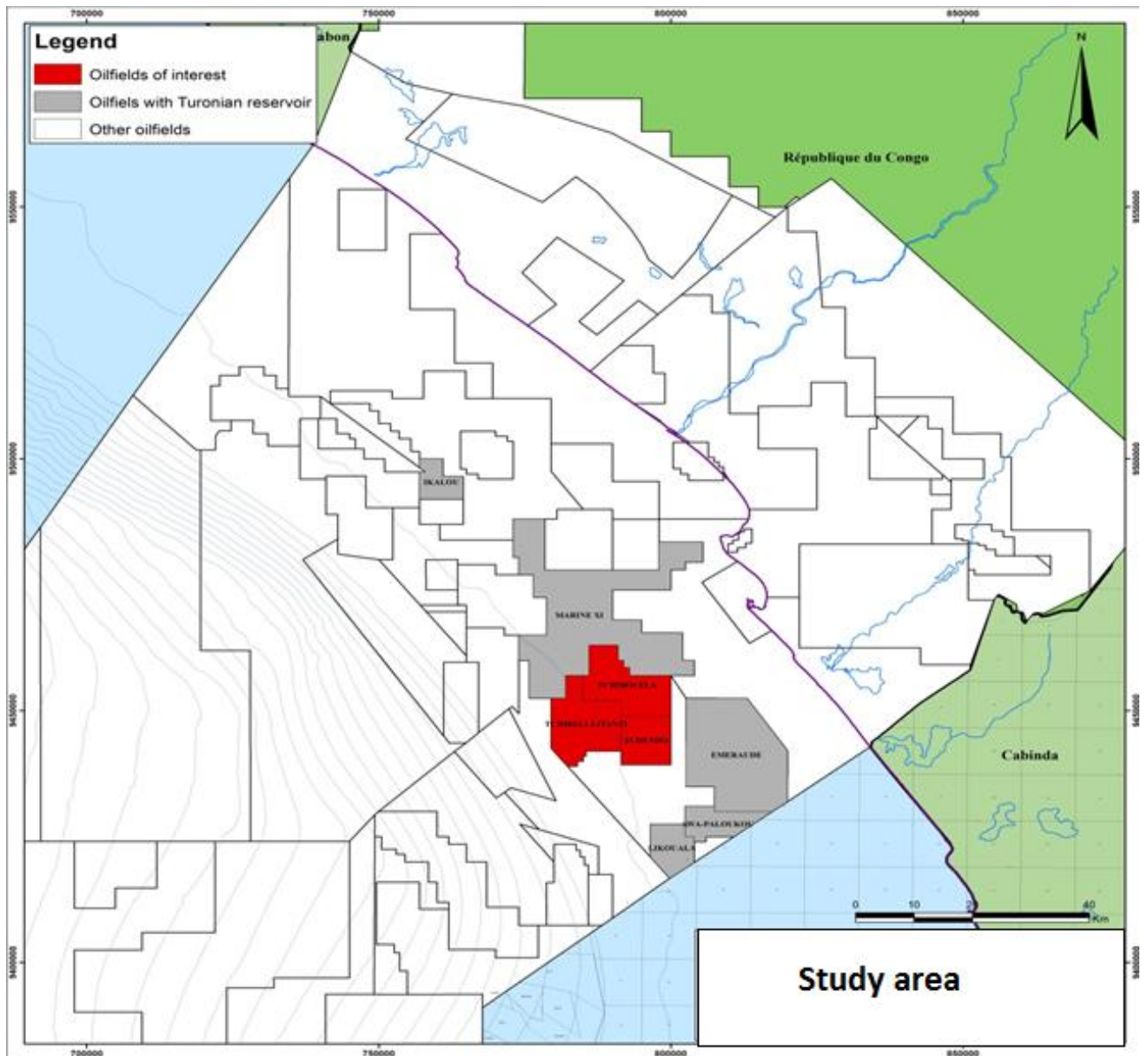


Figure 1: Congolese Coastal Basin oilfields (red blocks represent oilfield of interest wells, Grey blocks represent oilfields probable Turonian reservoirs, black line represent oilfields boundaries, purple line represent onshore-offshore boundary)

## 1.2. Geological setting summary

### 1.2.1. Tectonic setting:

The African plate became the core of Gondwana supercontinent after late Precambrian Pan-African earth movement and reined a stable tectonic setting for a long time until the supercontinent was broken up by the impact of Mesozoic plumes that caused the fragmentation of Gondwana into the Americas, India, Australia, and Antarctica (Chen *et al.*, 2013). As all the other western African basins, the Congolese Coastal Basin was developed during the break up of Gondwana and the opening of the South Atlantic Ocean.

Four tectonic episodes are distinguished within the basin, revealing a four stages evolution of the basin: pre-rift, syn-rift, transitional and post-rift episodes:

- The pre-rift episode started during late Jurassic-Barriasian epoch. During this episode, South America and African continents were still a united continent (Gondwana supercontinent) but affected by Tristan mantle plumes. Basalt rock erupted on these continents at about 130Ma (Dickson *et al.*, 2003); subsequently volcanic belts were formed between the two continents (Walvis ridge and Rio de Grande) ridge at separate sides of the African and South American continents (Fort *et al.*, 2004).
- The syn-rift episode began at the Valanginian- Barremian epoch of early Cretaceous. During this period, as a result of thinning; rifting was initiated and intercontinental rifts were developed between African and South American continents (Jackson *et al.*, 2000). Rifting started south and progressed northward (Numberg & Muller, 1991). According to Standlee *et al.* (1992), rifting may have been initiated by two hotspots: the Walvis hotspot and the Benue triple junction. Karner *et al.* (2003) reported that Gabon-Congo-Angola was thinned by the extension faulting landward of Atlantic hinge zone. Rifting led to development of asymmetrical horsts and grabens basin trending parallel to the present-day coastline (NNW-SSE trending faults) (Brownfield & Charpentier, 2006). Karner & Discroll (1999) assumed that the rifting phase comprises a series of pulses. Extension occurred by multiple slip across these eastward dipping border faults and they distinguished three rifting phases along Gabon-Congo-Angola margin: Barriasian-Hauterivian rift phase; Hauterivian-late Barremian rift phase and late Barremian-early Aptian phase.
- Transitional episode extended from Aptian to early Albian. During this period, lasting extension finally broke down the African and South American continents. South Atlantic

was progressively opening at the same time affected by the obstruction of volcanic topographic high formed by transverse Walvis and Rio de Grande (Lui *et al.*, 2008).

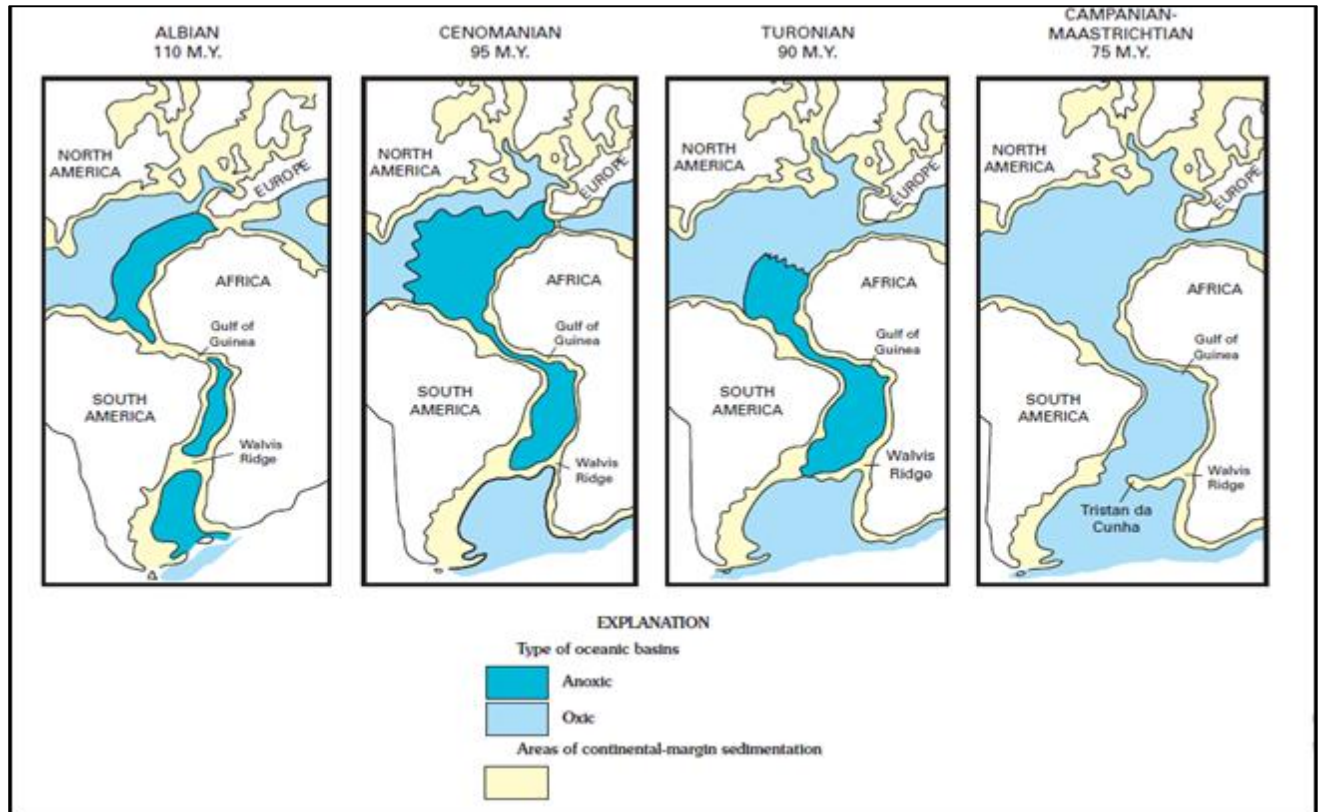


Figure 2: Paleogeographic map of the Cretaceous break up of Africa and South America (modified from Brownfield and Charpentier, 2006)

- Post-rift episode extends from Albian to recent. This period was representative of sea level change, uplifting and tilting of the African continent (Lui *et al.*, 2008). Duval *et al.* (1992) reported that during post-rift (post salt) period tectonic was characterized by raft tectonic which allowed extreme thin-skinned extension of overburden over a decollement of thin skinned. The simultaneous uplifting of the continent to the East and marine sediment burdening to the west African margin to tilt westward (seaward) and at the same time salt tectonics (raft tectonics) were formed as a result of gravity slipping deformation (Lui *et al.*, 2008; Savoye *et al.*, 2009).

### 1.2.2. Stratigraphy and sedimentary environment

As any other rifting basin, the stratigraphy and sedimentary environments evolution of the Congolese Coastal Basin were influenced by tectonic events related to the opening of the Atlantic. Hence, sediments and environments within the basin are classified on the basis of the tectonic event during which they deposited:

- Synrift rocks in the coastal Congo Basin range from Valanginian to Barremian and consist of lacustrine and fluvial rocks (Baudouy & Legorjus, 1991; Harris, 2000). Syn-rift sequence consists of Valanginian Vandji sandstone corresponding to quartzose sandstone light gray feldspathic and conglomeratic (Nombo-Makaya & Han, 2009). This sandstone is considered as developed in alluvial system. The Vandji sandstone is overlain by the Sialouvakou marl constituted of slightly micaceous claystone, with interbedded sandstone. The Sialouvakou marl is in turn overlain by Djeno sandstone constituted of alternating micaceous argillaceous–calcareous sandstone with siltstone and gray shale. These facies deposited in fluvial–lacustrine environment (Brownfield & Charpentier, 2006; Nombo-Makaya & Han, 2009). The fluvial-lacustrine depositional setting of Djeno sandstone and sialouvakou marl is succeeded by lacustrine depositional setting in which Pointe-Noire marl developed (Brownfield & Charpentier, 2006). This period characterized a quiescent period.

During Barremian, the basin was subjected to extensive block faulting and erosion forming a graben -lacustrine setting. The rocks were deposited in lacustrine, alluvial and fluvial depositional setting. The formation was eroded prior to deposition of Toca carbonate made of bioclastic carbonates with rare shale and considered as lateral equivalent of Pointe Indienne shale constituted of grey-green silty, micaceous shale with sandstone, siltstone and carbonate interbedding. Brownfield and Charpentier (2006) reported that Toca carbonate represented the uppermost syn-rift rocks in the Congo Basin. It was divided into four units (McHargue, 1990).

- Basal post-rift rocks of the coastal Congo Basin are lower Aptian chela sandstone consisted of sandstone and shales deposited in a variety of environments including marine, lacustrine and fluvial (Harris, 2000).

Succeeding to Chela formation, salt was deposited across the equatorial western Africa due to barrier formed by migrating Tristan Da Cunha hot spot that restricted circulation from open Marine Ocean to south (Brownfield & Charpentier, 2006). Four evaporate cycles were recognized within the units (Brice & others, 1982). It contains both sodic and potassic salt (sylvinite) (Nombo-Makaya & Han, 2009).

The salt grades upward to a regionally extensive 50m thick unit representing freshening of the basin and the end of the salt deposition in the Congo Basin. It corresponds to Albian Sendji carbonates made of high energy dolomitic, oolitic, limestone and interbedded sandstone deposited in tidal channels in the lower part of an offshore bar and shoreface units in the upper part (Brownfield & Charpentier; 2006).

During Cenomanian, regression that started in Albian continued and continental facies began to deposit influenced at the same time by fluctuating shoreline. This led to the formation of Likouala silt and Tchala sandstone.

During Turonian–Senonian period, the basin underwent transgression which led to the formation of the Turonian Loango dolomite constituted of grey sandy dolomite, siltstone and dolomite and Senonian Madingo marl overlying Loango dolomite. Madingo marl consists of silty- sandy marl with clayey limestone and fossiliferous silty shale (Nombo-Makaya & Han, 2009).

- During Oligocene-Miocene, the basin became an open ocean and Paloukou formation consisted of shale intercalated by sand and limestone deposits.



UNIVERSITY *of the*  
WESTERN CAPE

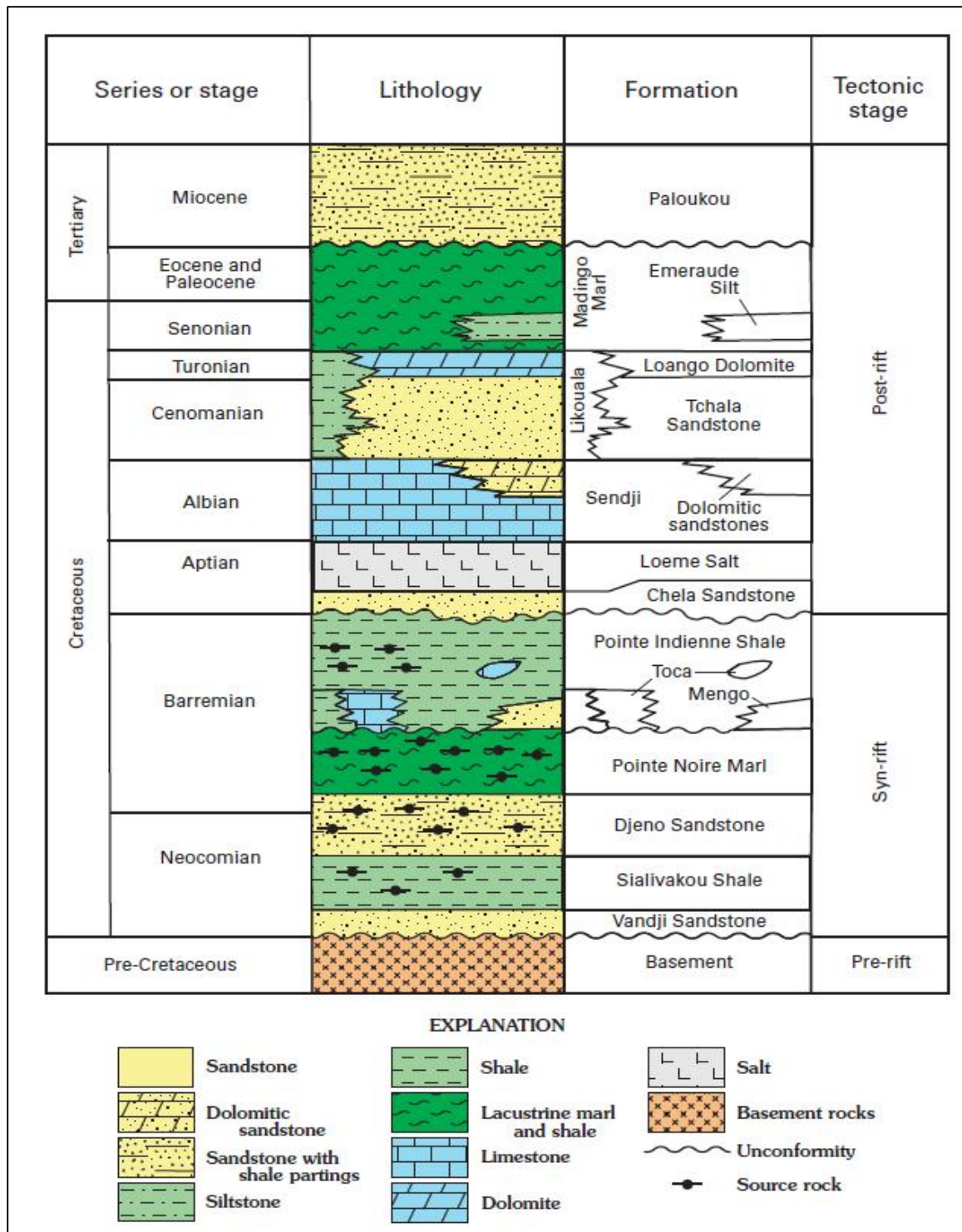


Figure 3: Generalized stratigraphic column of the Congo Basin (from Brownfield & Legorjus, 2006)

### 1.2.3. Previous works on Turonian series:

Turonian series of the Congo Basin were studied by various authors particularly those having worked for oil companies exploiting the basin hydrocarbon reserves. The Turonian series of the Congolese coastal basin were evidenced both onshore and offshore of the basin.

#### 1.2.3.1. Offshore

Offshore of the basin, the Turonian has been studied mainly by the following workers:

Doerenkamp & Jardine (1973) studied the micro-flora of the Congo Basin and delineated each epoch. With regard to the Turonian epoch, these workers related the series with the Gabonese formation and characterized the series as corresponding to zone Co C XIV. They distinguished two subzones within the Co CXIV zone:

- Subzone Co CXIVb corresponds to predominance of *C3 P3 R SP 162 (Deflandrea)*, *C3 P3 G SP 64*, apparition of rare *tri-pores SP101*, multi-pores *SP 36 sporadic*
- Subzone Co XIVa is characterized by maximum of *C3 P6 E SP 61a* and *Ephederals Sp56*, disappearance of *Dinogymnium* and *Deflandrea*, pollen spores *C3 P3 Sp. 155*, Pp multiporopollenites *SP 36* and *Sp 35* and definitive disappearance of *Deflandra* and *Dinogymnium*, apparition of *pseudoceratium D219*, *xiphophoridium D44*, *coronifera*, *Cyclonephelium D 128*.

Comparing the definition criteria in Congo and in Gabon, these workers found that they are the same. They noticed that micro-flora Co XIV b is the same in both countries and corresponds to the Anguille formation dated Coniacian but based on calcareous nanofossils zone Ga XIV b belongs to Coniacian – Santonian interval whereas in the entire basin it corresponds to *G.Renzi* and *P. turbinata* foraminifera meaning Cenomanian -Turonian interval.

In Gabon GA CXIV zones correspond to the Azile formation dated Turonian whereas in Congo calcareous nanofossil pre-XIVb is totally absent. The Zone Co C XIVa in Congo corresponds to the Ostracods biozone. The limit Co C XIVb – CO C XIVa corresponds to Senonian- Turonian limit considering palynological hypothesis of the Ostracods, it is included in Turonian considering the foraminifera's hypothesis.

The workers concluded the limit Turonian- Senonian is fuzzy that as in all the other basins; that the Co C XIVa subzone corresponds to Turonian epoch (Azile formation) and the subzone Co XIVb corresponds Coniacian (Anguille formation).

On the other hand, many authors have lithologically and sedimentologically studied the Turonian formation during different oil exploration campaigns

Le Fournier & Mathieu (1972) described the following lithofacies as corresponding to Aptian-Turonian interval:

- Oolithic facies with rare rounded quartz; interpreted as representing tidal delta deposits

- Oolitic bioclastic limestone with pellets and various debris more or less recrystallized into sparite (outer lagoon deposits)
- Calcareous mud with pellets, lamellibranch debris echinoderm plates with preserved textures (dolomitization) seen as representing internal lagoon deposits
- stromatolithic dolomitic facies (littoral bay deposits)
- dolomitic facies with spherolithe and silt concretions
- heterometric fine to coarse grained sandstone with irregular cementation facies considered as representing Ouadi deposit type
- white porous dolomitic facies with sandy matrix and mudcracks
- siltstone and fine sandstone facies with green argillaceous matrix (cement)

These two workers explained the formation of dolomitic facies by dolomitization of continental deposits or by pedogenic action (for Ouadi deposit type) and meteoritic water action (for lagoon deposits).

Monsaigeon (1983) described Turonian series of the Congolese Coastal Basin as comprising two formations:

- Loango dolomite: constituted from bottom to top by more or less silty and dolomitic shale, shaly-dolomitic siltstone to fine sandstone with intercalation of heterogranular sandstone and saccharoidal dolomite with more or less vacuole and sandy to silty locally calcareous.
- Loukoula silt deposited in outer part of the basin lies directly on Cenomanian formation of the same name. This formation consists of argillaceous siltstone more or less dolomitic related to marine domain, silty dolostone to sandy dolostone sometimes bioclastic, fine sandstone. It is interpreted as corresponding to littoral domain, locally calcareous to dolomitic (outer platform deposits).

The author considered the silt to siltstone facies as representing a deep marine barand the silty shale as representing an outer platform domain.

Massamba (1985) identified two mesosequences within the Turonian series: lower Turonian and the upper Turonian.

- Lower Turonian mesosequence consists of alternating shaly-sandy facies considered as representing margino-littoral domain and silty-sandy bioclastic carbonate facies interpreted as representing carbonate reef of outer shallow carbonate platform.
- Upper Turonian mesosequence appears as transgressive mesosequence delineated in the upper part by limestone forming MS2 seismic marker.

This upper Turonian mesosequence encompasses two domains:

- Outer shallow platform domain, for which the facies vary from one oil field to another:

- at DSM, TAM, ZAM and BOAM oilfields, it is represented by dolomicrite to silty- sandy, bioclastic sparite with phosphate debris, pyrite and glauconite overlain by dolomitic siltstone to sandy silty-dolostone;
  - at EMM, LOM, KOM and KAM oilfields, it consists of marine incursion deposit constituted of silty shale to shaly siltstone overlain by bioclastic silty-sandy microsparite deposits with foraminifera;
  - at LVM, LVMP, KOUM and IKAM oilfields, it consists of silty shale with limestone interlayers.
- Deep platform domain comprises silty shale with foraminifera, micritic, shaly siltstone interlayering and terminates by argillaceous with rare silt and rare phosphate debris compact micrite

The upper Turonian mesosequence is overlain by Madingo marl

Menard (1996), on stratigraphic synthesis of terminal Cenomanian/Turonian (Loango dolomite) reported 8 facies corresponding to 8 distinctive sedimentological environments for the Turonian deposits:

- Estuarine to fluvial facies: consisting of fine to medium sandstone with oblique beds, presence of flora and dolomitic clast at the base (erosion surface);
- deep bay: characterized by grey- green very biotubated (*teichichnus*) dolomitic argillaceous silt to silty shale;
- shallow bay bioturbated (*thalassinoides*) dolomitic silt to silty dolostone;
- Shallow bay to bioclastic reef: dolomitic silty peloidal wackestone with bivalves' shells and gastropods often dissolved;
- Bioclastic reef: Shelly packstone limestone sometimes dolomitised
- Medium to upper shoreface: characterised by dolomitic silt with locally HCS and SCS indicating a strong storm influence;
- Medium to lower shoreface: corresponding to shaly dolomitic silt with undulate beds (storm influence)
- Offshore: dark grey silty shale locally bioturbated indicating an environment protected from storm influence.

Biondi (1996) also described and interpreted the same facies as Menard in the same year during sedimentological study of terminal Cenomanian/Turonian of Tchibouela Marine, Tchibouela East Marine oil fields.

Massamba (1985) description of the Turonian series unlike palynologic zonation by Doerenkamp & Jardine (1973) proposed a stratigraphical chart in which Turonian series are constituted of Loango dolomite overlain by calcareous formation and both laterally equivalent to Madingo marl considered by Doerenkamp & Jardine as Senonian formation.

Masse (2008) described Turonian series and reported that Turonian series were subdivided into two lithological parasequences:

- Calcareous parasequences comprised of the following facies:
  - ◆ Grey to green, slightly silty, pyritic and slightly bioturbated
  - ◆ Bioturbated silty mudstone with coarse white molluscs' fragments
  - ◆ Silty wacke-packstone with bioclasts (dominantly echinoderms, *ephiuridea*)
  - ◆ Floastone (silty wacke-packstone matrix) with lamellibranches and valves
  - ◆ Floastone (silty packstone matrix) with lamellibranches and gastropods
  - ◆ Silty floastone with lamellibranches (*oestreidae*) in place.
- Silicoclastic parasequence consisting of:
  - ◆ Grey to green shale, slightly silty, pyritic and bioturbated
  - ◆ Bioturbated silty shale/bioturbated mudstone
  - ◆ Well sorted, fine grained massive silty sandstone
  - ◆ Well sorted fine grained silty sandstone with hummocky cross stratification
  - ◆ Fine grained silty sandstone with parallel laminations
  - ◆ Coarse grained sand, poorly sorted, with some bioclasts and pyrite

The author also reported dolomitization of the previously mentioned facies which he considered as a secondary process and interpreted the calcareous parasequences as representing carbonate platform specifically ramp recombined to bioclastic Chenier deposits and silico-clastic parasequence as representing either coastal plain or fluvial-estuarine type of deposits.

#### *1.2.3.2. Onshore*

The upper Cretaceous rocks (from Turonian to Santonian) crop out along the Congolese Atlantic coast from Pointe Kounda to Djeno (Pointe Kounda, Pointe Indienne, Pointe Noire seaport lighthouse, Pointe M'vassa, Djeno (Dartevelle, 1957; Louango-Tchikaya, 1972). These rocks were the subject of multiple dating and description studies by various workers favoured by early oil exploration and diverse mapping projects.

Lombard & Schneegans (1930) (quoted by Dartevelle, 1957), recognized occurrence of ammonites *Texanites soutoni*, *Texanites sp.* at Pointe M'vassa and dated these rocks as upper Santonian whereas Schneegans (1932) (referenced by Dartevelle, 1957) dated these rocks as corresponding to lower Santonian.

Haas (1934) described the rocks at Pointe M'vassa lithologically as corresponding to alternating lumachel beds and fossiliferous sandstone. He dated the rocks as Santonian on the basis of bivalves (*e.g. Cytherea, Plicatula hirsuta, Inoceramus*) and gastropods. Djeno rocks were stratigraphically considered as overlying Pointe M'vassa rocks and dated Santonian by Hirtz (1951) and Dartevelle (1957).

The study of Pointe Noire lighthouse cliff yielded different ages depending on the workers. After Schneegans (1954) the all package of rocks comprising the cliff corresponds to Senonian age on the basis of *Lima obliquistriata* present in the rocks and also observed in Senonian rocks of India whereas a later work by Louango-Tchikaya (1972) revealed occurrence of Turonian age rock through the study of microfossil content (this was the first time that Turonian was directly dated from outcrop).

Pointe Indienne outcrop was studied by Hirtz (1951). He described the rocks as corresponding from base to top to: blue sandstone with pyrite slightly laminated and with non-calcareous cement, followed by brecciated sandstone with argillaceous clasts overlain by conglomerate with dominant silex, quartz and quartzite and with clayey sandstone clasts and with slightly calcareous cement. Hirtz reported that these rocks lacking fossils were dated Turonian through parallelization with study of a well realized at Pointe Noire in which the same lithology was observed.

Pointe Kounda outcrop was first described by Emilianoff in 1934. He characterized lithologically the rock at this location as constituted of the succession calcareous sandstone, marly sandstone with fish debris, black bituminous marl and marly limestone dated Coniacian. Further work by Dorenkamp (1973) on microfossils showed occurrence of *Hexaporticolprites sp6* of zone Co C XIVa characteristic of Turonian stage in rocks from Pointe Kounda.

Most recent work By BRGM (Callec *et al.*, 2014) during the last Congolese map updating gave a Turonian-Santonian age for this outcrops. This campaign described the rocks as corresponding to Loango dolomite, which is stratigraphically considered as equivalent to Turonian rocks (mainly offshore). Furthermore, the authors added that the outcrops can be correlated with Turonian rocks offshore of the basin.

The previous works did not consider both onshore and offshore data at the same time. These studies were done considering only a particular oilfield or a small onshore area.

Hence, the described Turonian formations differ from one worker to another (*e.g.* different vertical successions between Monsaigeon (1983) and Massamba (2007)). The workers yielded different descriptions and interpretations for Turonian sediments (*e.g.* Le Fournier & Mathieu (1972) versus Massamba (1984) versus Masse (2008) facies models).

This inconsistency could be related to the fact that the workers did not study the formation basinwide which could lead to the misunderstanding of the environments in which the series developed and as a consequence the misunderstanding of the Turonian reservoirs.

The present research studied the Turonian series basinwide from onshore to offshore.

## Chapter2: Material and method

### 2.1. Data

The data used during this research include outcrops, cores, wire- line logs and seismic (2D and 3D).

#### 2.1.1. Outcrops

The outcrops recognition was based on previous works performed during Chemin de Fer Congo Océan railway construction, Pointe Noire port dredging, colonial geological fieldtrips along the Congolese Atlantic coast (Emialianoff, 1934, Haas, 1934; Schneegans, 1954; Louango Tchikaya 1972; Dorenkamp, 1973) and the last geological mapping update (Callec *et al.*, 2014). These outcrops are located in five different locations along the Congolese Atlantic coast:

- Pointe Djeno (32M 0825261, 9455083)
- Pointe M’vassa (32M 0821122, 9460502)
- Pointe Noire seaport lighthouse’s cliff (32M 0814791, 9469585)
- Pointe Indienne (32M 0808681, 9484335)
- Pointe Kounda (32M 0763495, 9537809)

Pointe M’vassa and Djeno outcrops were studied. Each bed along the two outcrops was sampled and 58 samples were collected (38 samples from Pointe M’vassa and 20 samples from Djeno) for facies description while 13 samples were collected from the two outcrops samples at 50 cm interval and were submitted to palynological analysis done in (Buratti *et al.*, 2017) Whose results were used in this research. Thin sections were made from the 58 samples collected for facies description.

#### 2.1.2. Offshore Data

Fifty wells were selected from Total E&P Congo database on Co CXIVa palynological zone occurrence (Turonian). That selection was performed only on post salt wells on which a biostratigraphic study was performed.

Two wells out of the sixteen wells with Turonian interval cored were selected to be used as reference wells

The offshore Data include:

- Cores: the studied cores are more than eighty metres long each; the palynological data from core study and thin sections were provided by Total E&P Congo.
- Well logs: they consist of gamma ray, neutron-density, sonic logs and check shot or psv

Tableau 1: Well summary table

Number of wells	Wells with cored Turonian interval	Total core length	Core with wireline log
50	16	1060m	46

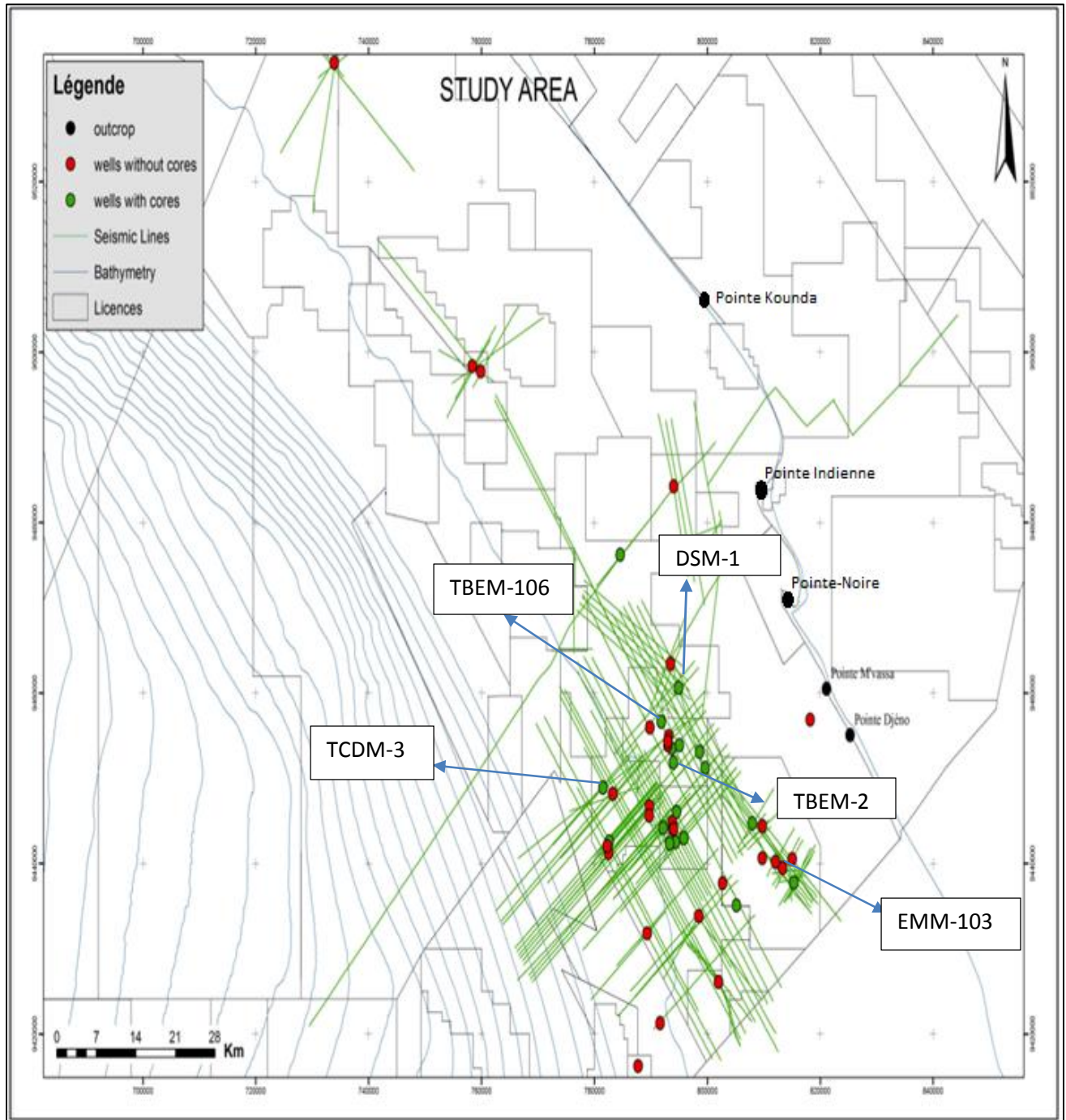


Figure 4: Studied wells and outcrops locations( green lines represent seismic lines, green dots represent well with available cores, red dots represent wells without core) (the names of the seismic lines were not provided due to confidentiality)

## 2.2. Methodology

This research thesis was performed using coastal outcrops, offshore cores and well logs, 2D and 3D seismic data.

The methodology followed corresponds to the approach developed by Durand (1996) and taught in the Basin Evaluation Honours Course at the University of Wits. It consists of three different scale changes:

- Outcrop and core scale change, to define and calibrate facies, facies association, and facies model. Two reference outcrops of the so-called Turonian series were selected (Pointe Mvassa and Djeno) (fig. 4) and studied. This allowed a better understanding and description of the offshore wells cores. From the defined facies model, sequence stratigraphy concepts were applied to the vertical and horizontal successions of the environments (see below 3.3). Stratigraphical surfaces (Maximum flooding surfaces, sequences boundaries) and patterns (progradational, retrogradational, aggradational (Van Wagoner *et al.*, 1988)) were recognized from cores and outcrops **to establish the chronostratigraphical correlation framework with well logs and seismic interpretation.**
- Core to well scale change, to calibrate facies and the depositional environments, the stratigraphical surfaces and patterns defined in the previous section on the wells. The stratigraphical surfaces and the patterns were tied with well-logs (gamma ray, neutron-density, sonic and seismic synthetic logs), this led to recognition of stratigraphical surfaces response on a well-logs. The log markers were hence identified to serve as **framework for well to well correlation.**
- Well to basin scale change, to calibrate the markers defined in the preceding section on a seismic profile. The log markers identified above were tied on seismic profile through the use of seismic synthetic logs. This log-seismic tie indicated the corresponding response of the environment changes on seismic profile (Recognition of maximum flooding surface on seismic profile). **This allowed identifying the seismic horizons corresponding to these log markers; these seismic horizons have been used for basin correlation.**

The successive steps for this research were as follows:

- Summary of the geological setting of the Congolese Coastal Basin.
- Re-constitution of stratigraphic column of the Turonian series by the use of literature review and identifying and defining the characteristic of Turonian formation stratotype.
- Performing outcrops selection and well with Turonian interval well identified.
- Reviewing paleontological data from the wells and their stratigraphic assignments in the light of current paleontological and stratigraphic knowledge. This review was performed in order to summarize and correlate the biostratigraphic findings of various paleontological data dealing with sediments in selected wells.

The criteria established for Upper Cretaceous stages during international symposium in 1995 notably for Cenomanian (Troger & Kennedy, 1996), Turonian (Bengston, 1996), Coniacian (Kauffman *et al.*, 1996), Santonian (Lamolda *et al.*, 1996), Campanian (Hancock & Gale, 1996) and palynological subdivisions (Deaf *et al.*, 2014) were used here in order to distinguish and refine the age assignment of different sections of the wells.

- Studying outcrops and cores facies and defining a facies model: Lithofacies analysis was conducted on both outcrops and cores in order to place each facies within its hydrodynamic and environmental contexts. The lithofacies were established by including abrasion, fragmentation, articulation, degree of encrustation, nature of the organism, nature of the matrix, sedimentary structures, degree of bioturbation and ichnofacies.

A microscopic analysis was carried for a certain number of facies in order to have a clear description of the lithology.

In this section 80kg of rocks from two reference outcrops were sampled, cut and 50 thin section were made and described. 80m long each core from 5 wells were also described and only two reference wells were presented here. 450 thin sections from the cores were also described and the most representative were shown in this manuscript.

- Determining stratigraphic surfaces through the use of core-wireline logs tie (meaning establishing a chronostratigraphic sequence) and calibrating core facies description with wireline responses.
- Coupling biostratigraphic data with either lithofacies, well logs or seismic to establish the chronostratigraphy of the Turonian series.
- Performing outcrop-core- well logs tie at different locations of the basin and correlating them in order to determine the geographical extension of the Turonian formations.
- Performing onshore and offshore seismic lines selection, well-logs-seismic tie and seismic-biomarkers tie.
- Performing petrographic study of the core (Core plugs) and field samples in order to define the diagenetic processes that have occurred during Turonian. Identifying the different diagenetic environments to which the sediments were exposed.
- Determining petrophysical characteristics of the Turonian series formations through the use of well logs to assess their petroleum interest. Two reference wells were chosen for this section: TBEM-2 and TCDM3

Petrophysical study was conducted in order to evaluate the changes in petrophysical properties (porosity and permeability) with depth, their relationship with facies (environment) and to understand the effect of diagenesis on these properties. On the other hand reservoirs continuity strikeward and dipward of the basin was considered to evaluate how the petrophysical properties change.

## Chapter 3: Results and Discussions

### 3.1. Biostratigraphy

#### 3.1.1. Outcrops

##### 3.1.1.1. Pointe M'vassa

Pointe M'vassa yields accumulations of various shells. The findings are consisted of (appendix 1, 2, 3 and 4):

- ✓ bivalves and oysters: *Trigonarca curvadonta*, *Trigonarca camerounensis*, *Trigonarca angolensis*, *Lopha lombardi*, *Lopha aucapitanei* (Coquand), *Plicautla ferryi*, *Plicatula flattersi*, *Plicatula hirsuta*, *Agelasina pledonta*, *Anofia aro Reymont*;
- ✓ gastropods: *Turitella haustator*, *Nerita angolensis*, *Fusus sp.*, *Anchura (Dicroloma) sp.*, *Tibia (Calyptraphorus) palhata* (Forbes);
- ✓ ammonites (**the present research evidenced for the first time ammonites in this site** as all previous articles lie on work by Lombard from which the existence of the form remains hypothetical): *Protexanites*, *Texanites venustus*, *Texanites Soutoni*, *Menuites sp* (**evidenced for the very first time in the section**);
- ✓ Fish debris: *Enchodus crenulatus*.

The palynological assemblages recovered from Pointe M'Vassa are rich and well preserved. The forms evolution along the outcrop is presented in figure 5 below. They consist of a terrestrial fraction made of pollen grains and spores and a marine fraction, mainly including dinoflagellate cysts and acritarchs.

The terrestrial fraction of the assemblages is dominated by the pollen *Hexaporotricolpites emelianovi*. It is associated with the common occurrence of *Ephedripites spp.*, sporadic *Constantinisorites spp.*, *Myrtacidites spp.*, *Cretacaeiporites spp.*, *Tricolporites spp.* and a few other accessory pollens.

Within the marine fraction dinoflagellate cysts are mainly represented by *Cleistosphaeridium spp.*, *Cribroperidinium spp.*, *Spiniferites spp.* and some scattered *Florentinia spp.*, *Trithyrodinium spp.* and *Cyclonephelium spp.*

The assemblages are also characterised by *peridonioid* cysts such as *Dinogymnium spp.*, *Senegalinium spp.*, *Isabelidium spp.* and rare *Alisogymnium spp.*; smooth cysts, referred to the genus *Leiosphaeridia* are abundant all over the section.

The foraminiferal content from Pointe M'vassa consists of *Nodosaria sp.*, *Textularia sp.* and *Solitary Quinqueloculina sp.*



## Discussion

The examination of the forms such as *Trigonarca*, *Lopha lombardi*, *Lopha aucapitanei*, *Plicatula flattersi*, *Plicatula ferryi*, *Plicatula hirsute* and *Anofia aro* Reymant showed that these organisms had a extent from Turonian to Maastrichian (table 2). Hence, they only indicate a broad upper Cretaceous age.

The relative abundance of ammonites *Protexanites* (bed 3, 5, 7 and 11), *Texanites venustus Collignon* (bed 14 and 16), *Texanites soutoni* (bed 24 and 30) and *Menuites sp.* (bed 32) at Pointe M'vassa is meaningful as these taxa lived in specific periods. *Prototexanites* is an upper Coniacian to Santonian genus (Wright 1957, Toshimitsu, 1988); *Texanites venustus Collignon* is known only from middle Santonian of Madagascar (Collignon, 1966), Angola (Cooper 1998); *Texanites soutoni* belongs to middle to upper Santonian (Klinger and Kennedy, 1975) while *Menuites* is known as a lower Campanian genus (Wright, 1996).

In addition, *Enchodus crenulatus* was found in Santonian to lower Campanian terrains of Cabinda basin (Dartevelle, 1949), in Vonzo (DRC) terrain (Casier & Dartevelle, 1959) and in Senonain terrain of Angola (Antunes & Cappetta, 2002).

Table 2: Macrofossils time range

Period	epoch	stage	<i>Plicatula Hirsuta</i>	<i>Plicatula ferryi</i>	<i>Lopha Lombardi</i>	<i>Trigonarca</i>	<i>Agelasina Pledonta</i>	<i>protexanite</i>	<i>Texanites Venustus</i>	<i>Texanites T. Soutoni</i>	<i>Menuites</i>
Cretaceous	Upper	Maastrichian	↕	↕	↕	↕	↕	↕	◆	◆	◆
		Campanian									
		Santonian									
		Coniacian									
		Turonian									
		Cenomanian									

The analysis of the palynomorphs at Pointe Mvassa section indicates that *Hexaporocolpites emelianovi* belongs to Coniacian of Gabon (Boltenhagen, 1967; Potonei, 1970), to Turonian to Campanian of Gabon (Boltenhagen, 1967) and it has been also identified in late Albian to Senonian rocks of Brazil and South America (Jardine *et al.*, 1972).

The occurrence of both *Spiniferites sp.* and *Spiniferites bejui* from the base of this section indicates Coniacian to Santonian age for the sediments (Mantel, 1850; Sarjeant, 1970). The occurrence of these specimens from the base of the section indicates that the sediments are younger than Turonian.

The base occurrence of dinoflagellate *Dinogymnium spp.* (base Santonian) may argue that the interval from Albian to Turonian interval does not exist at Mvassa. This occurrence of *Dinogymnium spp.* coincides with the first occurrence of ammonites *Protexanites* (figure 6) considered as a late Coniacian to early Santonian genus.

The abundance of genus *Senegalinium* with a particular predominance in the upper part of the section at Mvassa shows a Campanian to Maastrichtian age (Jain & Millepied, 1973).

The foraminiferal analysis of the specimens at Mvassa does not present an age determination interest but present a paleo-environmental interest.

**Due to the occurrence of the ammonites *Prototexanites*, *Texanites venustus*, *Texanites Soutoni*, *Menuites sp.* and the pollens periods of occurrence (Buratti *et al.*, 2017); Pointe M'vassa section is now considered as deposited during upper Coniacian, and for the first time, to lower Campanian.**

These results are coherent with previous results by Lombard & Schneegans (1930), Schneegans (1932). But they diverge with Callec *et al.* (2014) results that attributed Pointe Mvassa outcrop to Turonian.

UNIVERSITY of the  
WESTERN CAPE



### 3.1.1.2. Djeno

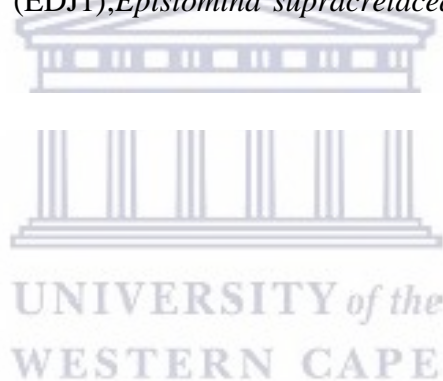
Djeno section mainly consists of beds made of shells beds. They are constituted of (appendix 7):

- ✓ Bivalves: *Trigonarca angolensis*, *Trigonarca camerounensis*, *Plicatula locardi*, *Plicatula ferryi*;
- ✓ Gastropods: *Volutomorpha (?) mungoensis* Reymont;
- ✓ Ammonite: *Puzosia sp.*

The palynological assemblages from Djeno section are largely dominated by dinoflagellate cysts; their evolution along the outcrop is presented in figure 7 below. The genus *Senegalinium* is very abundant and is associated with *Spiniferites spp.*, *Dinogymnium spp.* and some scattered *Florentinia sp.* and *Odontochitina sp.*

The terrestrial fraction is very similar to that of Pointe M'Vassa, but with a relative higher frequency of the pollen *Constantinisorites sp.*

The foraminiferal investigation along the outcrop reveals poorly fossiliferous samples consisted of *Haplophragmoides spp.* (EDJ20), *Nodosaria sp.* (EDJ5), *Pseudopolymorphina ovalis*, *Dicarinella concavata* (solitary) (EDJ1); *Epistomina supracretacea* (EDJ1) and micro bivalves (EDJ1).



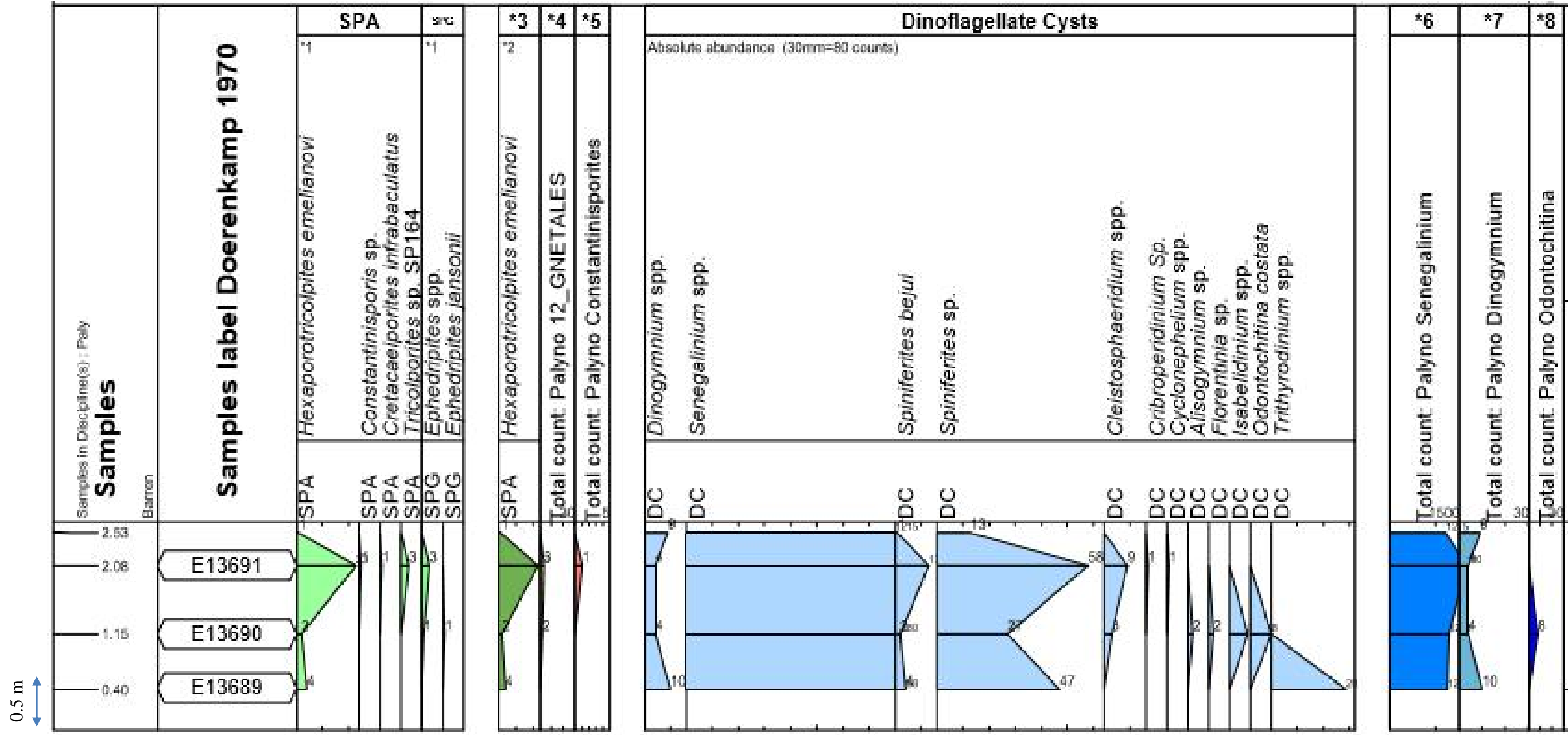


Figure 7: Distribution of palynomorphs at Djeno.

## Discussion

Analysis of the above forms indicates that the bivalves *Trigonarca angolensis*, *Trigonarca camerounensis*, *Plicatula locardi*, *Plicatula ferryi* had a long extent from Turonian to Maastrichtian. The ammonite *Puzosia sp.* was encountered in terrains from early Aptian to Maastrichtian (Kossmat, 1985-1898; Matsumoto, 1954; Collignon, 1961 and Kennedy & klinger, 2014).

The composition of the palynological assemblages recovered from the Djeno section suggests an attribution to the CXIV b subzone considered as Senonian.

The predominance of *Hexaporotricolpites emelianovi*, the presence of common *Ephedripites* associated with the occurrence of *Tricolporites sp.* 164, *Cretacaeiporites infrabaculatus* and *Myrtaceae* pollen grains is characteristics of subzone CXIVb corresponding to Senonian interval. The first stratigraphic occurrence of *Constantinisorites spp.*, is also characteristic of this subzone. However, *Hexaporotricolpites emelianovi* has been also identified in late Albian to Senonian rocks of Brazil and South America (Jardineet *al.*, 1972).

Among dinoflagellate cysts a relative increase in Senegalinium frequencies is recorded at the CXIVb subzone as it corresponds to Campanian- Maastrichtian interval (Jain & Millepied, 1973) and is accompanied by common *Dinogymnium*, *Oligosphaeridium* and more sporadic *Florentinia* and *Oligosphaeridium*.

The occurrence of solitary foraminifera *Dicarinella concavata* at the base of the section indicates a Coniacian-Santonian interval. This excludes the occurrence of Turonian age sediments along Djeno section, as the first *Dicarinella concavata* indicates the upper Turonian boundary.

Hence, **the sediments at Djeno are younger than Turonian age**. This is different with what had been proposed by Callec *et al.* (2014) and it is coherent with Doerenkamp (1972). The Coniacian-santonian age of the outcrop is strengthened by the occurrence of genus *Spiniferites bejui* in the lower part of the section and Campanian to Maastrichtian age is advocated by Senegalinium increase in the upper section.

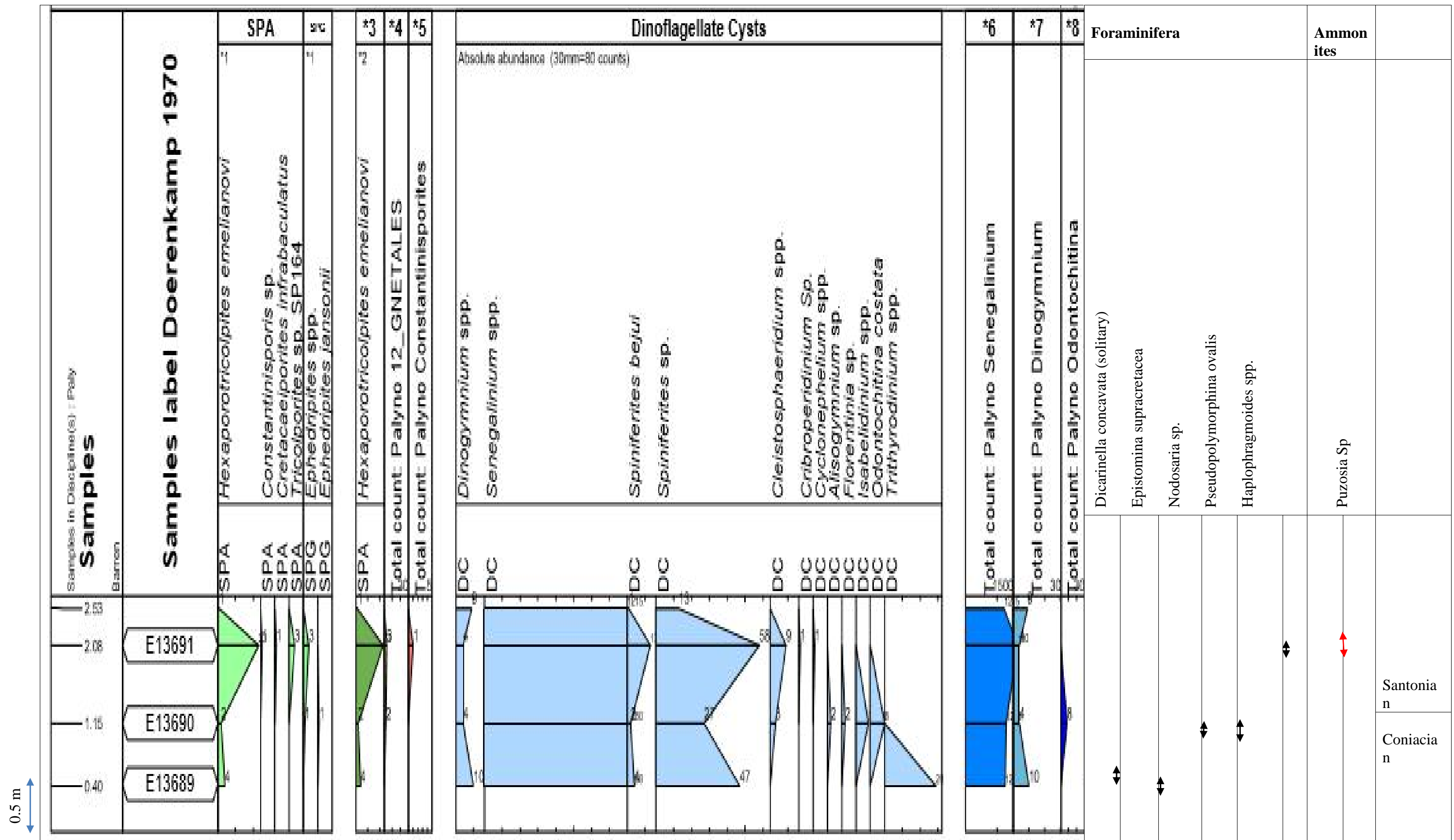


Figure 8: Stratigraphic distribution of palynomorphs, foraminifera and ammonite at Djeno

### 3.1.2. Wells

Biostratigraphic Works published to date on Cretaceous terrains offshore of the Congolese Coastal Basin rely mostly on foraminifera by Mboro (1981), Massala (1993), Massala *et al.* (1996) and on spore pollens. The biostratigraphic findings including spore pollens, foraminifera, and ostracods have been reconsidered in the light of international chart in order to relocate each depth interval within selected wells in its time interval in order to serve as basis for chronostratigraphical correlations between wells and outcrops.

The results for the present research were summarized in a table for each well (plate 1).

	North Africa		West Africa			North South America	
	NW Egypt Schrank & Ibrahim 1995	NW Egypt Present study	Senegal and Ivory Coast Jardine & Magloire 1965	Upper Benue Basin NE Nigeria Lawal & Moulade 1986	Gabon Blotenhagen 1980	NS America Muller et al. 1987	NE Brazil Regali 1989
Maastrichtian	IX <i>Costastricolpites reticulatus</i> <i>Spinizonocolpites cf. echinatus</i> A. Z.		II <i>Aquilocolpites</i> , <i>Echitropites</i> III <i>Tricolpate-syncolpate</i>	VII <i>Spinizonocolpites baculatus</i>	SII <i>Translucentipolis picatilis</i> SIIa <i>Butinia andreevi</i> SIIb <i>Syncolpites subulius</i>	VI 13 <i>Proteac. dehaani</i> 12 <i>Crasstricolpites</i> 11 <i>Auricullidites reticulans</i>	<i>Spinizonocolpites Proteacidites dehaani</i> <i>Syncolpites Tricolpites</i> <i>Proteacidites spp.</i>
Cenomanian			IV <i>Proteacidites</i> , <i>Trionites</i> J	V <i>Longaportites</i> sp. 3	SIII <i>Sporopollismagloirei</i>	10 <i>Drosendites senonicus</i>	Angiosperma <i>Cretacaeiporites Hexaporotricolp.</i> <i>Foveotricolpites giganteus</i> group
Santonian		V <i>Canningia senonica</i>	V <i>Monocolpogollites Drosendites senonicus</i> <i>Foveotricolpites giganteus</i> group	IV <i>Drosendites senonicus</i>	SIV <i>Punchoratipolis krutzschii</i>	V 8 Interval Zone	
Coniacian	VIII <i>Drosendites senonicus</i> T. R. Z.		VIa <i>Cretacaeiporites</i>				
Maastrichtian	VII <i>Foveotricolp. giganteus</i> - <i>F. spp. aff. ggentor.</i> A. Z.		VIb	III <i>Cretacaeiporites scabratus</i>			
Late Cenomanian	VI <i>D. cf. dunviganensis</i> <i>triporates</i> A. Z.	IV <i>Proteacidites cf. africaensis</i> <i>Classopollis classoides</i> <i>Afropollis jardinus</i> <i>Proteacidites cf. africaensis</i>	VII <i>Trionites" africaensis</i> <i>Cretacaeiporites polygonalis</i> <i>Afropollis</i> <i>Galeacomea ephedroids</i> <i>Classopollis</i> <i>Cicatricosisporites</i>	II <i>"Trionites" africaensis</i>	CI <i>Elaterocolpites castelainii</i>	6 <i>"Trionites" africaensis</i>	<i>"Trionites" africaensis</i>
Cenomanian	V <i>C. brasiliensis</i> <i>E. castelainii</i> <i>C. densimorus</i> A. Z.	III <i>Elaterocolpites castelainii</i>	VIII <i>Elaterocolpites Eucommidites Araucariacites</i>	I <i>Hexaporotricolpites potonieii</i>	CI <i>Elaterocolpites castelainii</i>	7 <i>Elaterosporites protensus</i> <i>E. verrucatus</i> <i>Afropollis</i>	<i>Brenneripollis</i> <i>Afropollis</i> <i>Hexaporotricolp. triporates</i>
Late Albian	IV <i>E. verrucatus</i> <i>Galeacomea causea</i> <i>C. polygonalis</i> A. Z.	II <i>Sofrepites legouxiae</i> <i>Elaterosporites acuminatus</i> <i>Sofrepites legouxiae</i> <i>Elaterosporites verrucatus</i>	IX <i>Cretacaeipor. polygonalis</i> <i>Galeacomea perulites</i> <i>tricolpates</i> , <i>tricolpates</i> <i>Cicatricosisporites</i>	<i>Afropollis jardinus</i>	AI <i>Sofrepites legouxiae</i>	6 <i>Elateropollenites jardine</i>	<i>Stellatopollis</i>
Albian	III <i>E. Klasi-Afropollis</i> <i>Tricolpites</i> <i>Tricolpites</i> <i>Afropollis jardinus</i> <i>C. perulatus</i> A. Z.	I <i>Elaterosporites klasi</i> <i>Galeacomea causea</i>	XI <i>Afropollis</i> <i>Classopollis ephedroids</i> <i>Cicatricosisporites</i>			III 6 <i>"Tricolpites" Exesipollenites tumulus</i>	<i>Cretacaeiporites</i> <i>Tucanopollis crisopolensis</i>
Aptian							

Figure 9: Palynological biozonation correlation in North and West Africa and Northern America (from Deaf *et al.*, 2014, modified after Schrank, 1992).

PAM1		
Depth	Palyno-zone and spore pollen	stage
620	<i>CXIVb</i> <i>Hexaporotricolpites emilianovi</i> , <i>SP 132</i> , <i>Sp133</i>	Coniacian
730		
740	<i>CXIVa</i> <i>Sp 36</i>	Turonian
824	<i>Multipropollenites Sp, Sp 28</i> <i>Perotroletes Sp, Sp 168</i> <i>Dissaccates</i>	
826	<i>CXIII</i> <i>Classopollis, triorites africaensis</i>	Cenomanian
1340		

EMM103			
Depth	Palynozone and pollen	Nannofossils	stage
251	<i>CXVa</i> <i>Prp.</i>	<i>Lithastrinus grilli</i> ,	Santonian
286			
291	<i>CXIVb</i> <i>C3P6E, CP3 Sp 162</i>	<i>Masthasterites furcatus</i>	Coniacian
424			
429	<i>CXIVa</i> <i>C3P6E, Ephedrales, P3 Sp 101,</i> <i>PP Sp 36</i>		Turonian
523			
524	<i>CXIII</i> <i>Classopollis, Triorites</i>		Cenomanian
573	<i>africaensis</i>		

TBEM2			
Depth	Pollen and palyno-zone	Foraminifera	stage
543.15		<i>Heterohelix globulosa, Rotalide</i>	Coniacian
543.15		<i>Hedbergella Spp., Dicarnella Sp,</i> <i>Gavelinopsis</i>	
564.62			
613	<i>CXIVa</i> <i>Hexaporotricolpites emilianovi, Ephedrite, Florentia Cf ressex,</i> <i>Batiacasphaera</i>		Turoian
624			
623	<i>CXIII</i> <i>Classopollis, Triotrites africaensis</i>		Cenomanian
646.85			

Depth	Pollen and palyno-zone	Stage
492	<i>CXIVb</i> <i>Constantinispuris jacquei, hexaporotricolpites emilianovi, E. barghoornii/staplinii, Dinigymnium Spp.</i>	Coniacin (Senonian )
492	<i>Hexaporotricolpites emilianovi, Steevesipollenites multilineatus, Cretaeiporites scabratus, Ephederites Spp., Dinogymnium acuminatum</i>	Turonian
593		
593	<i>Classopollis brasiliensis, C. classoides, Triorites africaensis, perotrites pannuceus.</i>	Cenomanian
850		

TCDM3			
Depth	Pollen		stage
482			
564	<i>Rotalide CNG F 10</i>		
587			
593	<i>Gabonita billmani</i>		Turonian
612			
621	<i>Gabonita levis</i>		

DMI		
Depth	Pollen and palyno-zone	Stage
78	<i>CXVa</i> <i>Deflandrea D20,</i>	Santonian
84	<i>Dynogymnium D25 b and D25c</i>	
90	<i>CXIV</i> <i>Hexaporotricolpites Sp 61a,</i>	Coniacian
96		
200	<i>CXIVA</i> <i>Hexaporotricoltes Sp61a, Ephederales Sp56, Perotriltes Sp28, Tropore scabre Sp101, Disaccate Sp168</i>	Turonian
236		
239	<i>CXIII</i> <i>Classopollis Sp 60a, Triorites africaensis</i>	
278		

Following the biostratigraphic refining of each well, the impedance log was produced for each well to be used for well-seismic tie and to distinguish seismic markers corresponding to each stage base or top.

The stage intervals hence defined for each well, the correlation was performed in order to establish stage continuity throughout the basin.

Particular cross sections were used to perform correlation for Turonian age interval; they are:

- Correlation cross section from Pointe Mvassa to TCDM3 through DSM1 and TBEM2 (figure 10):

In this section Turonian boundaries determined on wells using biostratigraphy coincide with major seismic horizons. The propagation of these horizons from well TCDM3 to Pointe Mvassa indicates that the outcrop is located well above the Turonian upper Boundaries and is within the Coniacian to Santonian interval as defined by their relative horizons.

This result is coherent with age range determined by the use of macrofossils and microfossils.



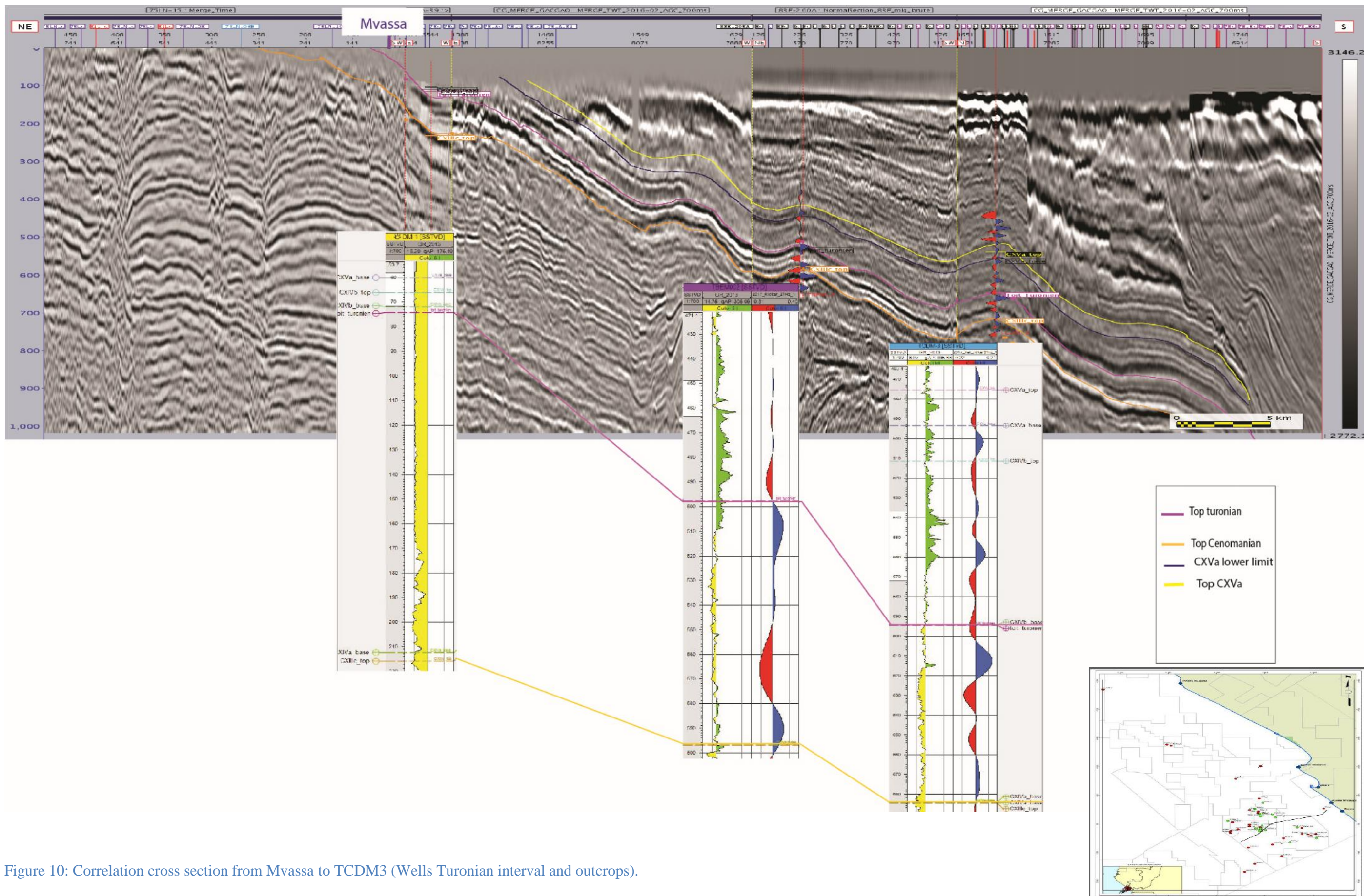
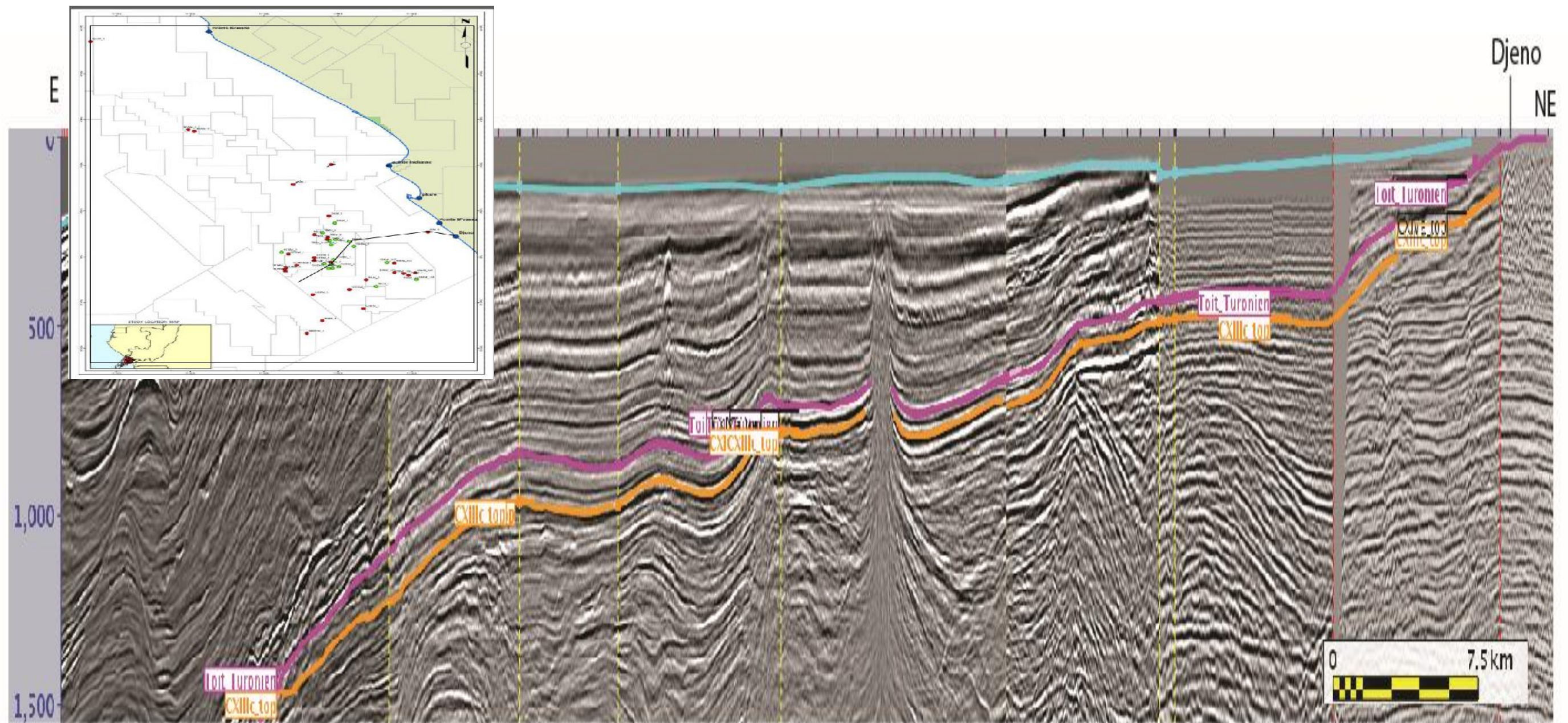


Figure 10: Correlation cross section from Mvassa to TCDM3 (Wells Turonian interval and outcrops).

- Correlation cross section from SUEM2 to Pointe indienne (figure 11)  
This section also shows that the Turonian upper and lower boundaries correspond to major seismic horizons (the same horizons with the previous cross section). The propagation of these horizons from well SUEM2 to Pointe Indienne outcrop indicates that the outcrop is located within the Turonian Boundaries. Hence, Pointe Indienne is of Turonian age.





- Top CXIIc
- Top Turonian

Figure 11: Correlation cross section from Pointe Indienne to SUEM2

- Correlation cross section from Sea port to Well SUEM2 (figure 12) also shows that Turonian boundaries coincide with major seismic horizons. The outcrop at the seaport is limited by Turonian upper and lower boundaries; hence the outcrop is of Turonian age.



UNIVERSITY *of the*  
WESTERN CAPE

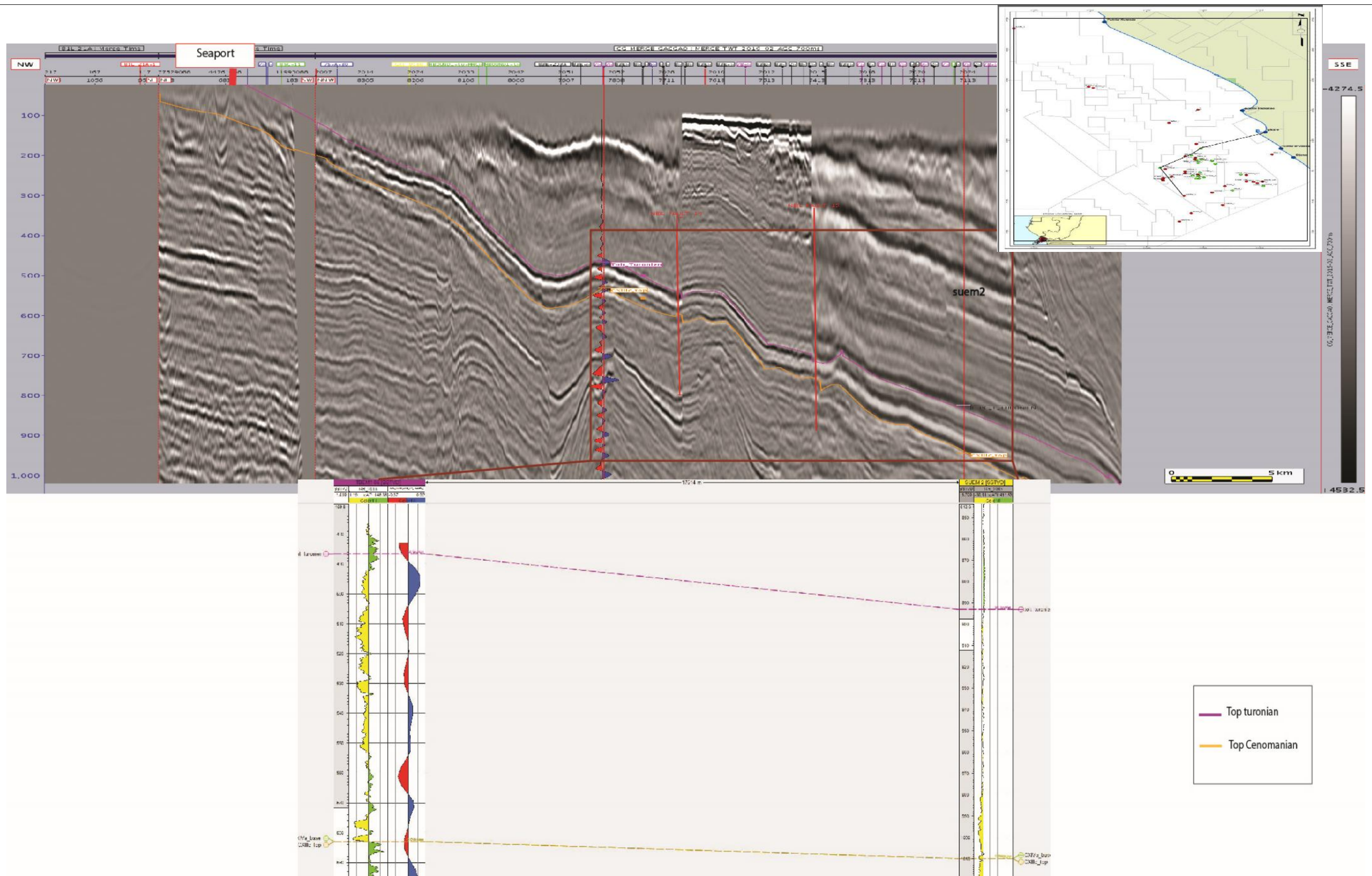


Figure 12: Correlation cross section from Sea Port towell SUEM2–offshore Turonian

- Correlation cross section from DSM1 to LKFM1 (figure 13): this correlation from the most distal well to the most proximal well shows that Turonian markers found through the use of biostratigraphy coincide with the same seismic horizons (base and top horizons) throughout the basin. This is very consistent throughout the basin.



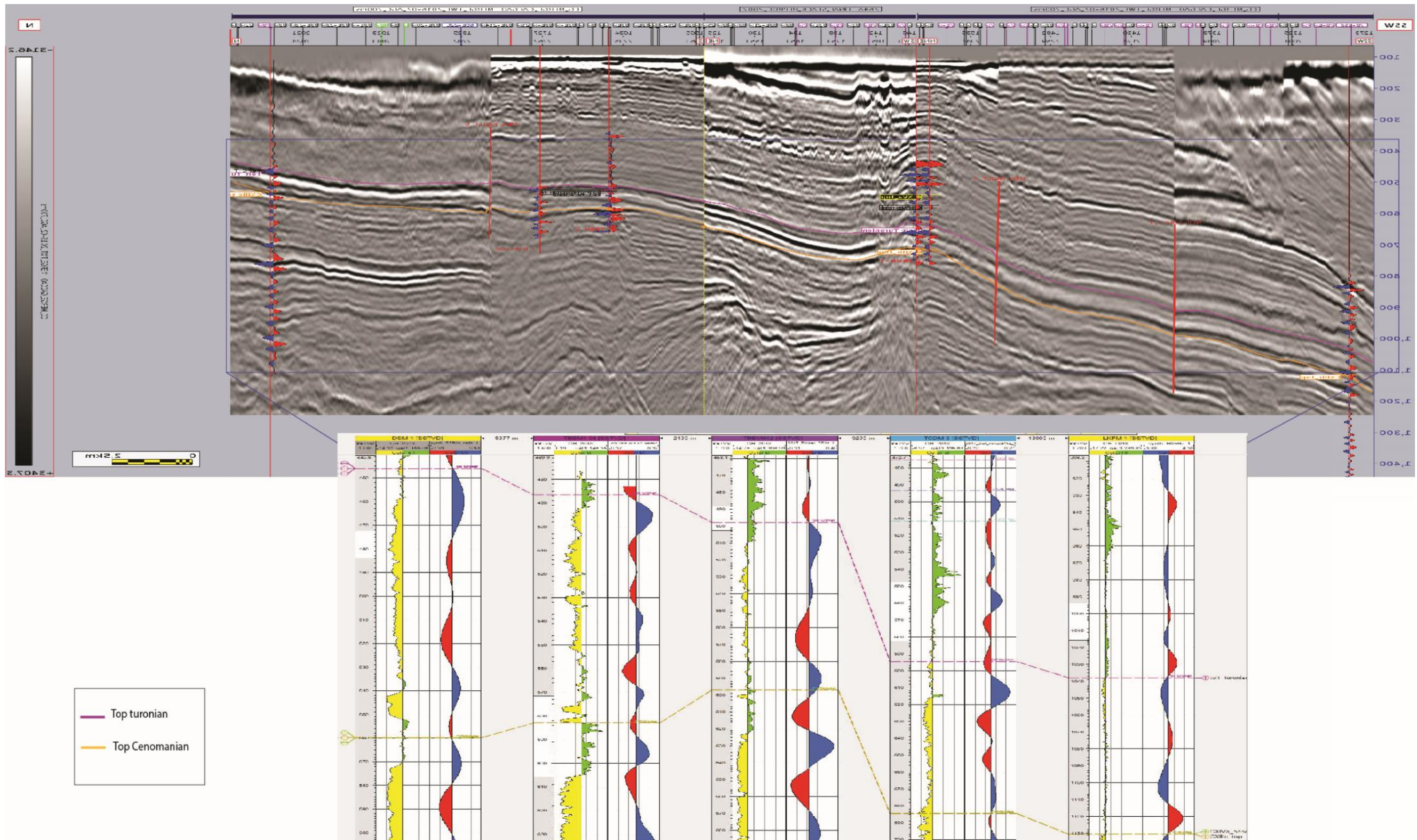


Figure 13: Correlation cross section from well DSM1 to LKFM1 (Turonian correlation).

The correlation cross section from well DSM to EMM fields illustrates lateral continuity of the Turonian interval. It also shows that thickness remains the same through the depositional strike. Turonian biostratigraphic markers corresponding upper and lower Turonian boundaries coincide with the same seismic horizons from one field to the other.

,



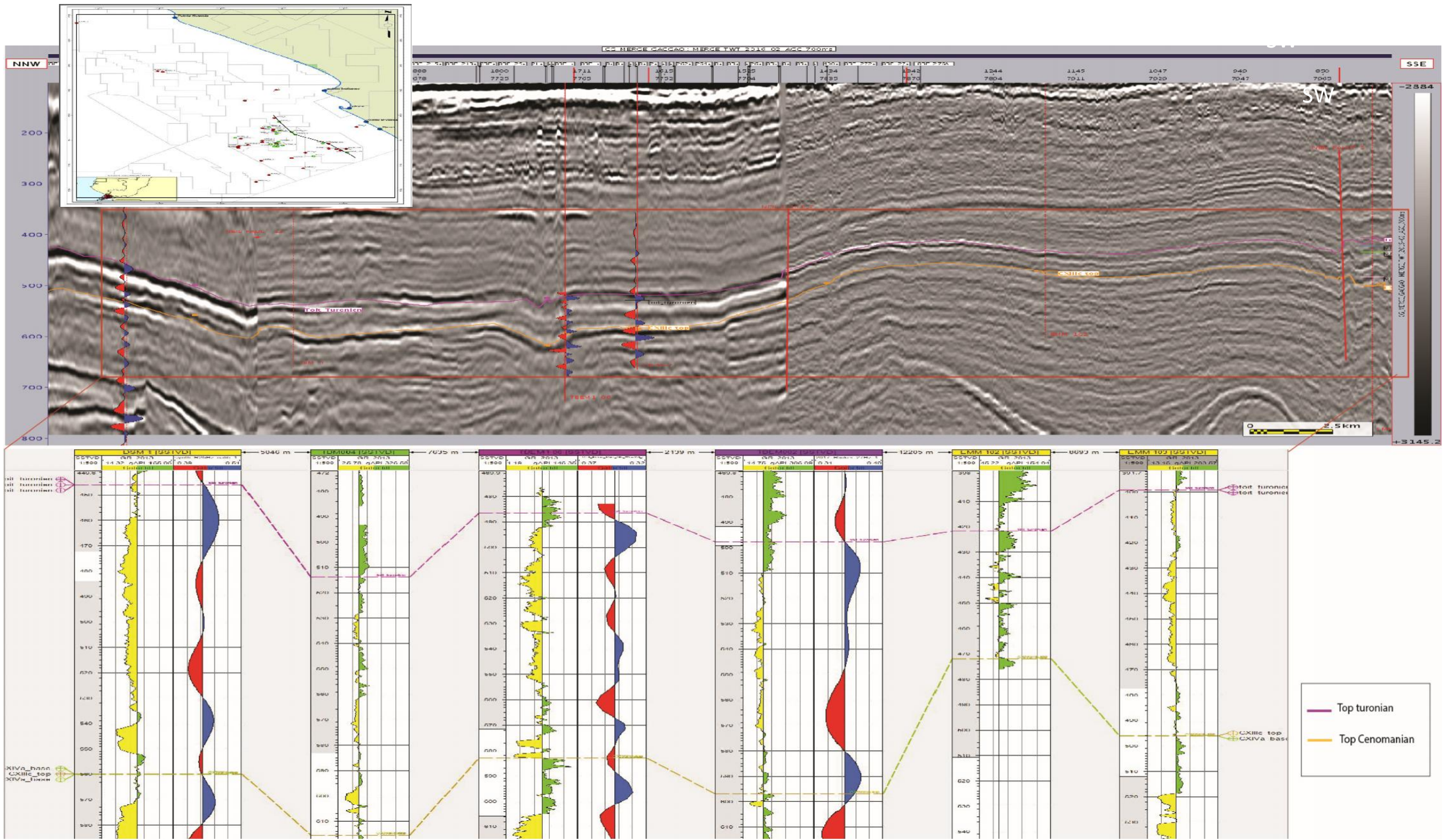


Figure 14: Correlation cross section from well DSM 1 to EMM103 Wells(Turonian correlation)

The correlation dip from well TBEM 106 to well TCDM3 through TBEM2 shows a high consistency between Turonian markers determined through by the use of biostratigraphy and the corresponding seismic horizons throughout the depositional dip. It also shows decrease in thickness from proximal TBEM field to TCDM field.



UNIVERSITY *of the*  
WESTERN CAPE

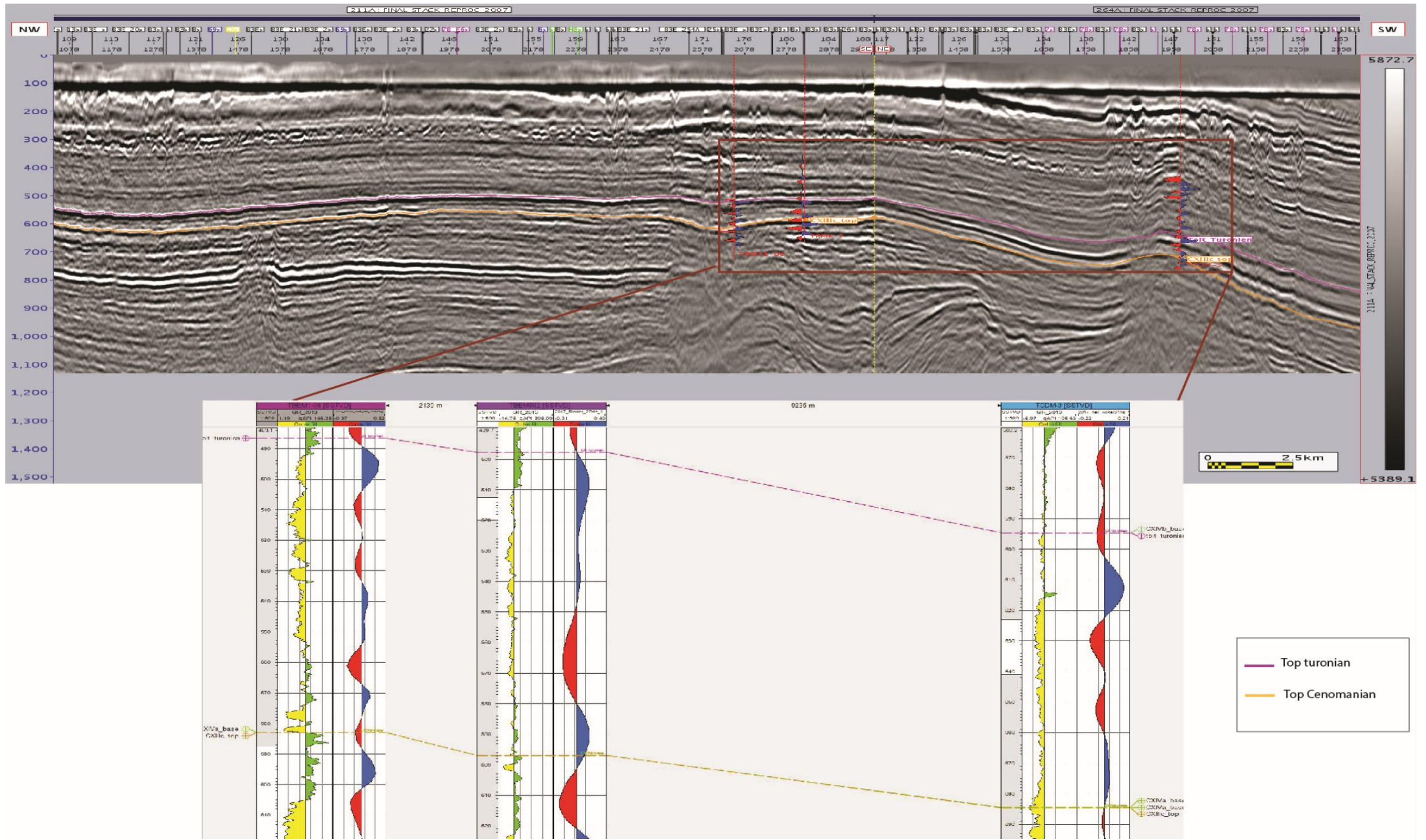


Figure 15: Correlation cross section from TBEM106 to TCDM3 Wells.

Hence it is now shown that:

- **Pointe Indienne outcrop is Turonian due to the outcrop being located within the Turonian interval, (above the Cenomanian upper limit).**
- **Pointe Noire sea port outcrop is also Turonian; this result is consistent with those by Louango Tchikaya (1972). Hence, the sea port outcrop can be considered as of Turonian age.**
- **Pointe Mvassa (located above the Turonian upper limit on cross section) is younger than Turonian, this results is consistent with *Texanites* ammonites found this location. Hence, it is a Santonian to Campanian age.**
- **Djeno located just above the upper Turonian limit near CXIVb zone on cross section, hence is considered as being Senonian age.**



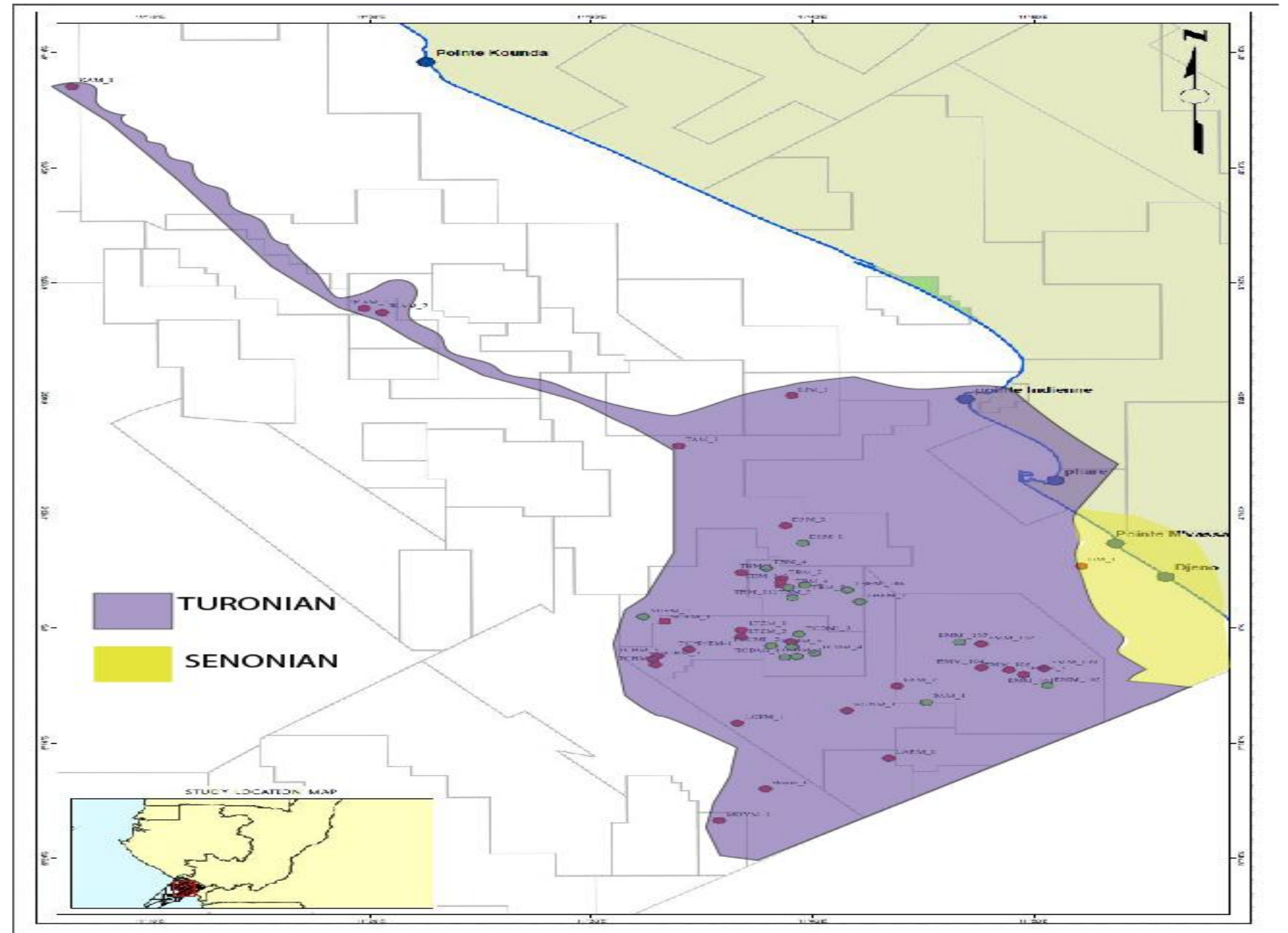
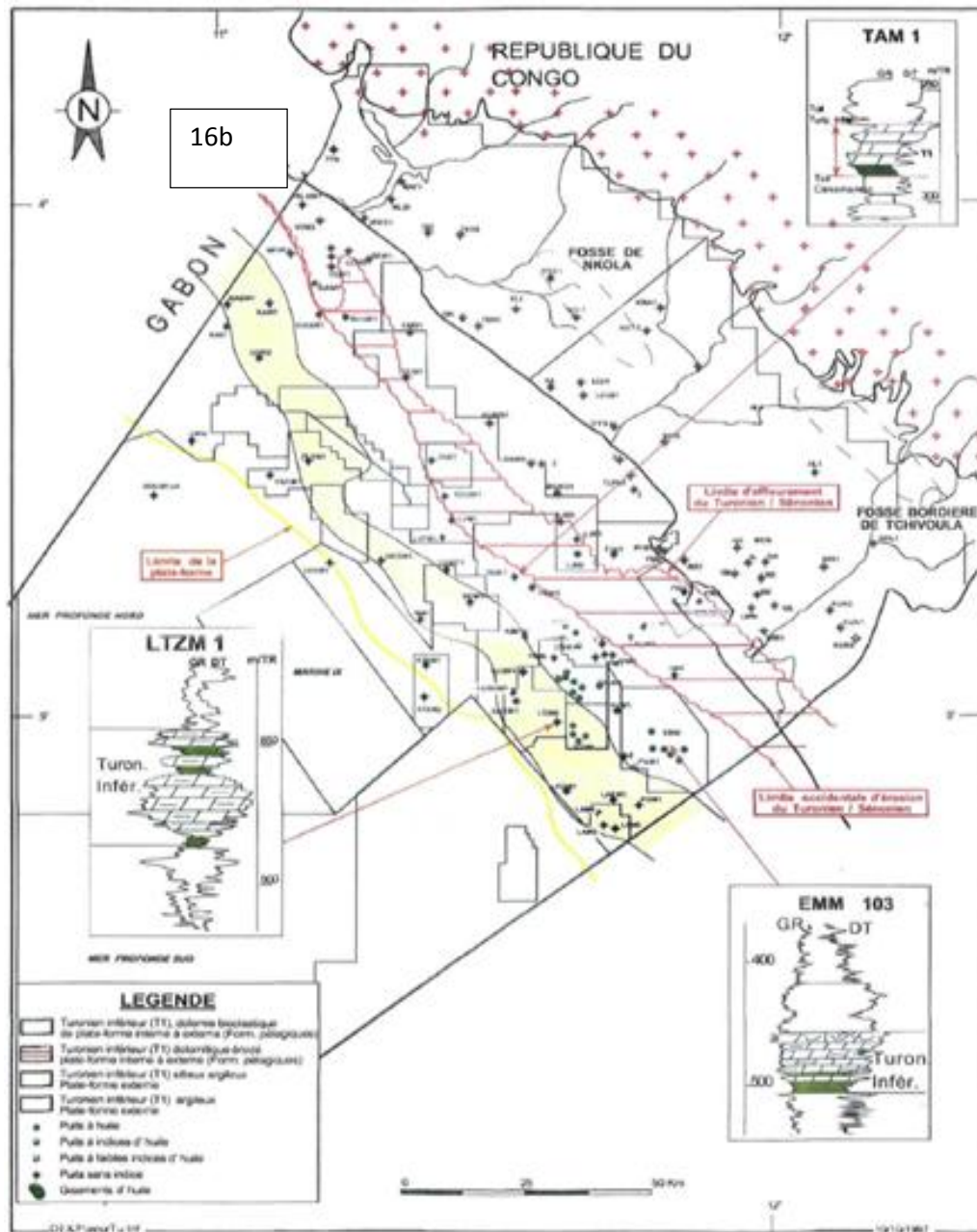


Figure 16a: Upper Cretaceous paleogeographic map and Turonian geographical extension (Massamba, 1985)

Figure 16b: Proposed paleogeographic extension as now proposed.

## 3.2. Facies model

### 3.2.1. Outcrops

Two main outcrops were described and they are from south to north: Djeno (32M 0825261, 9455083) and Mvassa (32M 821122, 9460502) (figure 17).

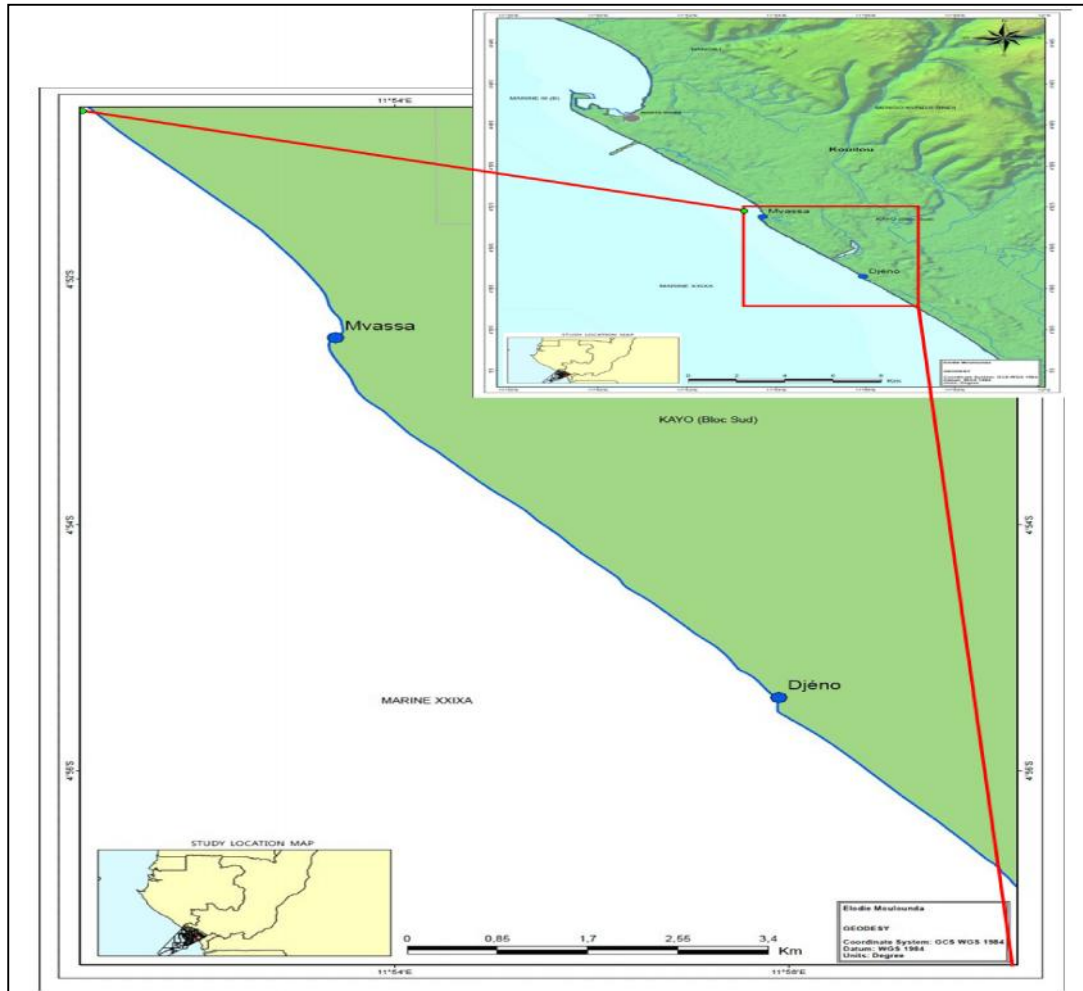


Figure 17: Outcrops locations

Eight facies were encountered during the study of Djeno and Mvassa. Each facies was discussed and interpreted in order to define the environment in which it developed.

#### **Facies 1**

This facies consists of 5 to 15 cm wide and 10 to 20 cm deep burrows filled with bioclasts. The bioclasts within the burrows are found both articulated and disarticulated. The articulated shells are found in life position while the orientation of the disarticulated valves varies. The horizontal and concave-down valves are consistently present in low proportions whereas vertically oriented and concave-up shells are dominant. The horizontal concave-up shells also are important.

The bioclasts are constituted of ammonites *Texanites* (in the lower beds), *Plicatula ferryi*, *Plicatula hirsute* and dominantly (80%) *Trigona arca camerounensis* and *Trigona arca angolensis*. They are embedded in a silty argillaceous calcareous matrix.

Examination under the microscope showed that it consists of very fine, well sorted, angular silty sandstone to sandy silt with an argillaceous matrix and a microcrystalline to microsparry cement. The bioclasts consist of dissolved shells debris showing sparry cement in mould space. Thin sections also show dolomitization of former calcite with formation of hedral dolomite.

### **Discussion**

This facies formed by burrowing and a sediment sorting activity of infaunal organisms such as *Anofia* and *Agelasina plectonota*. This is evidenced by whole bivalve trapped between burrow and wall rock (plate 1, figure 1). The burrows may have been then enlarged by a current prior to the deposition of the shells.

Salazar-Jimenez (1982) showed that orientations of the shells in such burrows result mainly from passive deposition within burrows rather than from active reorientation through bioturbation. When falling or sliding into opened burrows, most of the shells evidently come to rest in vertical or horizontal concave-up positions (Salazar-Jimenez, 1982). However, this facies does not directly indicate the environmental setting in which it developed, but it gives indication of low sedimentation rates time during which the organisms burrowed the sediment. Based on the fossil content, the occurrence of ammonites *Texanites* and the *Plicatulids* indicate deposition in near shore shallow water setting or intertidal zone and they can be found in both marine and brackish water while the occurrence of *Anofia aroreymont* indicates variety of environments and depths. However, coexistence of these genera in the same burrows shows that they deposited in the same environment.

**Hence, this facies containing *Plicatulids* and *Anofia* deposited in near shore shallow water or intertidal zone. Silty argillaceous matrix indicates that the facies deposited in low energy protected setting.**



Plate 1: Figure 1 and 2 - sample showing pod facies (note whole shells trapped between pod and surrounding rocks; figure 3 - pod on outcrop; figure 4 - microscopic view of the facies showing silt size grains in calcareous matrix)

## **Facies 2**

This facies consists of densely packed bioclastic beds made up of more than 70% shells. The accumulation of the shells shows low diversity, highly dominated by epifaunal bivalves: *Plicatula hirsute*, *Plicatula ferryi*, *Plicatula flattersi* and *Lopha lombardi* and in lesser extent semi infaunal bivalves: *Trigonaarca camerounensis* and *Trigonaarca curvadonta*.

The accumulation of shells comprises 60% of articulated shells in life position, 30% of disarticulated concave up shells and 10% of disarticulated convex up shells. The shells are arranged concordantly to the beds. They are embedded in silty argillaceous matrix. The shells are well preserved and without incrustation on their surface. This facies shows no sedimentary structure.

## **Discussion**

The abundance of articulated epifaunal shells in life position advocates that the sediments were buried in situ and thus are autochthonous. They have been transported over a very short distance and thus can be regarded as para-autochthonous.

According to El-Hedeny *et al.* (2001) and Abbott *et al.* (1995), *Plucatulids* belong to warm-water, near shore, low energy environment saltwater. Furisch & Pandey in 1999 in southern India found that dominance of articulated shells in particular epifaunal oyster (*Lopha Lombardi* for this study) in life position indicates low energy conditions probably in connection with a short high energy event interlude during which the fauna was smothered.

Hydrodynamically unstable concave up orientation of the shells (about 30%) indicates rapid movement and burial (Dixon, 2007). Moreover, the low degree of incrustation on the shells surface also testifies about rapid burial. The articulated shells' outnumbering disarticulated concave upward shells shows a reworking by a single event probably. However, silty argillaceous matrix shows a deposition in a low energy protected environment.

**Considering the organisms near shore habitat, considering matrix size, this facies deposited in a protected low energy environment such as bay in which an exceptional single event such as flood, storm or tide may have reworked and dismembered 30% of the bioclasts.**



Figure 18: Bed of densely packed epifaunal bivalves



### **Facies 3**

It consists of grey, densely packed bioclastic grainstone to bioclastic sandstone made up of single valve shells.

The bioclasts are constituted of 60% *Trigona* *camerounensis* and *Trigona* *angolensis*, 30% *Plicatulids* and 10% *Lopha* *lombardi* embedded in dolomitic silty to very fine sandy matrix. Bioclasts present a red stained surface (probably resulting from the alteration of pyrite). Shells are oriented horizontally with 75% concave up, 20% concave down and 5% articulated. Sedimentary structures are mainly large through cross beds and recognizable ichnofabrics consist only of *Thalassinoides*. At the base of bed 26 of Mvassa, the bioclasts are heavily incrustated. This facies shows an erosive base.

Microscopic analysis of the facies revealed that it consists of well sorted, very fine grained angular quartz with microcrystalline to microsparry cement. Bioclasts consist of moulds of dissolved bivalves. This facies presents sparry cement developed in mould space and shows replacement of calcite by dolomite.

### **Discussion**

Vertebrates encountered in this facies indicate near shore shallow water. The Dense skeletal packing, the high degree of shells dismembering and the concave up orientation of the shells are consistent with development in high energy setting. Hence, this facies was deposited in near shore shallow marine environment as based on organism's biota.

**The Facies association with facies 6 and facies 7 shows that this facies may have developed deposited in shallow ramp or represents shoreline shelly ridge (chenier).**

UNIVERSITY of the  
WESTERN CAPE

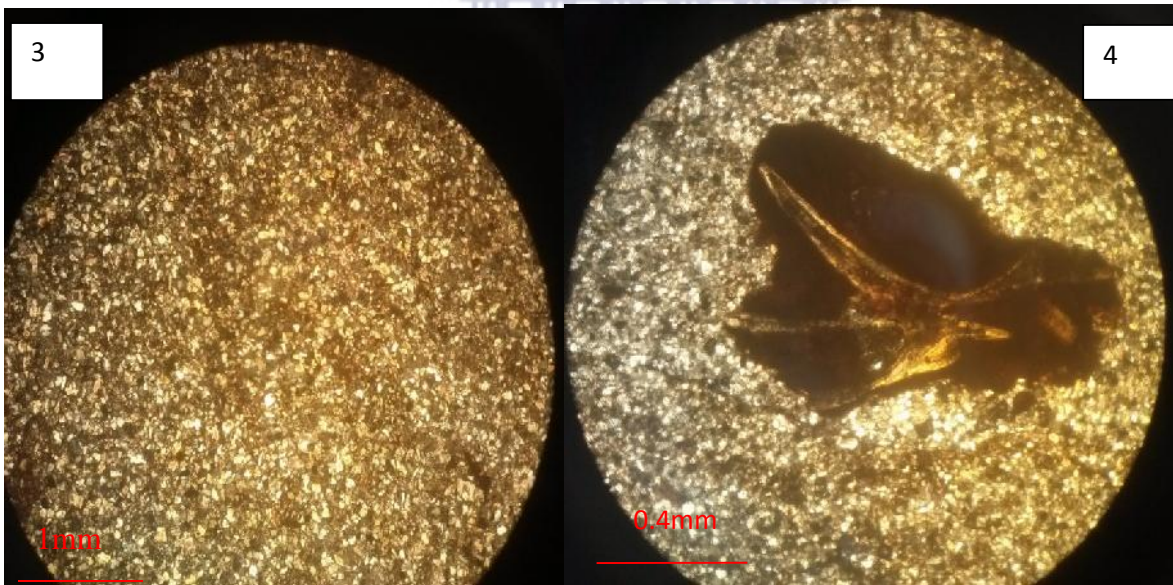


Plate 2: Figure1: bioclastic sandy facies with scoured base (note scored base), figure2: note upward grading of shells size from samples, figure3-4:thin section of the facies.

#### **Facies 4**

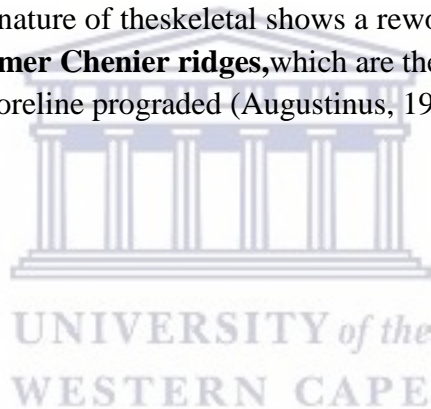
It consists of brown, densely packed bioclastic packstone to grainstone with a silty matrix. The bioclasts consist of calcite recrystallized fragments and concave up single valves of *Trigonids* (*Trigonarca angolensis*, *Trigonarca camerounensis*). The facies shows an erosive base and it is structureless.

Under the microscope, this facies shows a silty matrix and sparryequant cement. It also presents a moldic porosity.

#### **Discussion**

Packstone to grainstone texture of this facies indicates sediment deposition in high energy setting (James *et al.*, 1992). This suggests that this facies represents a high-energy, shallow platform environment, above or close to the fair-weather wave base. Wright (1986) and Tucker & Wright (1990) interpreted shoreline grainstone as characteristic of shallow ramp setting. They explained that the inner part of the shallow ramp is characterized by high-energy shoreline grainstones because of unimpeded wave travel across the shallower portions of the ramp.

The single valves concave up nature of the skeletal shows a reworking in high energy setting. **Hence, this facies may represent former Chenier ridges**, which are the relicts of former shelly beaches that have been left inland as the shoreline prograded (Augustinus, 1989).





0.4mm



1mm

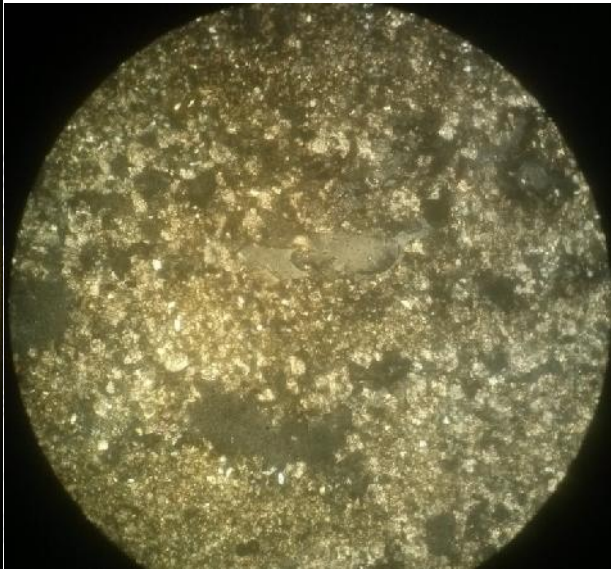
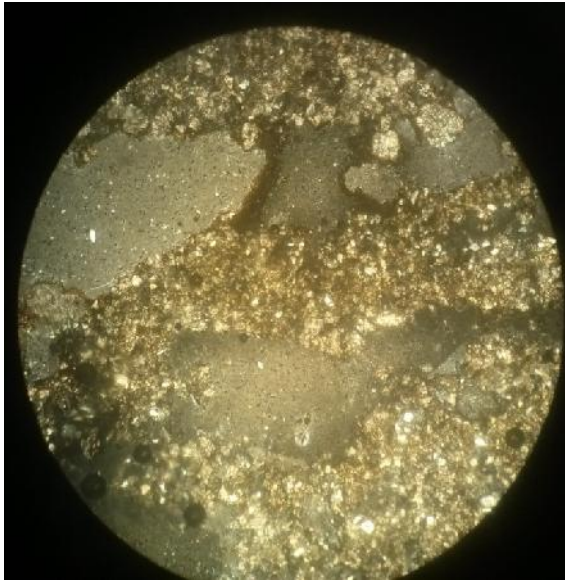


Plate 3: Figure 1:note trough cross bedding within the facies, figure 2: sample, figures 3- 4: sparry cement and moldic porosity (note silt within the matrix)

## Facies 5

It consists of grey to greenish, bioclastic packstone. The bioclastic dominant constituents are valves of predominantly semi infaunal *Trigonalca camerounensis* and *Trigonalca angolensis* representing 80% of the bioclasts, together with *Plicatula flatteri*, *Plicatula ferryi* and rare *Lopha lombardi* consisting the remaining 20% of the bioclasts. The bioclasts are embedded in a calcareous silty matrix. This facies shows an erosive base. The primary sedimentary structures were destroyed by bioturbation and the recognizable ichnofabrics include *Thalassinoides*, *Paleophycus*, *Rhizocorallium irregular* and *Teichichnus*(plate 4).

The matrix under microscope revealed that it consists of well sorted, sandy silt to very fine grained, angular quartz, cemented by micro-sparry cement. The bioclasts consist of dissolved bivalves showing a micrite envelop around. Some moulds are filled with microsparry to sparry cement which also shows replacement of calcite by hedral dolomite.

This facies is found in association with massive claystone on which it lies erosively.

## Discussion

The lack of bivalves in life position and the predominance of single valves indicate that the sediments are allochthonous or para-autochthonous. Abbott (1995) showed that *Trigonalca* belonging to *Trigonid* genus in turn belonging to *Glycimeridadae* family lives chiefly in warm moderately shallow to shallow water. The dominance of concave up semi infaunal shells indicates that the water was sufficiently agitated to overturn the shells.

The occurrence of feeding traces such as *Teichichnus*, *Rhizocorallium*, *Scallichnus* and dwelling traces such as *Arenicolites* and *Paleophycus*, shows that the environment served as feeding and dwelling habitat for the organisms. The dominance of horizontal structures produced by mobile fauna reflects the accumulation of detritus in sediment under moderate to low energy conditions (Bromley, 1996; Buatois & Mangano, 2004a). Buatois & Mangano (2011) in the study of ichnofacies showed that thin tempestites layers may occur in storm affected bay or subtidal setting. The authors showed that sandy tempestites bear low diversity *Rhizocorallium*, *Paleophycus*, *Planotites*. MacEachern & Gingas (2007) stated that *Glossinifungites* ichnofacies (*Rhizocorallium*, *Paleophycus*, *Arenicolites* and *planotites*) are commonly associated with autigenic firmgrounds due to local erosion.

The facies association formed by claystone facies and the above described facies was interpreted as characterizing distal bay setting (Buatois & Mangano, 2011; figure 19). **Hence, this facies deposited in distal bay setting.**

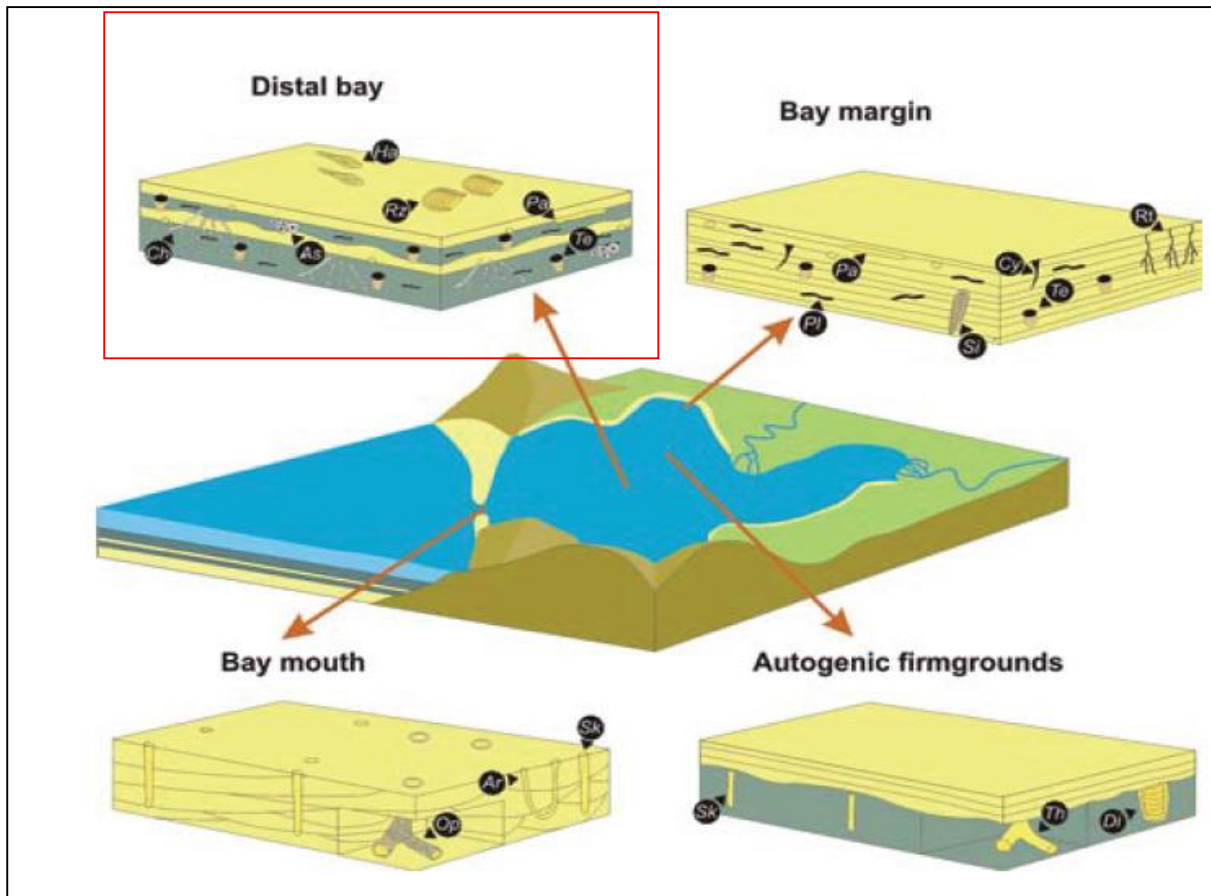


Figure 19: Bay facies (modified from Mangano & Buatois, 2011) (*Rhizocarallium*: Rz, *Teichichnus*: Te, *Paleophycus*: Pa)

UNIVERSITY of the  
WESTERN CAPE

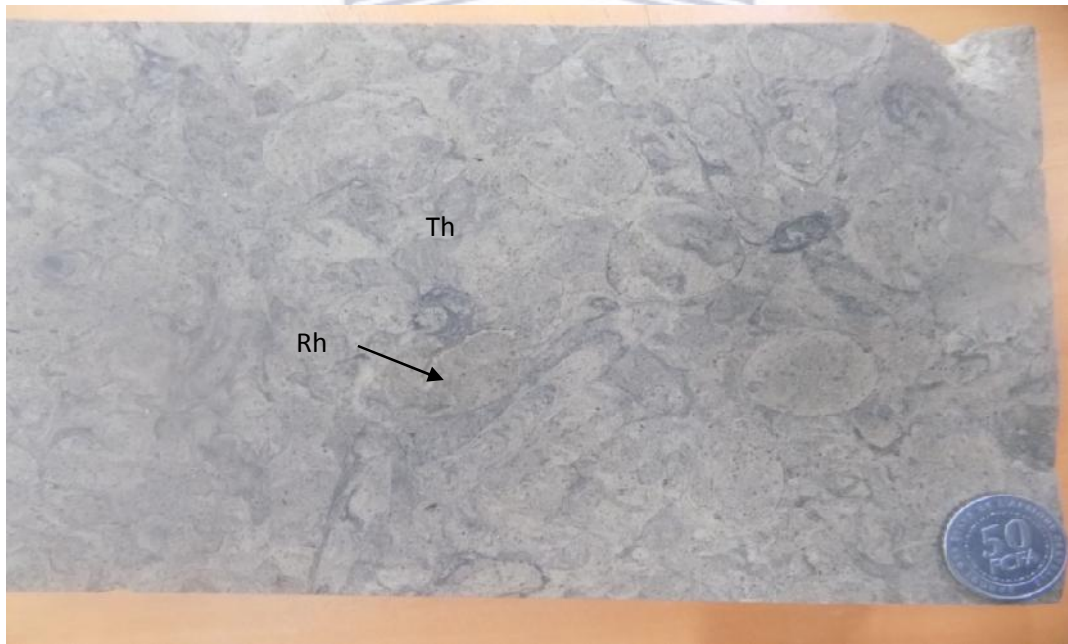


Plate 4: Te: *Teichichnus*, Ar: *Arenicolites*, Th: *Thalassinoides*, Pa: *Paleophycus*, Rh: *Rhynchonellium*, Sc: *Scolicia*

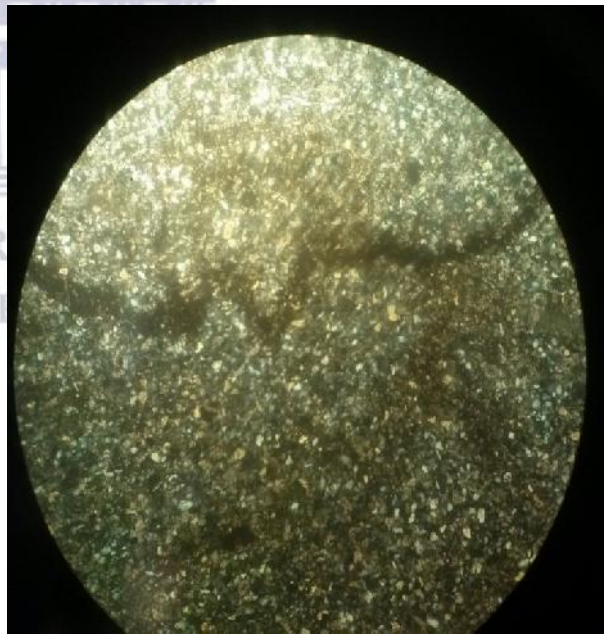
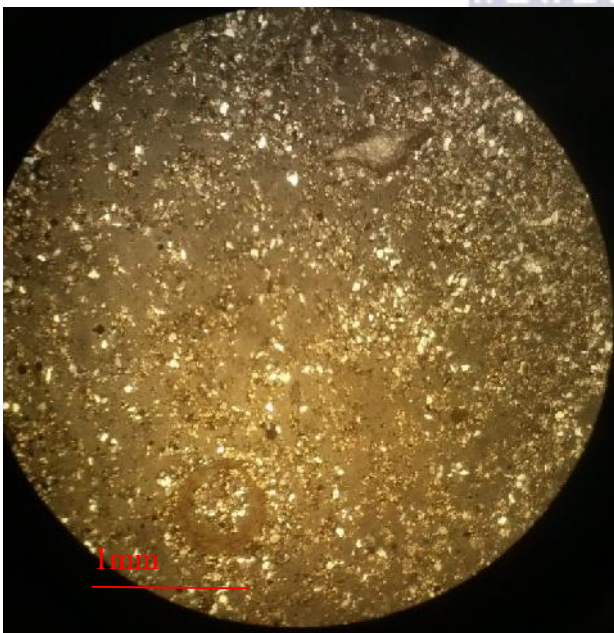
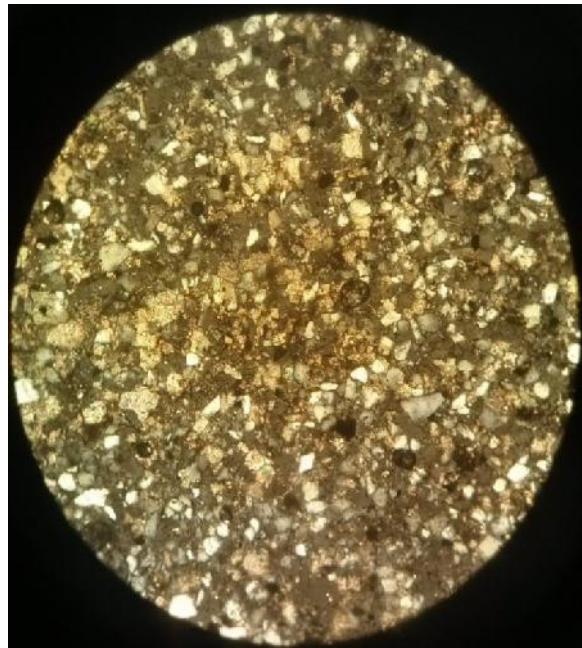
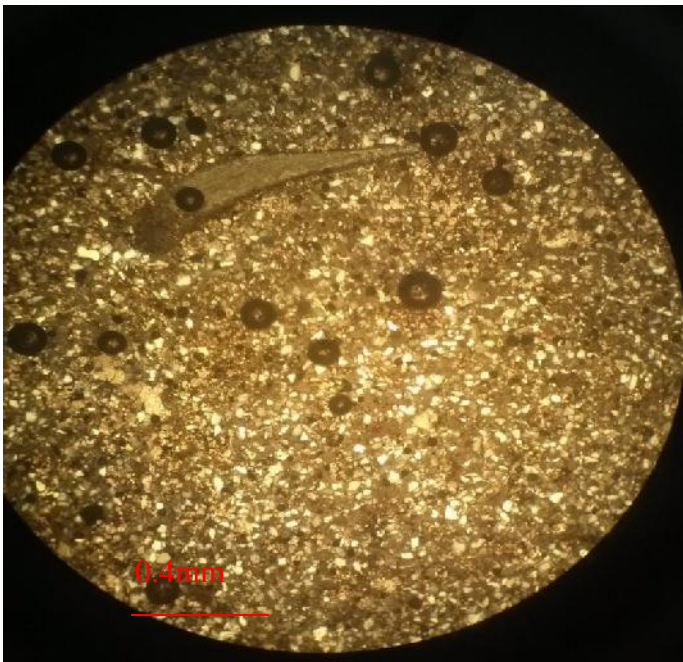


Plate 5: 1, 3, 4 bioclastic calcareous very fine to silty sandstone, 2 note replacement of calcite by dolomite

## **Facies 6**

It consists of grey, well sorted, massive, slightly silty claystone. This facies show low to no shells content. The rare skeletal found in this facies are found articulated and in life position. The facies shows a non-erosive base.

It is found in association either with facies 8 (*Ophiomorpha* dominated facies) or facies 5 both lying erosively on the claystone facies.

## **Discussion**

The above features show that the facies developed in low oxygen, low energy setting. Claystone (mud) indicates deposition by mud settling from suspension (Reineck & Singh, 1980). **The association with both facies 5 and facies 8 respectively deposited in distal bay and mouth bay shows that this facies deposited in distal bay setting.**



## **Facies 7**

This facies consists of loosely packed and poorly sorted bivalves. It presents cluster of bivalves locally, nesting and vertical stacks of concave up disarticulated valves of *Anofia aro* Reymont, *Trigonids*, rare *Lopha lombardi* and *Plicatulids*. The deposit shows single valves and slightly disturbed shells in life position.

The matrix consists of calcareous silty claystone (marly matrix). The facies shows a scoured base in which nested clusters of shells are found.

The analysis of thin section revealed that it consists of silt to very fine grained quartz in argillaceous matrix with calcareous cement. The matrix shows micrite to microcrystalline cement.

## **Discussion**

Nesting in various direction and concave up orientation of valves indicate the presence of a turbulent flow and a suspension settling (Middleton, 1967; Futterer, 1982). The occurrence of whole shells in life position indicates a catastrophic mortality model. Johnson (1957), Aigner & Futterer (1978), Aigner (1982) showed that the mechanism is related to a combination of cluster of life habitat of shells and storm induced sea floor scouring or submarine erosion and subsequent filling (depositional hiatus).

This facies is interpreted as resulting from a simple-event mechanical reworking and a rapid in-situ burial. Filling of storm generated scouring depression may have been responsible for the formation of this facies in an environment with low energy background conditions (Tomasovych, 2004). Hence, this facies developed by erosion by fair-weather or storm generated waves which resulted in exhumation and redeposition of pre-fossilized vertebrate skeletal elements in upper offshore or distal bay.

**This facies developed by wave generated by periodical storms in a generally low energy environment, this is consistent with a deposition in transition offshore or upper offshore.**

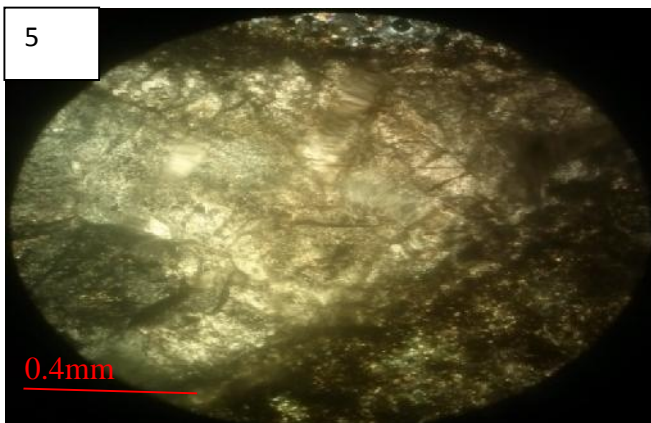
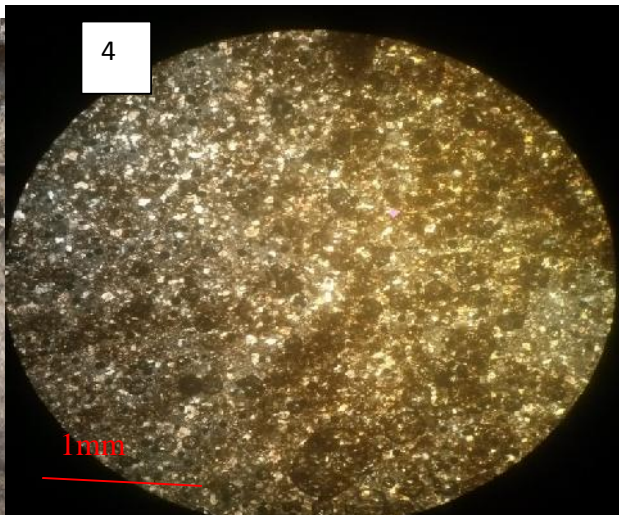


Plate 6: Figures 1-3: nested facies on outcrop (note scours at the base of the nests), Figure4: microscopic view displaying silt in argillaceous matrix and figure 5: note sparry cement.

## Facies 8

It consists of brown (by alteration but grey in other beds), moderately to highly bioturbated bioclastic packstone facies. It shows packed bioclasts dominated by disarticulated concave up valves. They are mainly *Trigonarca camerounensis* and *Trigonarca angolensis*; very rare *Lopha*, *Plicatula* and fishbone debris are shown by this facies.

The bioclasts are embedded in silty to very fine sandy calcareous matrix. The primary sedimentary structures have been perturbed by bioturbation and only ghost of low angle horizontal laminations are visible in certain beds. The principal ichnofabric found is *Ophiomorpha* (plate 7, figure 1 and 2).

Under the microscope it shows very fine, well sorted angular quartz grains, in microcrystalline to microsparry cement. Skeletal consists of shells debris with some showing micrite coating around. Skeletal are either dissolved or filled by secondary microsparry to sparry cement showing replacement of calcite by dolomite rhombs. This facies is characterized by intercrystalline and moldic porosity.

The facies is interbedded with massive argillaceous beds together forming decimetric alternances.

## Discussion

*Trigonarca* genera observed in this facies belong to *Trigonid* subfamily which in turn belongs to family of *Glycimerididae*. Abbott (1995) showed that this family lives chiefly in warm moderately shallow to shallow water.

The large number of concave up valves as compared to those concave down indicates that the bioclasts accumulated either in quiet environment where predators, scavengers, and sediment-reworking animals, in conjunction with the life and death histories of given molluscs, are among the principal agents affecting shell orientation (Emery, 1968; Clifton, 1971 and Frey, 1972) or through turbidity currents. The latter is coherent with remains of primary sedimentary structures which are low angle planar cross beds defined by Reineck and Singh (1980) as characterizing high energy setting.

Bromley (1990, 1996); Buatois & Mangano (2001, 2011) indicated that monospecific suites of *Ophiomorpha* indicate high energy shoreline or post event suites in tempestites and turbites. *Ophiomorpha* are typical elements reflecting abundant organic particles kept in suspension by energetic wave forced current. Mangano & Buatois (2011) showed that bay mouth deposits tend to contain ichnotaxa indicative of relatively high energy conditions. **Hence, facies with *Ophiomorpha* represents development in bay mouth setting.**

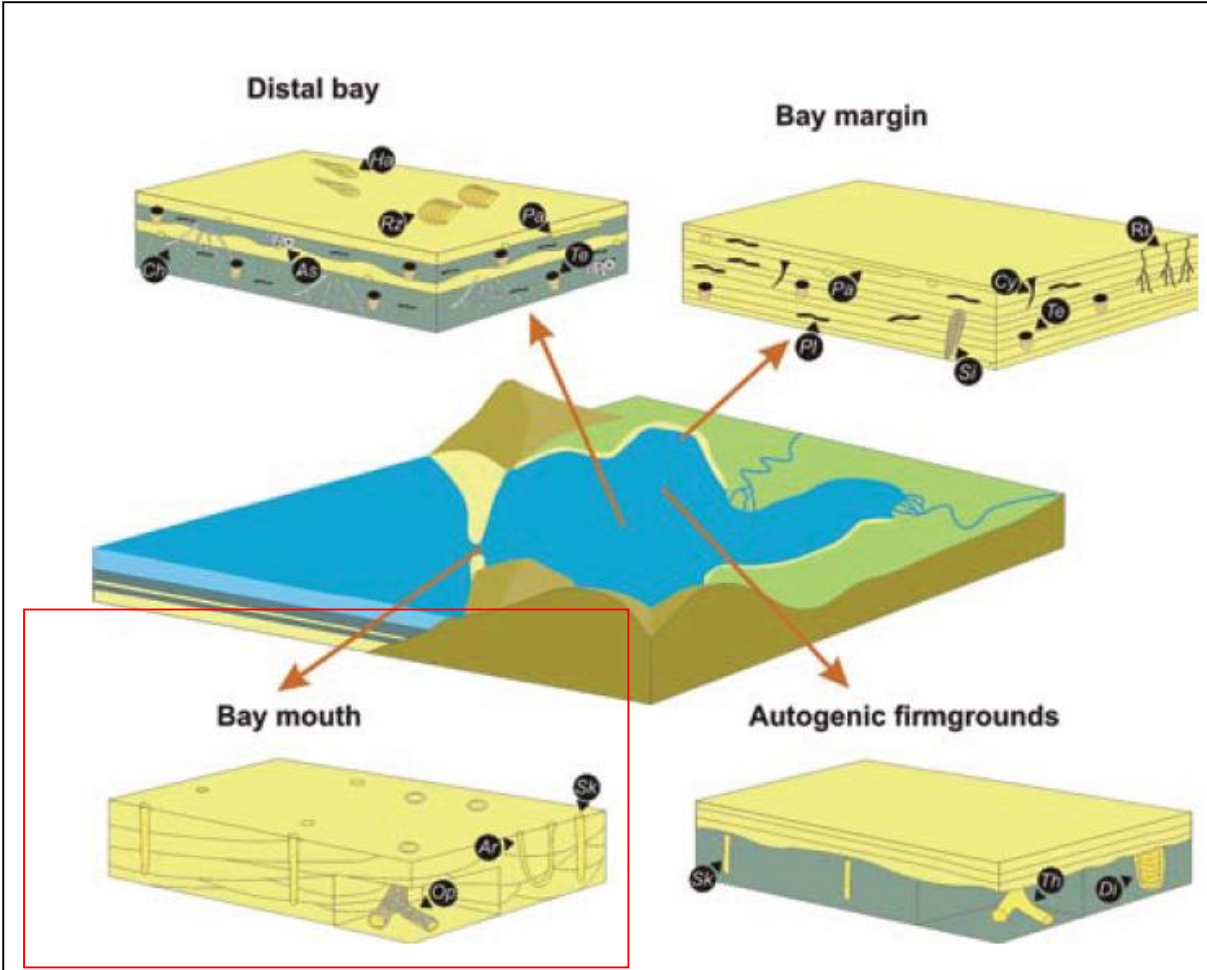


Figure 20: Bay facies (modified from Mangano & Buatois, 2011)

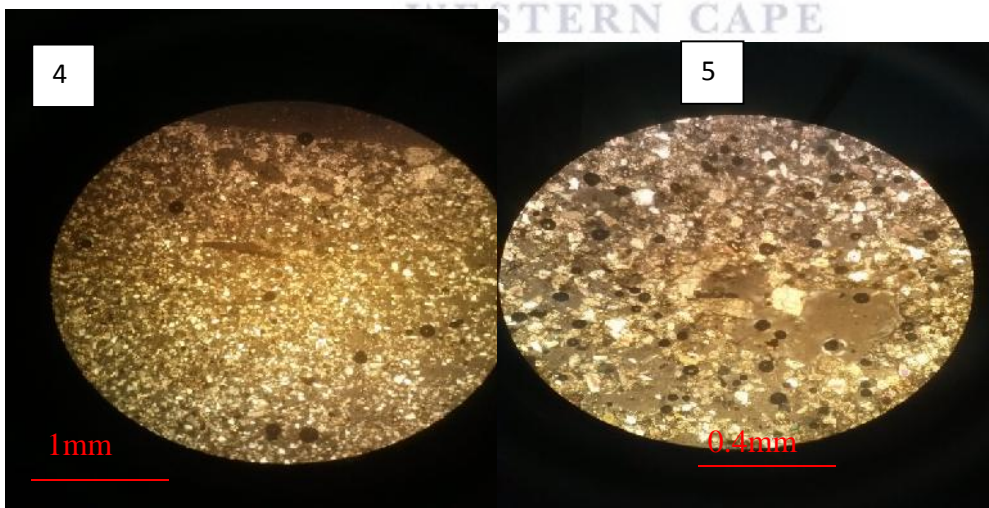
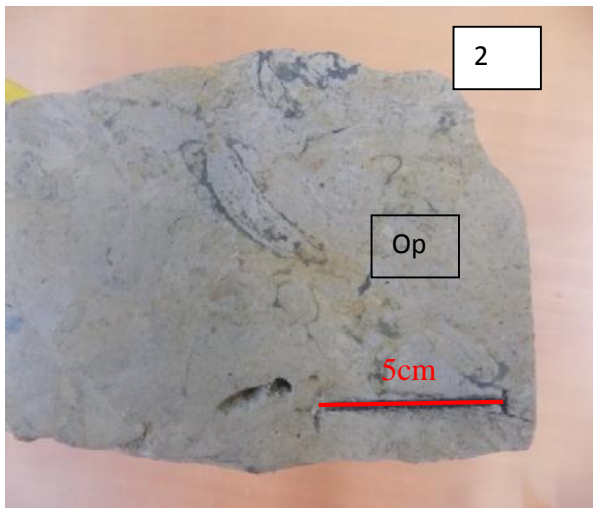


Plate7: Figures 1-3: very fine bioclastic calcareous sandstone, Figures4-5: formation of secondary dolomite in moldic space.



BEd	Facies	Lithology	Limestone						
			Mudst	Wackest	Packest	Grainst			
			Shale	silt	Vf	f	Coarse	V coarse	Granule

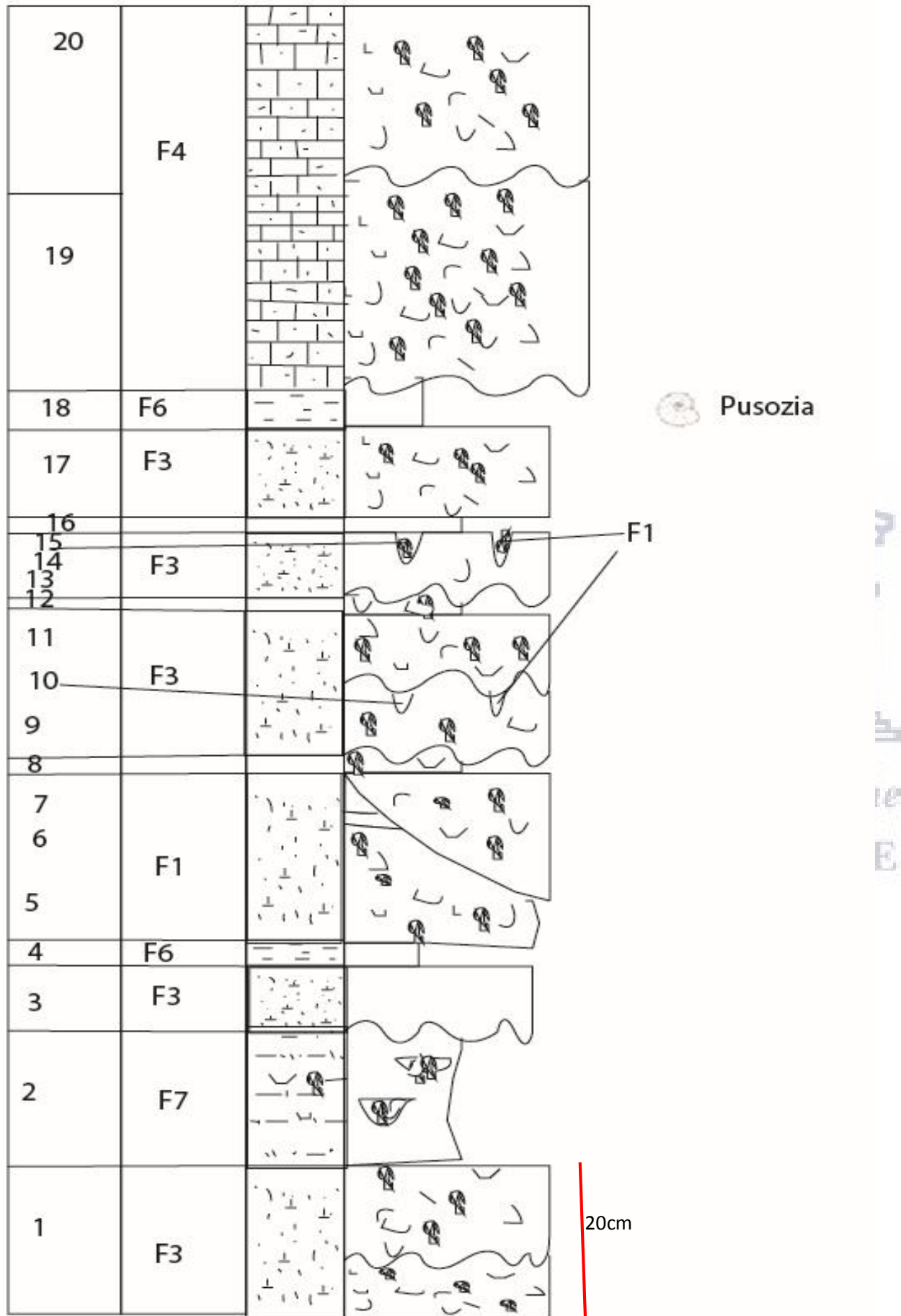


Figure 22: Djeno sedimentological log

### 3.2.2. Wells

Two wells were chosen to serve as reference wells for this study. This choice was based on cores availability, well defined biostratigraphy and moreover their locations which allowed the definition of transect illustrating the facies lateral variation in dip and strike.

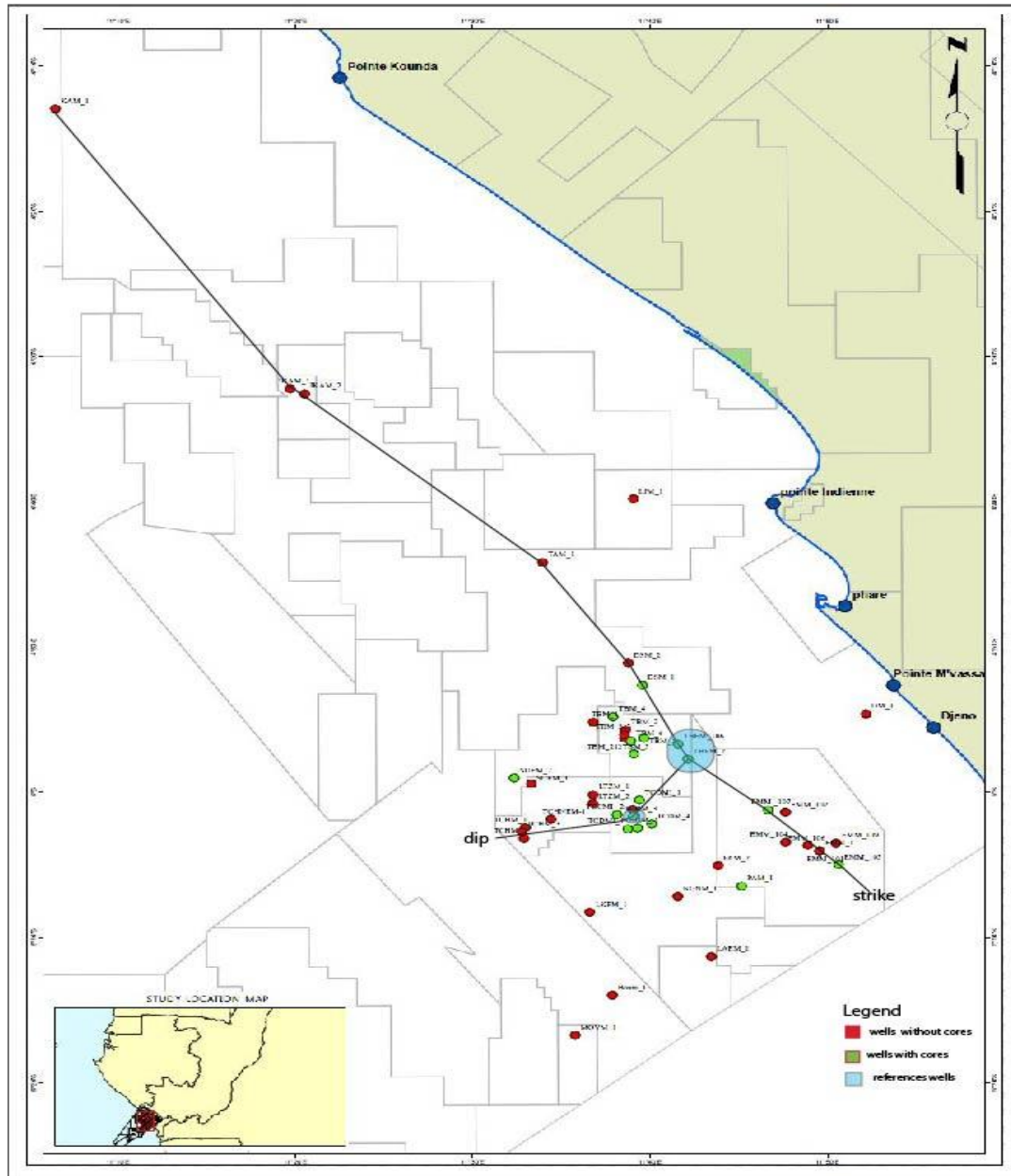


Figure 23: Locations of reference wells.

Twelve facies have been encountered during cores description; these facies have been described and then each facies has been analysed and interpreted in order to determine the paleo-environment in which it developed.

### **Facies 9:**

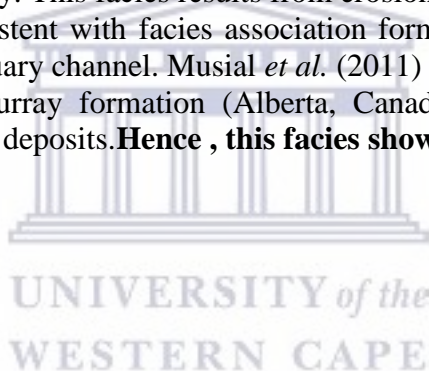
This facies consists of poorly sorted, matrix supported conglomerate. It displays upward fining of grain from coarse to medium grains and matrix with large mud clasts without a specific orientation. This facies also shows some bioclasts. This conglomerate displays slightly erosive to sharp base.

The facies has been found in association with planar cross bedded sandstone facies (facies 10). Facies analysis under the microscope showed that it consists of sub-rounded to sub-angular quartz grains cemented by dolomitic micro-sparry to sparry equant cement. The cement shows rare (low) crystallization of dolomite rhombohedra between quartz grains. The facies also displays bioclasts (bivalves' shells) and intergranular porosity.

This facies shows a porosity of 22% and a permeability of 1024mD

### **Discussion**

The angular shape of the grains in this facies shows a short distant transport while the upward fining shape of the grains indicates decrease of current strength. The abundance of mud clast in this facies is consistent with clay flocculation due to change in salinity in estuary environment. Moreover the presence of shell in this facies advocates for proximity to shells source such as beach bar or bay. This facies results from erosion of point bar during fluvial or flooding period. This is consistent with facies association formed with planar cross bedded facies which characterizes estuary channel. Musial *et al.* (2011) in the study of subsurface and outcrop of Cretaceous McMurray formation (Alberta, Canada) interpreted this facies as characterizing bottom channel deposits. **Hence , this facies shows deposition in point bar.**



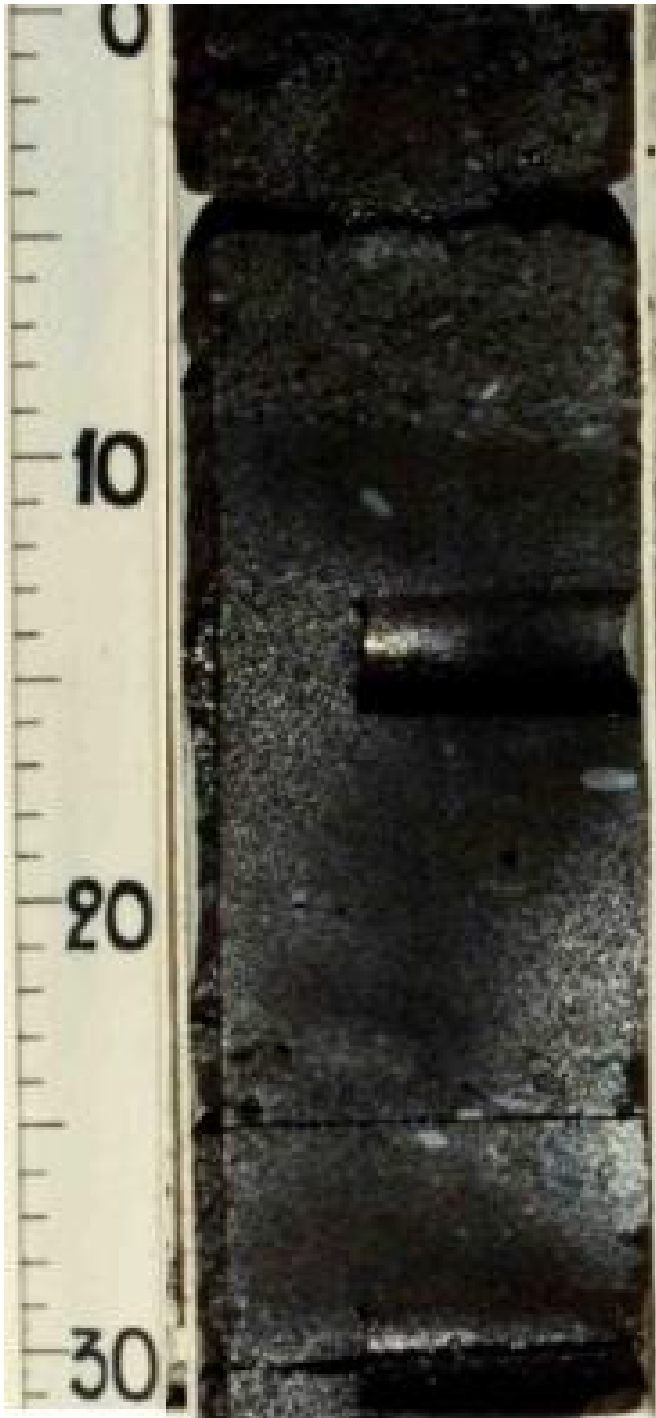


Figure 24: Debris flow facies

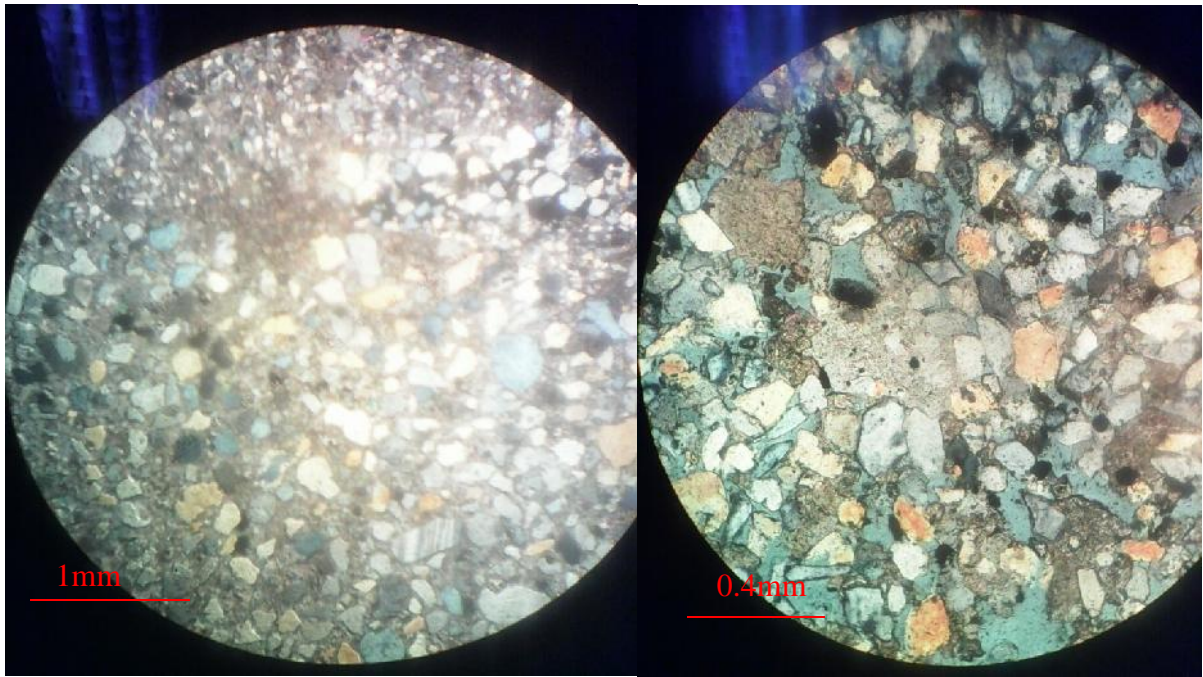


Figure 25: a. Sandstone with both anhedral; b. euhedral dolomitic cement (note both cements in right pictures)

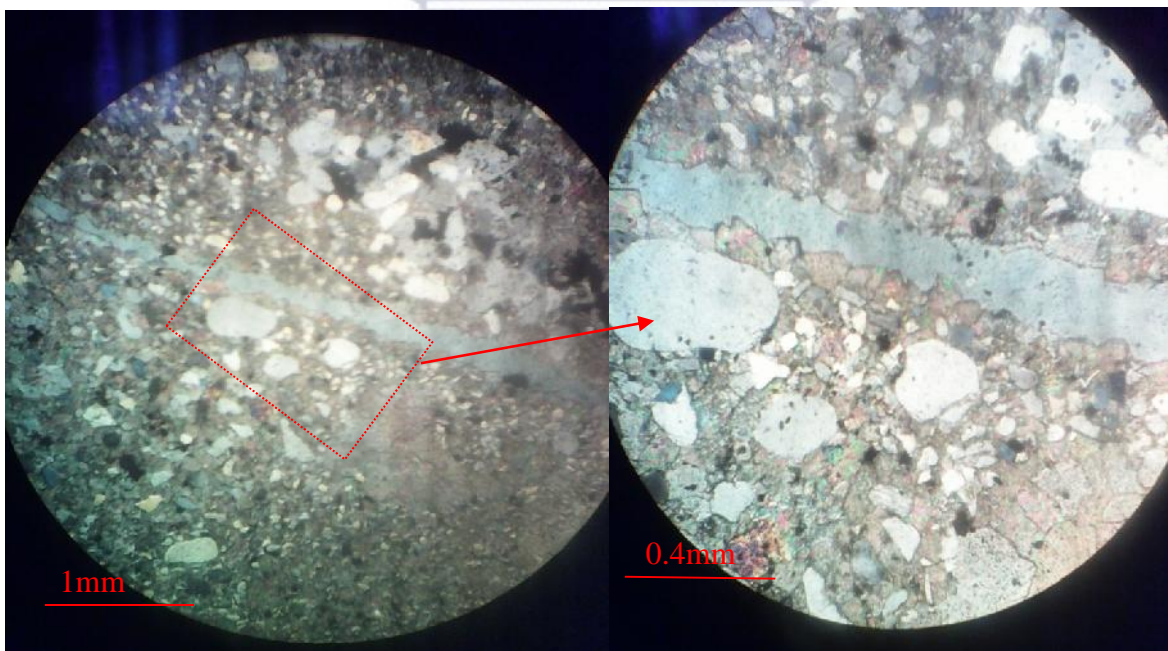


Figure 26: Sandstone with dolomitic sparry equant cement (anhedral dolomitic cement), note formation of dolomitic cement prior to formation of calcite.

## **Facies 10**

It consists of grey to brown (due to impregnation of oil), poorly sorted, upward fining from medium to very fine grained sandstone. It displays a slightly erosive to sharp base with argillaceous and sandstone clasts. It shows planar cross laminations grading upward to horizontal laminations and vertical burrows at the top (figure 27). This facies also shows scattered bioclasts and plant debris.

The observation under microscope shows: sub rounded to sub angular quartz grain, with dolomitic micro-sparry to sparry equant cement, showing rare (low) crystallization of dolomite rhombohedra. The facies also displays bioclasts (bivalve's shells) and intergranular porosity.

This facies is highly impregnated and petrophysical measurements on core from well TBEM2 show a porosity of 27% and a permeability of 1113mD.

## **Discussion and interpretation**

Upward fining sequence and erosive base with clasts show occurrence of decelerating unidirectional current flow with decrease of sediment laden (Reineck & Singh, 1973). Fining upward sequence as above described with erosive base, planar cross lamination and horizontal lamination indicates lateral migration (lateral accretion) of a point bar (Nichols, 2009; James & Dalrymple, 2010), this is strengthened by presence of plant debris which indicates continental influence.

**Hence, this facies indicates channel or distributaries channel.**

UNIVERSITY of the  
WESTERN CAPE

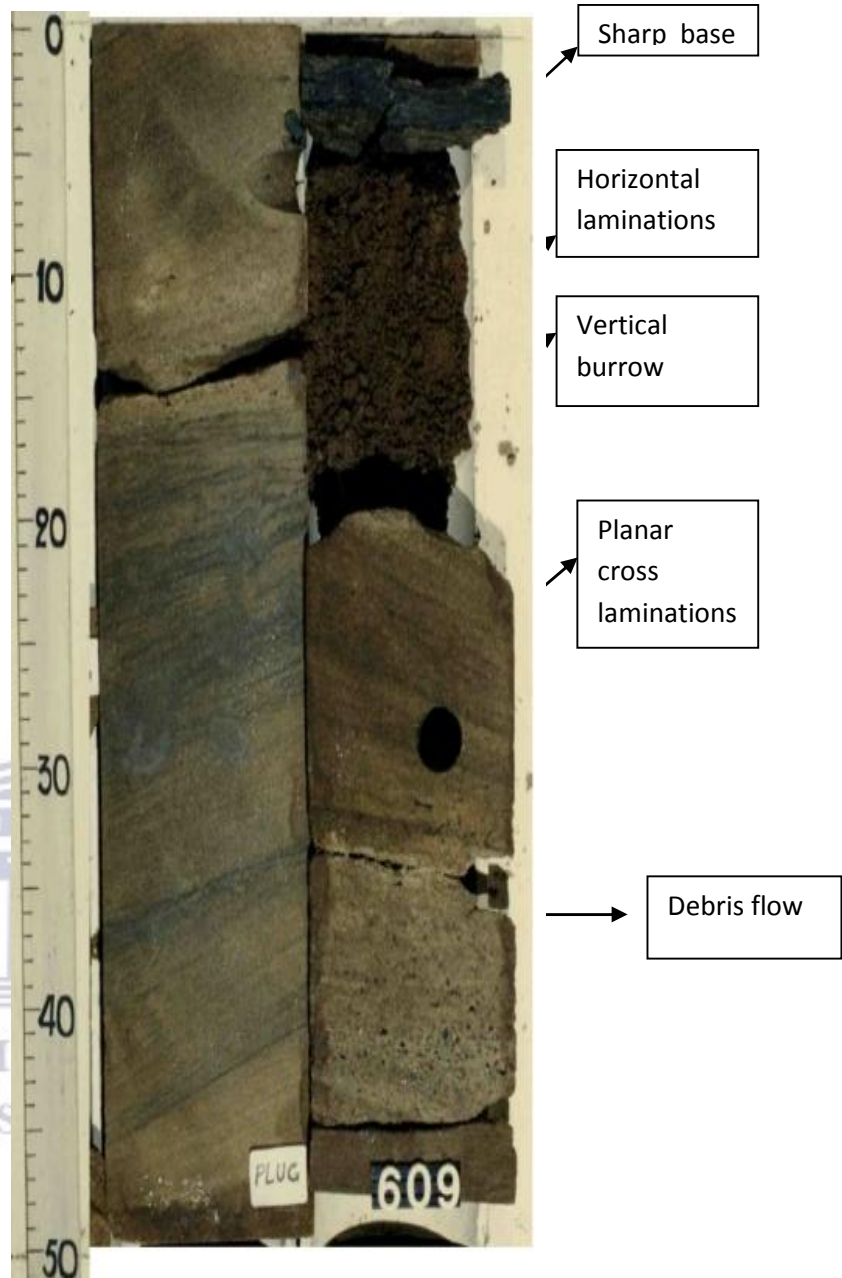


Figure 27: Planar cross bedded facies

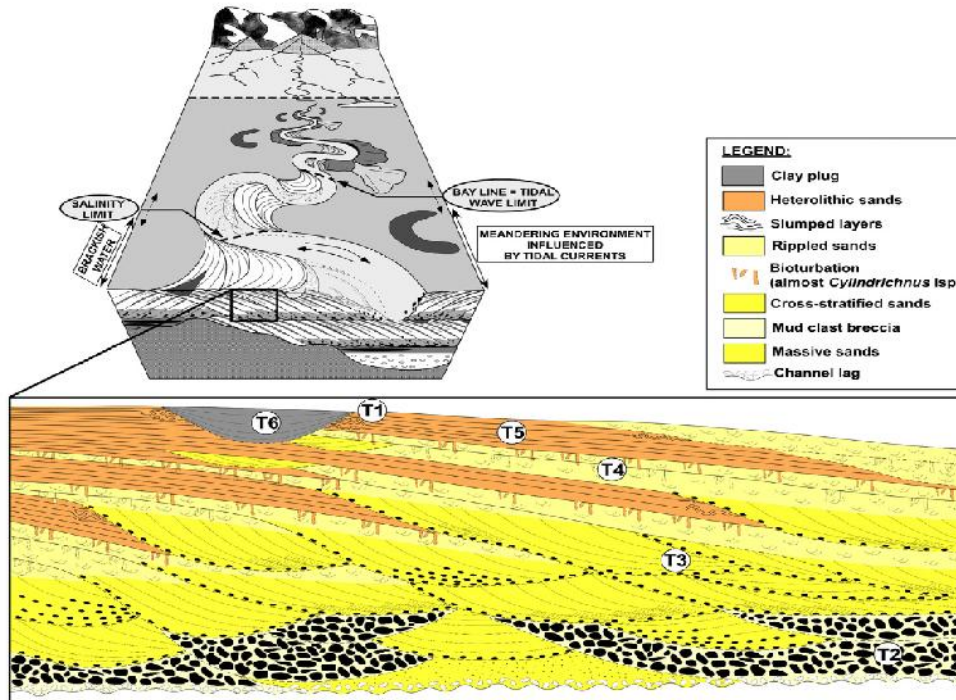


Fig. 10. Internal architecture of a tidally influenced point bar in the McMurray Formation. Six main facies are described from top to bottom: (T1) deformed and slumped layers; (T2) mud clast breccia; (T3) cross-stratified sands; (T4) low heterolithic and highly rippled sands; (T5) highly heterolithic sand; and (T6) thick clay layers.

Figure 28: Internal architecture of tidally influenced point bar, McMurray formation (Musial et al., 2011).

**Facies 11**

This facies consists of grey greenish, cylindrical, bioturbated, dolomitic argillaceous siltstone to argillaceous silty dolomite, with argillaceous matrix. It displays centimetric vacuoles; some are empty while others are filled with silt and with pyrite aureole. This facies shows trace of roots (clearly identified in well TBEM-106 at between 583 and 583.70m).

Microscopic analysis of the thin section showed that the facies consists of silt with argillaceous matrix and dolo- microsparry cement, vacuolar porosity and some roots. It shows replacement of original calcite by hedral dolomite rhombohedra. Vacuoles display pyrite aureole and are constituted of quartz (sandy silt sized), slightly argillaceous matrix. It also shows intercrystal porosity and roots' remnants.

This facies shows no oil staining; petrophysical measurement on well TBEM-2 revealed porosity from 19 up to 22% and permeability of 5 to 6 mD.

**Discussion:**

The characteristic of the above facies are consistent with development of soil in semiarid to humid climate. The occurrence of roots in this facies strengthens this. Reineck & Singh (1980) indicated that in such climate the presence of organic matter makes acidic condition, leaching and migration of various ions downward; this resulted in the formation of soil pyrite.

Leaching may have been responsible for formation of vacuoles observed in this facies. Moore (1989) explained formation of the nodules in process of caliche zone or vadose soil which also involves intense dissolution of original sediments and rapid precipitation, often driven by organic activity. Purvis & Wright (1991), Wright (1991) indicated replacement of original textures by fabrics such as nodules, concretions around the roots, crystal (microspar). This process clearly explains formation of the above facies fabrics.

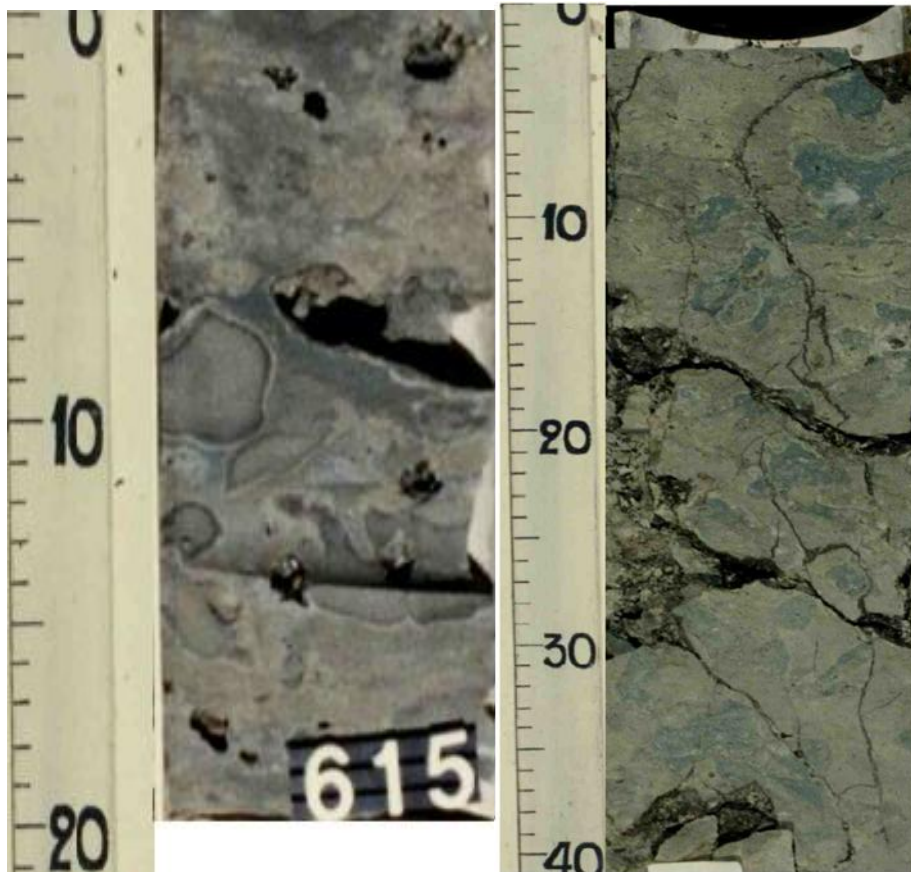


Figure 29: Soil facies (TBEM 2 from 614, 80 – 615m)

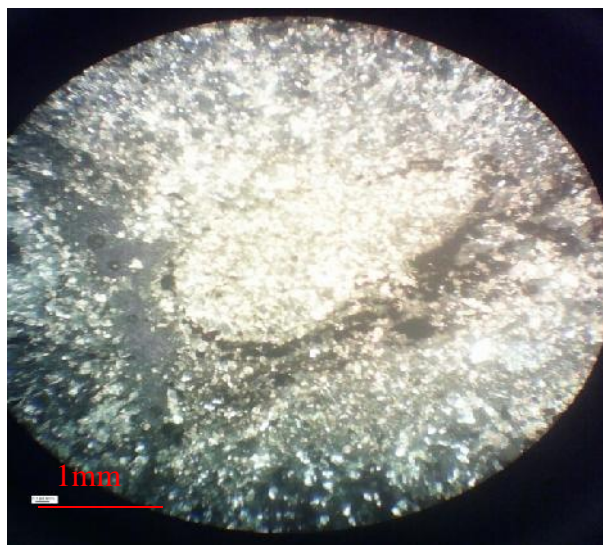


Figure 30: TBEM-106 at 606.85m)

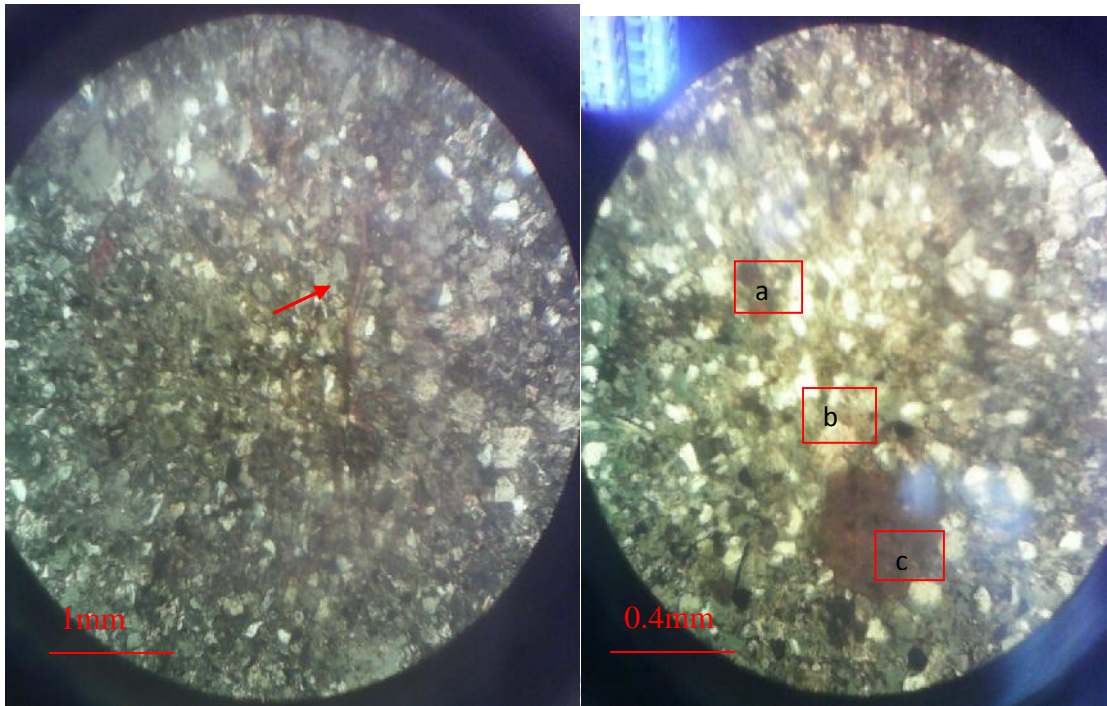


Figure 31: Note roots, vacuolar porosity (left picture, TBem2 at 621.45m), and intercrystal porosity and root remnant in filled vacuole or clast (right picture TBEM2 at 614.94)

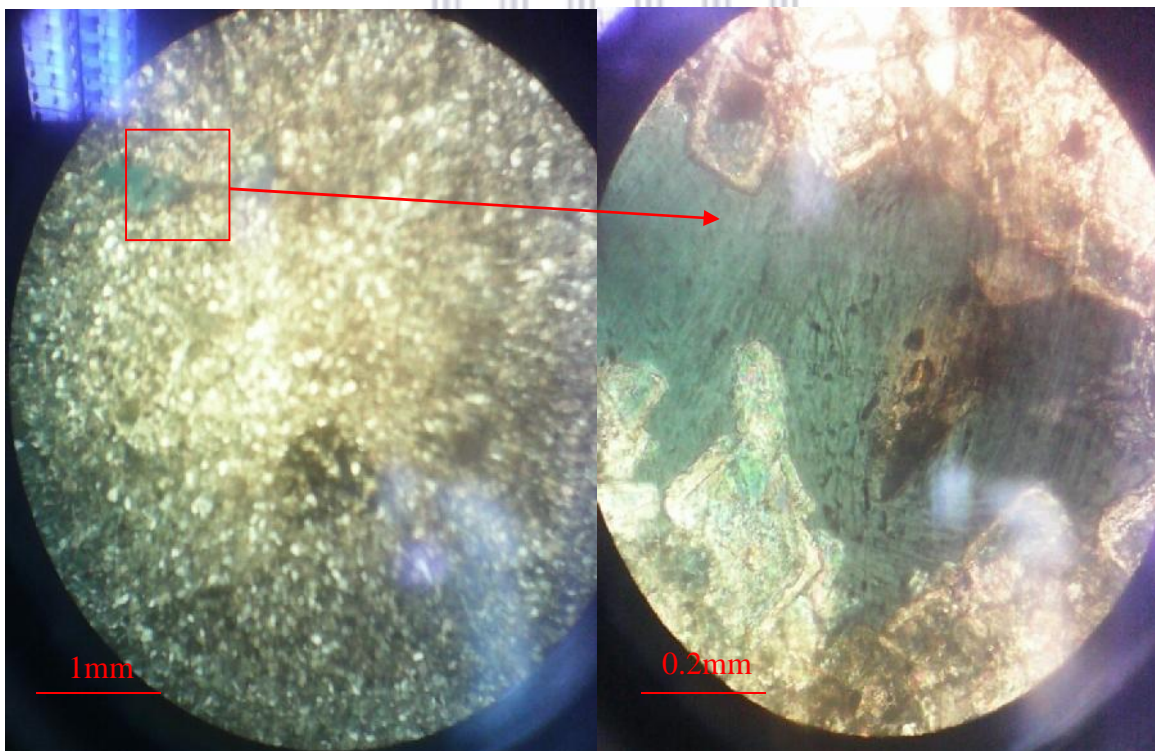


Figure 32: Hedral dolomite recrystallization from original calcite (TBEM2 at 621.77m)

## **Facies 12**

This facies consists of grey greenish, cylindrical, bioturbated, dolomitic argillaceous siltstone with argillaceous matrix. It is structureless (massive) and shows rare dissolved bioclasts, pyrite nodules and flame structure at the base. Some chondrites ichnofacies can be recognized at certain depths where it appears to be thinly laminated and with some plant debris.

The analysis under the microscope showed that this facies is made of quartz (silt sized) in argillaceous matrix enriched in organic matter. It contains rare dissolved bioclasts (bivalves' moulds) bound by dolo -microsparry cement. This facies shows no intergranular porosity and negligible vacuolar porosity. It can be seen from thin that dolomite formed by replacement of pre-existing calcite.

No oil impregnation occurs in this facies. Petrophysical properties measured show a porosity between 7 and 22% and permeability from 0.14 to 1.3mD.

## **Discussion**

The laminated claystone indicates the fall out of fine grained in low energy environment. The presence of plants debris suggests vicinity of the continent while the presence of pyrite nodule indicates the richness in organic matter. The presence of impoverished traces fossils assemblage indicates harsh conditions such as brackish water environment. **This facies have been interpreted as having deposited in restricted bay setting. Restricted bay setting is also supported by presence of chondrites which have been interpreted by Mangano & Buatois (2011) as corresponding to fully marine condition in proximal bay setting.**

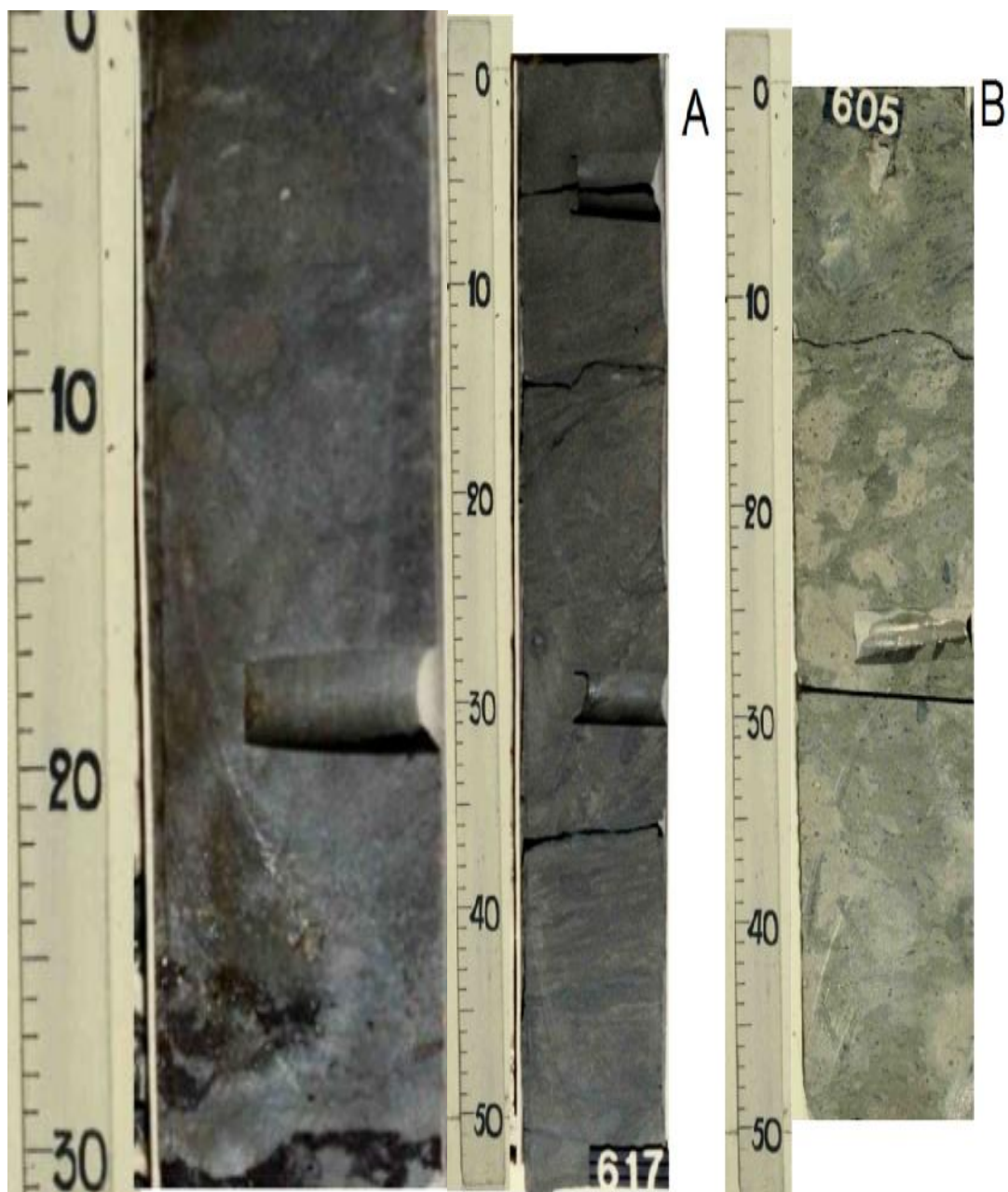


Figure 33: Argillaceous dolomitic siltstone facies, note flame structure at the base. (A.TBEM-2 between 616.5 and 616m; B.TBEM-106 between 605 and 605m)

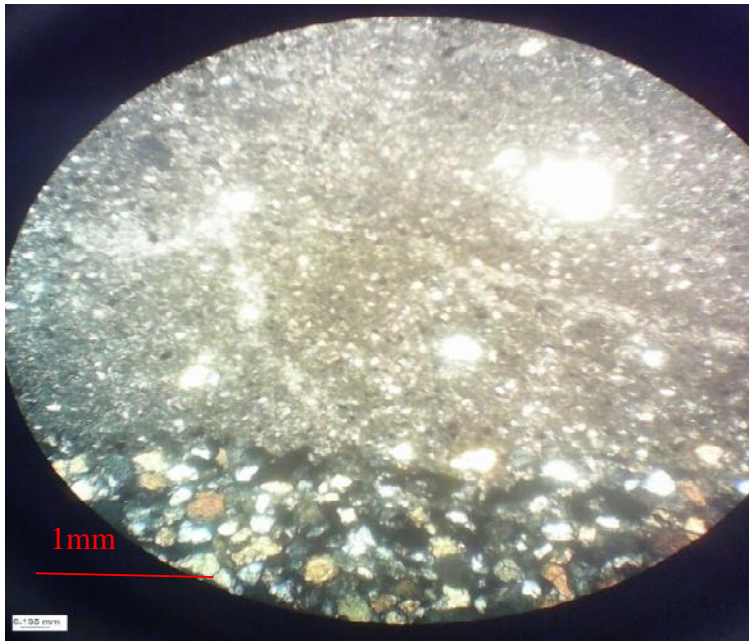


Figure 34: Argillaceous dolomitic facies (TBEM-106), note non-erosive contact

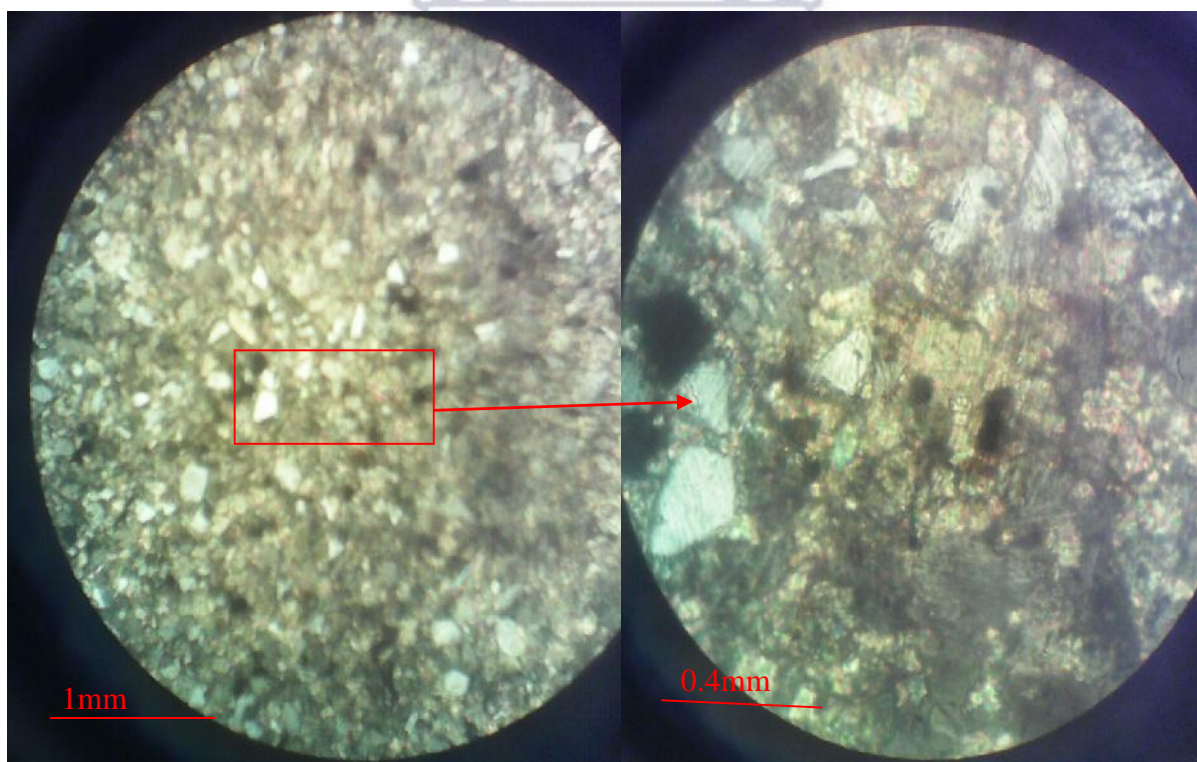


Figure 35: Micrite to microsparry cement; note replacement of former calcite (in red) by dolomite.

### **Facies 13**

This facies consists of grey greenish, bioturbated, silty bioclastic dolomudstone to dolomitic bioclastic siltstone. It shows slightly argillaceous matrix with single valve bivalves moulds. This facies is characterized by pluricentimetric vacuoles filled with Anhydrite. It also shows flame structures at the base.

The microscopic analysis of this facies shows that it consists of silt with slightly argillaceous matrix, dissolved bioclasts (bivalves) with dolo-microsparry cement with hedral dolomite formed by dolomitization of former calcite. This facies shows both moldic and vacuolar porosity.

#### **Discussion:**

Mudstone dolomite indicates that the deposit developed in low energy area (James *et al.*, 1992). The occurrence of nodular anhydrite was ascribed by Wilson (1975), Read (1985), Lyndsay & Kendal(1985) to Sabkha environment, however Moore (1989, 2013) described a set of major criteria for Sabkha environment with as the most important syngenetic nature of the dolomite. The above description showed that dolomite in the case of this facies is secondary dolomite as it developed from recrystallization of former calcite.

**Hence, this facies did not developed in sabkha environment as it can be thought base on nodular aspect of the anhydrite but Moore (1989) proposed for this facies a development in marginal bay environment (marginal marine evaporative lagoon) where the development of barrier or the seal in marine setting often modifies free hydrologic exchange between marine water and shelf-lagoonal environment and in the case total evaporative drawdown, desiccated Salinas.**

Adams & Rhodes (1961) related dolomitization to seepage reflux ion where highly saturated density-driven brine with high Mg/Ca ratio is capable of dolomitizing the lagoon or shelf floor and adjacent porous limestone units as it displaces lighter pore fluids.



Figure 36: Dolomitic siltstone with anhydrite nodules

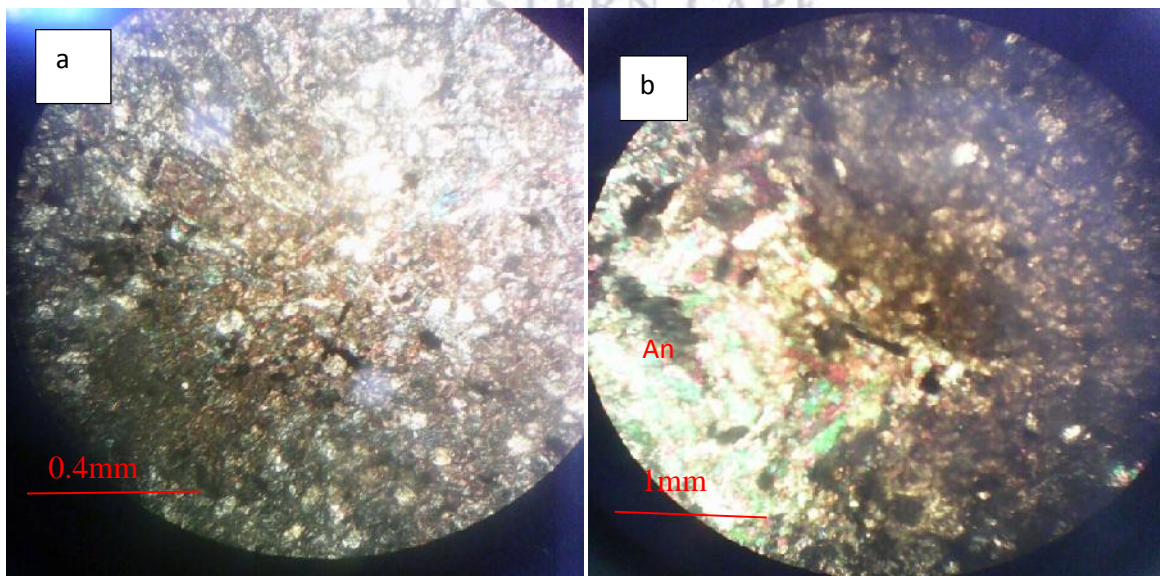


Figure 37: Dolomitization of former calcite (a), vacuole filled with Anhydrite, well TBEM-106 at 578.72m (An: anhydrite) (b).

## **Facies 14**

It consists of argillaceous dolomitic siltstone to silty dolomitic claystone. This facies is massive and moderately bioturbated. Recognizable ichnofossils consist mainly of *Teichichnus*. It also shows sulphur nodules with pyrite ring (aureole) and displays flame structures at the base. The facies shows some hummocky cross stratification toward the top.

Under the microscope, the facies shows silt size grain in argillaceous matrix and with dolomicrite cement. Dolomicrite cement formed from recrystallization of former micrite cement.

This facies shows no oil staining and it presents porosity from 22 to 27% and permeability between 0.85 and 9mD.

## **Discussion**

Silty argillaceous nature of the deposits indicates that the sediments deposited in sheltered area. Absence of root traces and pedogenic slickensides suggest subaqueous conditions.

Ichnofauna suggest a protected, low-energy environment with abundant organic matter in the sediment, here shown by the presence of pyrite grains.

The association of this facies with HCS sediment corresponds to mudstone-dominated with some interbedded storm induced deposits defined by MacEachern & Gingras (2007).

Buatois (2011) also described *Teichichnus* dominated facies in distal bay deposits (Mangano & Buatois, 2011). **Hence, this facies deposited in distal bay.**

UNIVERSITY of the  
WESTERN CAPE

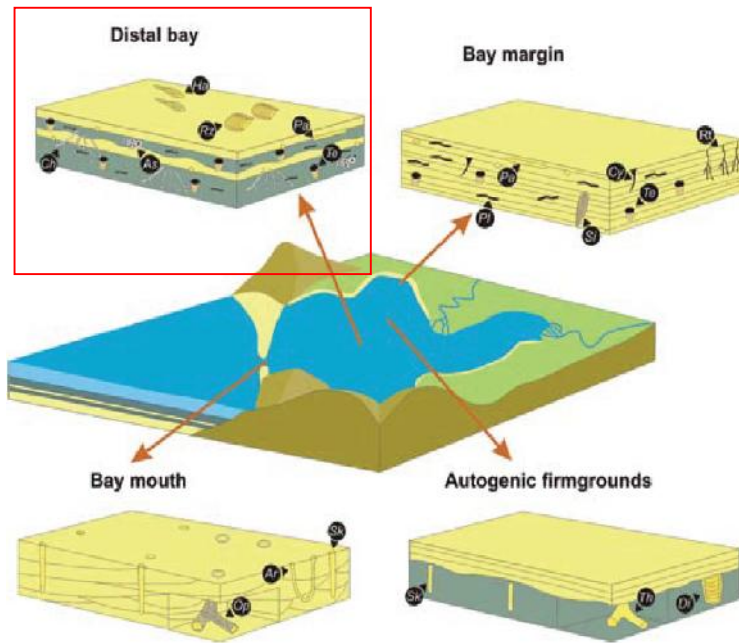


Figure 8.12 Schematic reconstruction of trace-fossil distribution in restricted bays. Bay-margin deposits commonly display low-diversity trace-fossil suites, including *Palaeophycus* (Pa), *Planolites* (Pl), *Siphonichnus* (St), *Teichichnus* (Te), *Cylindrichnus* (Cy), and root trace fossils (Rf). Distal-bay deposits may contain more complex forms indicative of slightly less-stressful conditions. Typical ichnotaxa are *Rhizocorallium* (Rh), *Halopoa* (Ha), *Chondrites* (Ch), *Asterosoma* (As), *Palaeophycus* (Pa), and *Teichichnus* (Te). Bay-mouth deposits tend to contain ichnotaxa indicative of relatively high-energy conditions, such as *Ophiomorpha* (Op), *Arenicolites* (Ar), and *Skolithos* (Sk). Autogenic firmgrounds may contain *Skolithos* (Sk), *Diploeraterion* (Di), and *Thalassinoides* (Th).

Figure 38: Bay facies (from Mangano & Buatois, 2011)





Figure 39: Argillaceous dolomitic siltstone, arrow shows *teichichnus*

## **Facies 15**

It consists of cylindrical, well sorted, non bioturbated grey to beige siltstone to very fine sandstone. It either shows massive appearance or thinly horizontal laminations or hummocky cross stratifications with sometimes with undulation at the top. This facies shows a sharp base. At certain depth *Ophiomorpha* has been recognized in this facies.

Microscopic study of this facies shows that it consists of very fine quartz (sandstone) to sandy silt with angular grained, sparse fine bioclasts with microcrystalline to dolomitic cement. The facies shows low intercrystalline porosity.

It shows porosity of 29% and 30mD permeability.

## **Discussion**

Well sorted, very fine sandstone to sandy silt with horizontal laminations facies has been described by Master (1965), Reineck & Singh (1971) as deposited in lower shoreface setting by high energy storm event. Reineck & Singh (1973, 1980) defined top wave ripples as characteristic of lower shoreface setting.

Mangano & Buatois (2011) showed that bay mouth deposits tend to contain ichnotaxa indicative of relatively high energy conditions, such as *Ophiomorpha*. Furisch (1998) defined this ichnofossil as characteristics of tempestites as corresponding to shoals facies in carbonate. Price (1933), Otvos & Howat (1996) described barrier (beach) ridges as often with *Ophiomorpha* ghost shrimp tubes. **Hence, facies with *Ophiomorpha* represents development in high energy bay mouth or barrier (beach) ridges.**

UNIVERSITY of the  
WESTERN CAPE

a

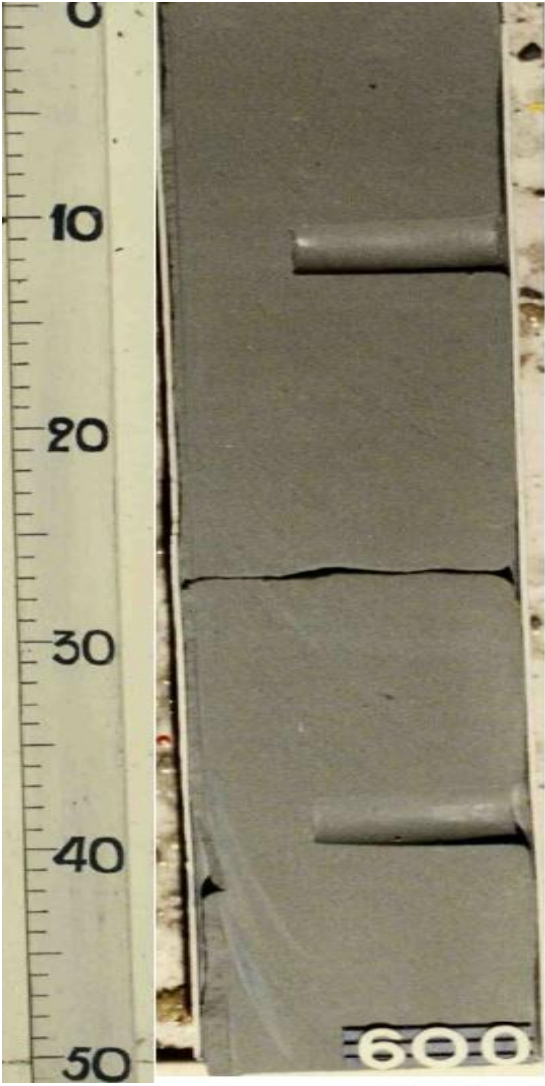


Figure 40: Cylindrical horizontal laminated facies: a. massive or thinly laminated, b. with *Ophiomorpha*

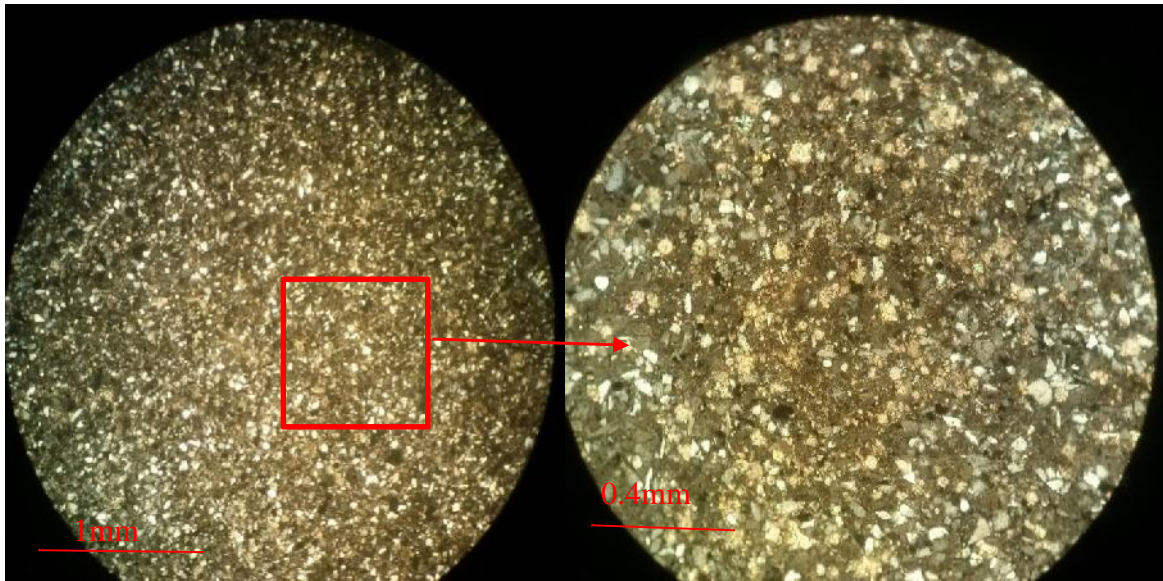


Figure 41: Facies silty matrix under microscope

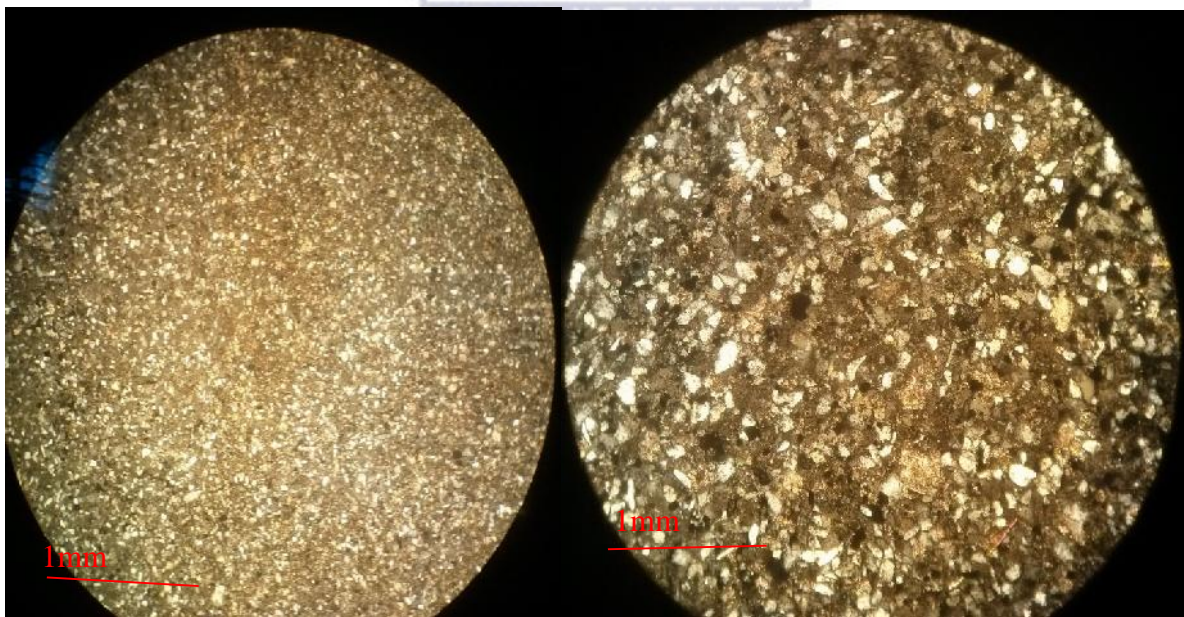


Figure 42: microcrystalline to dolomitic cement.

## **Facies 16**

It consists of grey, bioturbated silty bioclastic dolomudstone to dolomitic bioclastic siltstone with a silty argillaceous matrix. It shows moulds of bivalves' valves and centimetrical dissolution vacuoles filled with dolomitic silt. The facies displays no sedimentary structures and the most recognizable ichnofabrics found are *Thalassinoides*.

Investigations of this facies under microscope show silt sized grains (siltstone), slightly argillaceous matrix and bioclasts constituted of mostly rare dissolved bivalve's valves. The bioclasts show thin micritic cement and are bounded by micro-dolo-sparry cement showing pseudo-hedral to hedral dolomite.

This facies is poorly oil stained. It shows porosity from 15 to 27% and permeability from 1.63 to 34 mD (rare values of 434 and 1320 were measured at 584m in well TBEM2).

## **Discussion**

The bioclastic mudstone texture of this facies indicates deposition in low energy area. According to Moore (1989), Tucker & Wright (1990) and Nichols (2009), in deeper water below wave base the outer ramp deposits are principally redeposited carbonate mudstone and wackestone, often with the characteristics of turbidites.

Narbonne (1984), Maples & Archer (1986), Fraaye & Werver (1990) and Fürsich (1998) indicated that under lower energy conditions, such as those in distal carbonate ramps and platforms, more diverse suites dominated by horizontal trace fossils may be preserved, including *Thalassinoides*, *Rhizocorallium*, *Fürsichnus*, *Protovirgularia*, *Helicodromites*, *Palaeophycus*, *Teichichnus*, *Cruziana* and *Chondrites*. Moreover Mángano & Buatoï (1994) *Thalassinoides* is a common elite trace fossil in subtidal carbonates.

**Hence, this facies deposited in deep ramp setting.**



Figure 43: Bioclastic silty dolomudstone

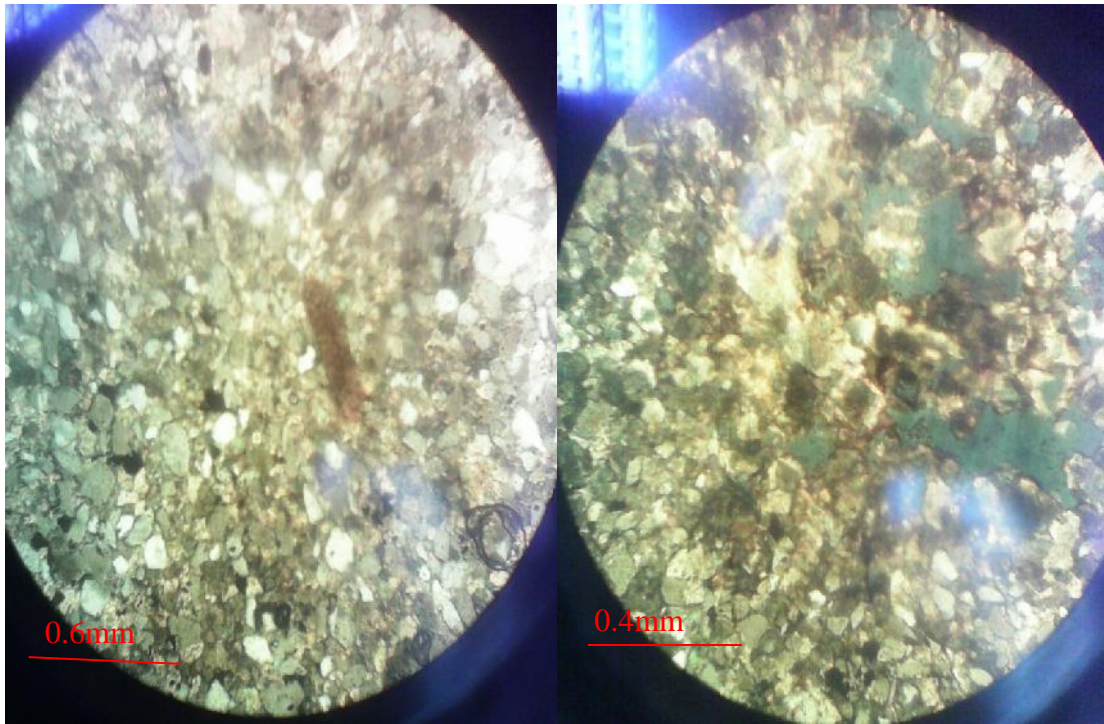


Figure 44: Micro-sparry cement with translucent aureole around the dolomite rhombs

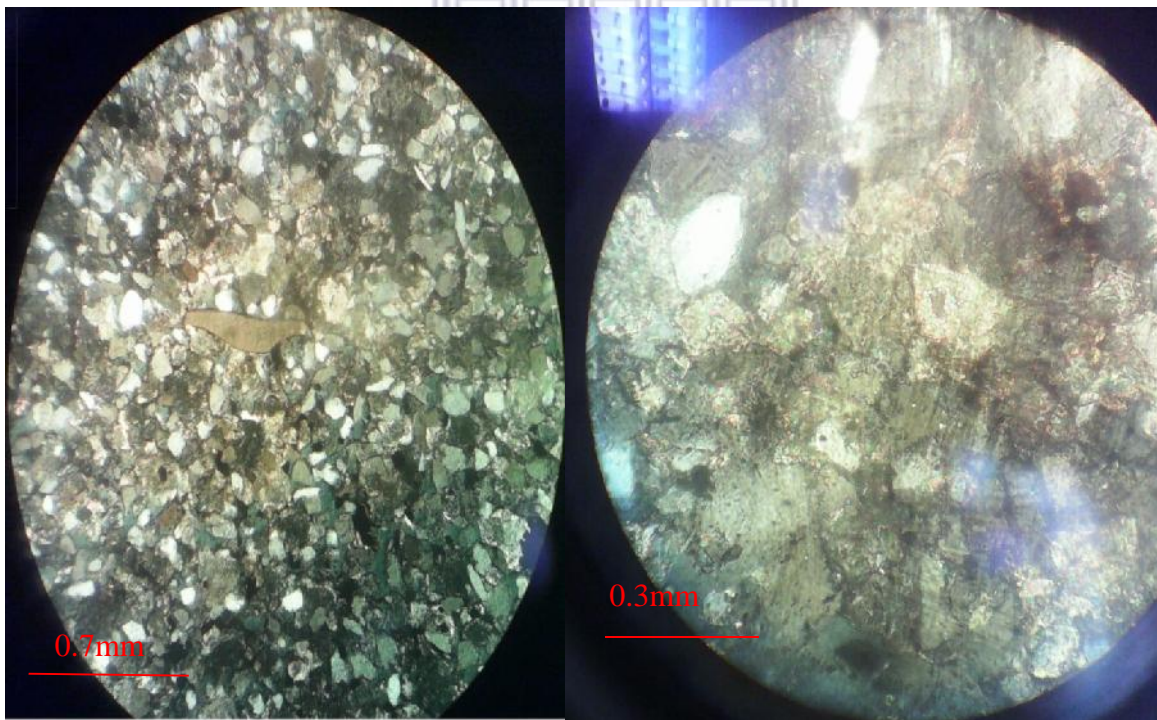


Figure 45: Silty dolo-mudstone facies; note calcite replacement by dolomite

## **Facies17**

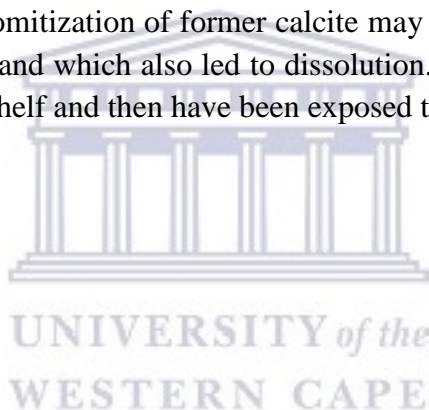
It consists of grey bioclastic mudstone with some skeletal (bivalves) debris. It displays silty argillaceous matrix and silty discontinuous lamina. This facies shows load cast at the base.

Microscopic analysis of thin section showed that it is consisted of bioclastic mudstone with debris of bivalves in micrite calcite matrix strongly cemented by dolomitized microsparry cement. The bioclasts either display micrite cement or are dissolved. This facies is characterized by both intercrystalline and moldic porosity.

This facies is not impregnated with oil and it shows porosity of 20% and permeability of 20mD.

## **Discussion**

The occurrence of bioclastic mudstone indicates deposition in low energy area (Wilson, 1975; Wall & Burrowes, 1985; Lindsay & Kendall, 1985). According to Moore (1989) Moore, Tucker (1990) and Nichols (2009) in deeper water below storm wave base the outer ramp deposits are mainly redeposited carbonate mudstone and wackestone, often with the characteristics of turbidites. Microsparry to sparry equant cement which indicates development in meteoric environment. Dolomitization of former calcite may have been induced by mixing of marine and meteoric water and which also led to dissolution. Hence, this facies developed in low energy lagoonal inner shelf and then have been exposed to meteoric diagenesis.



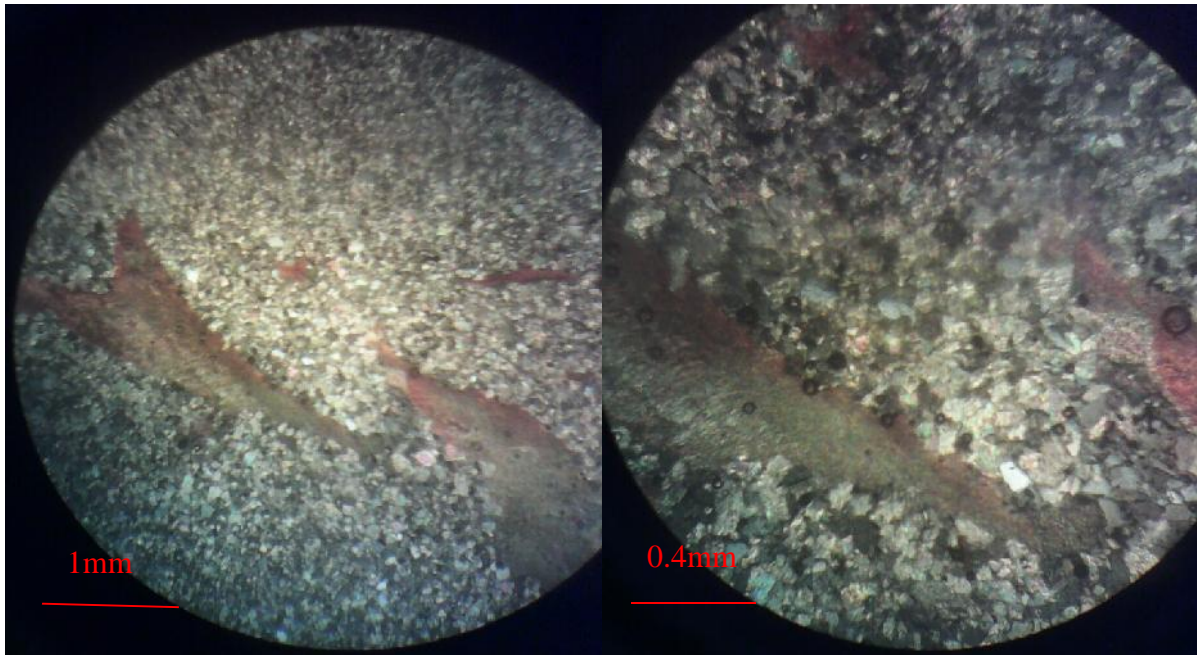


Figure 46: Note formation of calcite prior to replacement by dolomite (TBEM-2 at 562.70m)

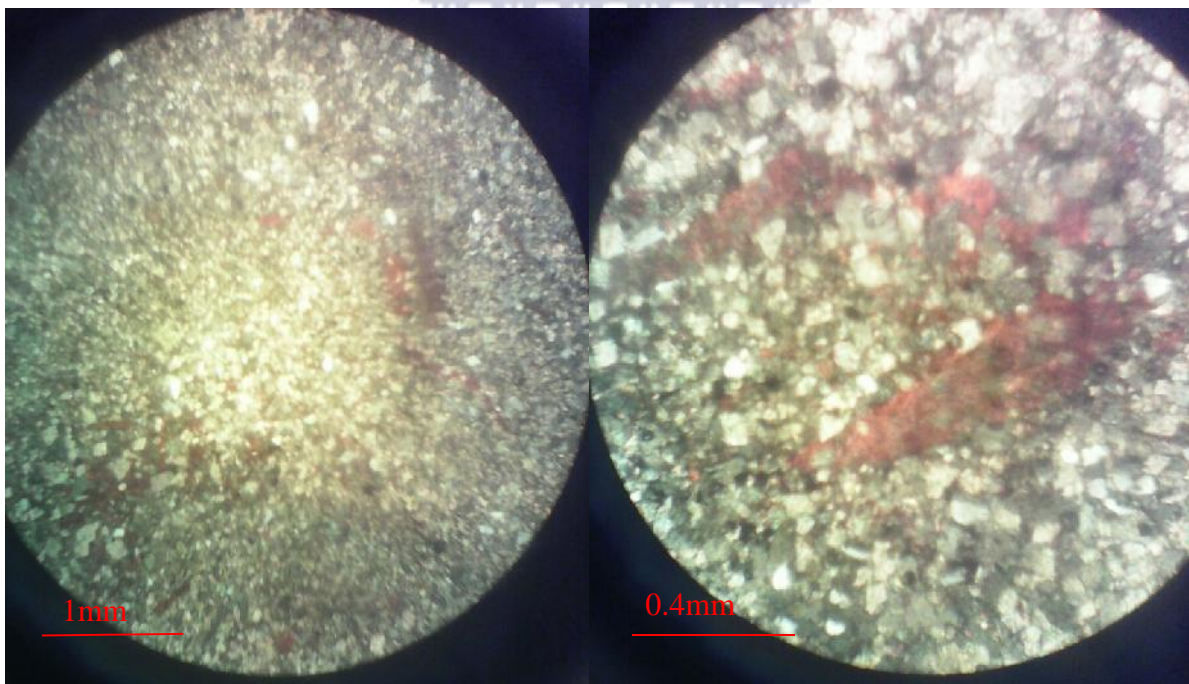


Figure 47: Note both moldic and interparticle porosity (TBEM-2 5 at 61.58m)

## **Facies 18**

It consists of grey, bioclastic mudstone to wackestone silty dolomite. Skeletals consist of moulds of bivalves' single valves in calcareous slightly argillaceous cement. This facies displays an erosive base (hardground) and no sedimentary structures.

The analysis of thin sections shows wackestone dolomite, made of entirely dissolved bivalves shells with sub hedral dolomite crystals (sucrosic dolomite), silt grains to very fine grained quartz. It also shows crystallization of the calcite, rare moldic porosity in which hedral dolomite developed and dominated par intercrystal porosity.

This facies is highly impregnated with oil and it presents high values of porosity from 23 to 40% (40% porosity was measured at 567.50min well TBEM2) and permeability from 1741 up to 5963mD.

## **Discussion**

Mudstone or wackestone are relatively low energy facies of protected or interior setting. Wilson (1975), Moore (1989) and Tucker and Wright (1990) described **this bioclastic mudstone to wackestone as developed in the mid ramp-outer ramp to deeper water below the storm wave base**. Purser (1985) explained sucrosic characteristic of dolomite in middle Jurassic of Paris basin by early dolomite dissolution by fresh water along the landward margin of a prograding coastal plain. He explained that fine dolomite rhombs that formed on coastal plain (tidal flat) were flushed and dissolved; he stated that the phenomena lead to both intracrystalline and moldic porosity as it is the case in this facies.

UNIVERSITY of the  
WESTERN CAPE



Figure 48: Wackestone silty calcareous dolomite

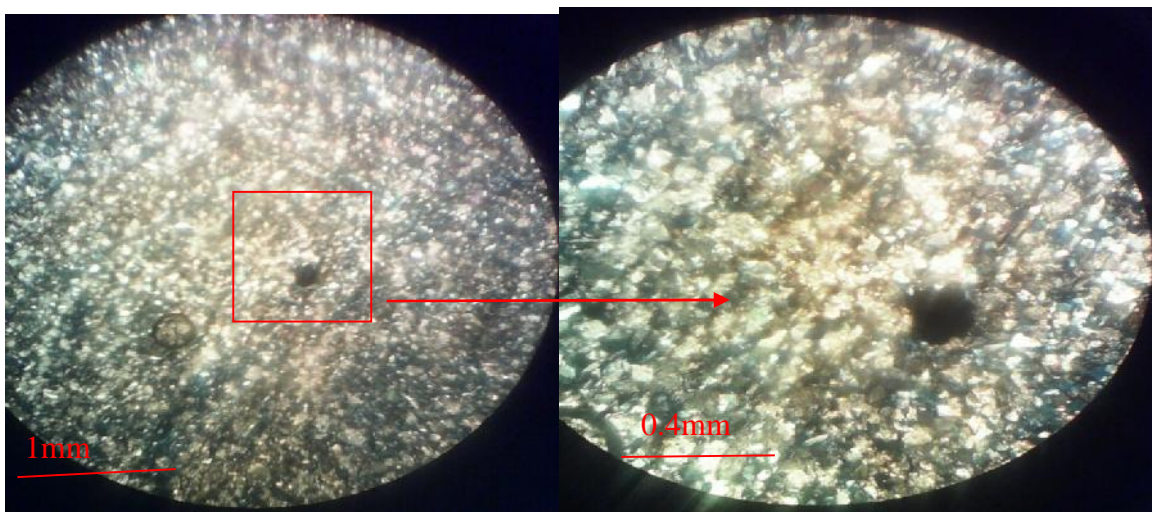


Figure 49: Intercrystal porosity

## **Facies 19**

This facies shows grey to beige, wackestone–packestone bioclastic limestone made of recrystallized shells, with silty argillaceous matrix, which also filled the lower part of the shells and rare argillaceous lamina. The bioclasts consist mainly of *Echinids*.

On thin section the facies shows wackestone to packstone bioclastic limestone with peloids (the peloids are well sorted and fine grained) in calcitic micrite matrix strongly dolomitized. The bioclasts show micrite envelop (coating).

It displays two generations of cement; the first generation consists of sparry cement developed inner part of the coated bioclast and in matrix, this cement was partially replaced by second generation of cement characterized by hedral dolomite.

## **Discussion**

The occurrence of the whole shells in life position indicates that the sediment accumulated in the living environment and hence is autochthonous or para-autochthonous.

Bioclastic and peloidal wackestone, packstone, and mudstone characterize the mid to deep ramp, in front of the high-energy zone and below fair-weather wave base (Moore & Wade, 2013). Coating around some of the bioclasts shows that they have been transported from high energy to low energy setting. The current that transported the coated bioclasts also winnowed most of the micrite. Hence this facies formed in high energy setting.

This process had also been described in deep ramp setting by Tucker & Wright (1990).

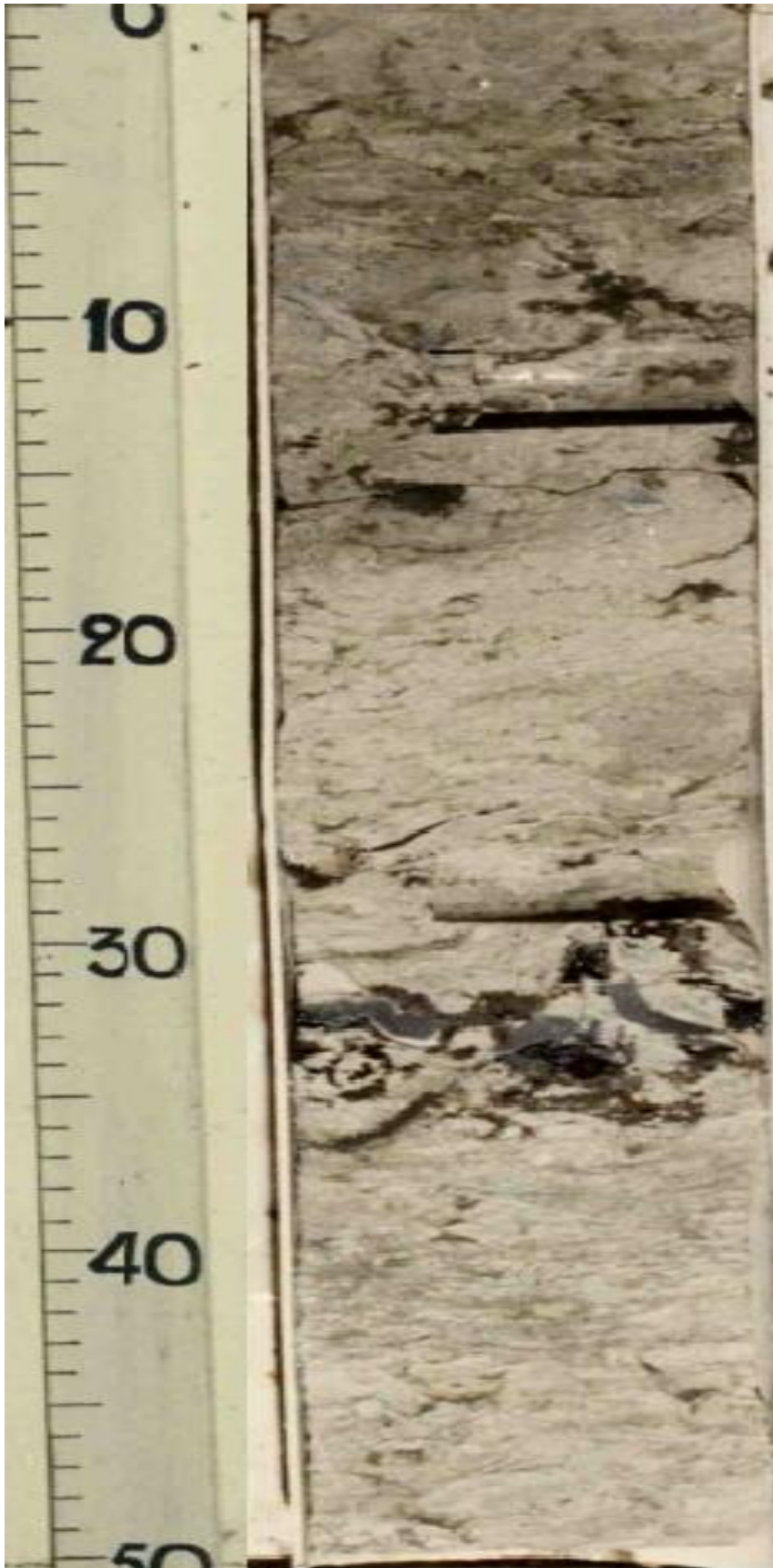


Figure 50: Silty bioclastic peloidal limestone (TBEM2 between 557 and 557.50m)

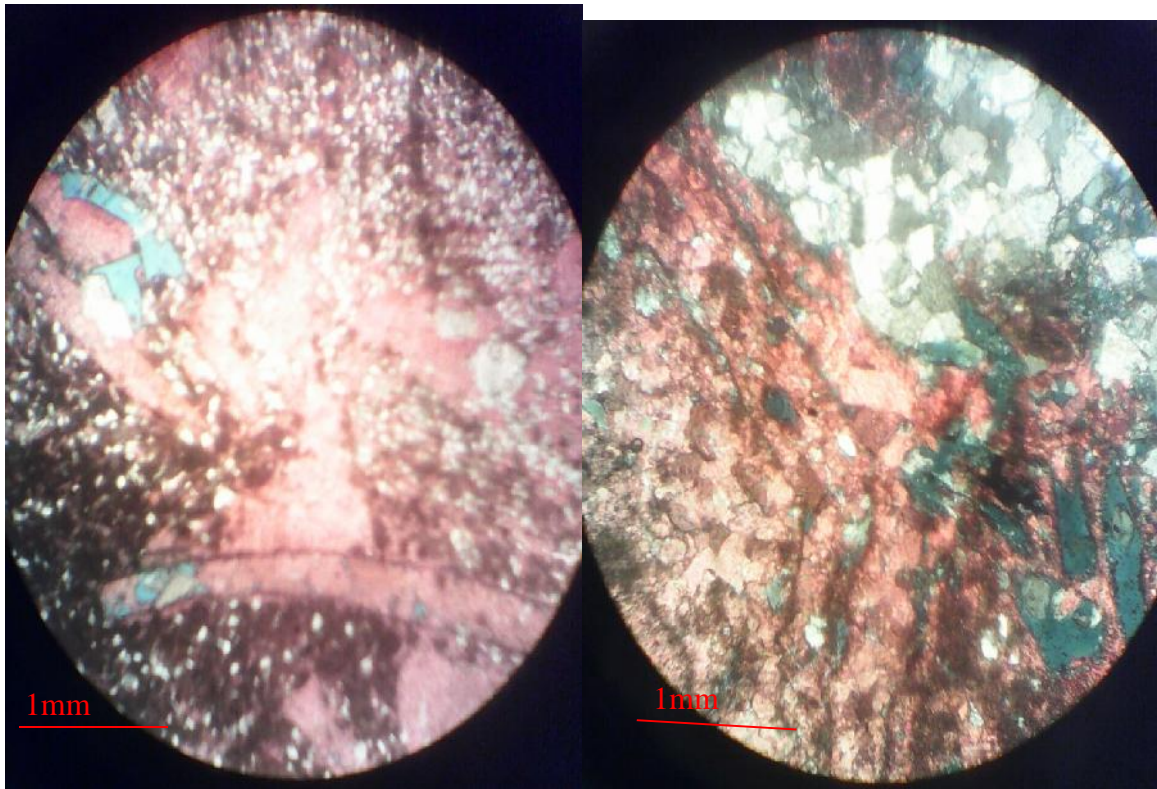


Figure 51: .A. silty bioclastic peloidal limestone, B. note hedral dolomite in molds.

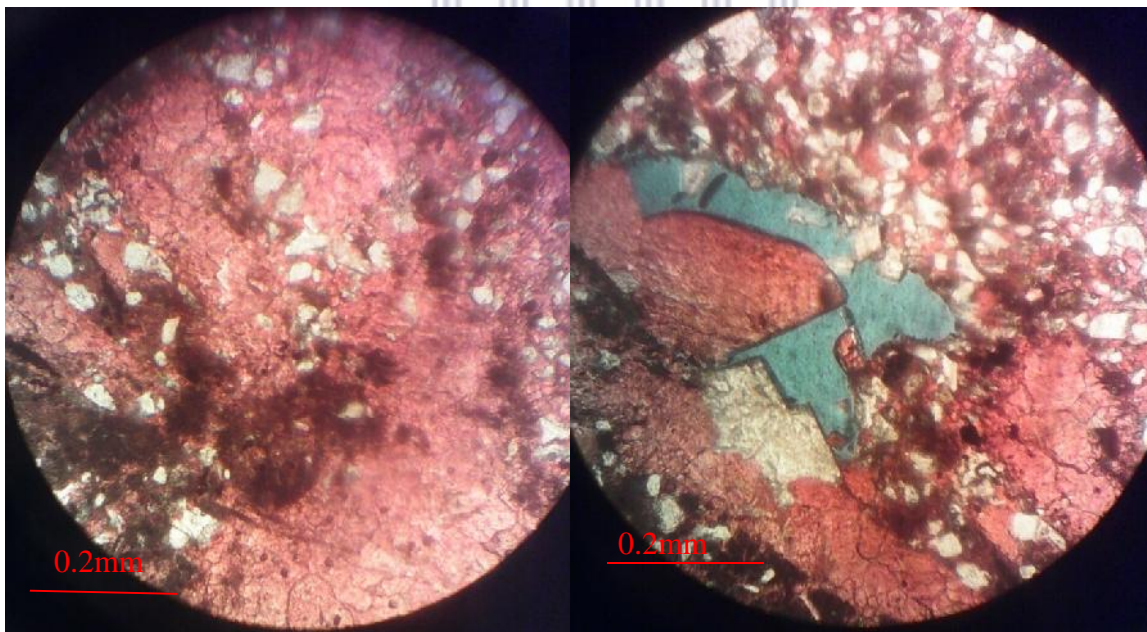


Figure 52: Silty bioclastic peloidal limestone; note dolomite in moldic space.

## **Facies 20**

It consists of Grey, bioturbated, silty bioclastic dolomite, packstone to grainstone. The bioclasts are constituted of bivalve's moulds, and some dolomitized shells debris. This facies shows a base characterized by erosive hardground surface.

Microscopic views of this facies revealed that it consists of packstone to grainstone dolomite, with rare quartz (silt) cemented by sparry equant cement. The facies displays moldic porosity. Molds are filled by calcite in depth whereas at lower depth no calcite recrystallization occurred.

This facies shows low porosity between 5 and 20% and permeability between 0.21 and 72mD. However, high values 28% porosity and 2021 to 2098 were measured at 574.73m and 573.51m.

## **Discussion**

Packstone and grainstone facies indicate sediment deposition in high energy setting (James *et al.*, 1992). This facies suggests that this facies type represents a high-energy, shallow platform environment above or close to the fair-weather wave base. Wright (1986), Tucker & Wright (1990) interpreted shoreline grainstone as characteristic of shallow ramp setting and explained that the inner part of the shallow ramp is characterized by high-energy shoreline grainstone because of unimpeded wave travel across the shallower portions of the ramp.

The single valves nature of this skeletal advocates for reworking in high energy setting as the shells are dominantly oriented concave up, **hence this facies could consisted of former chenier ridges, which are the relicts of former beaches that have been left inland as the shoreline prograded (Augustinus, 1989).**

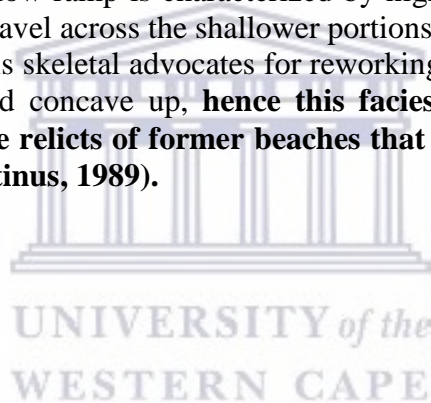




Figure 53: Silty bioclastic packstone (note hardground at 571.80m).

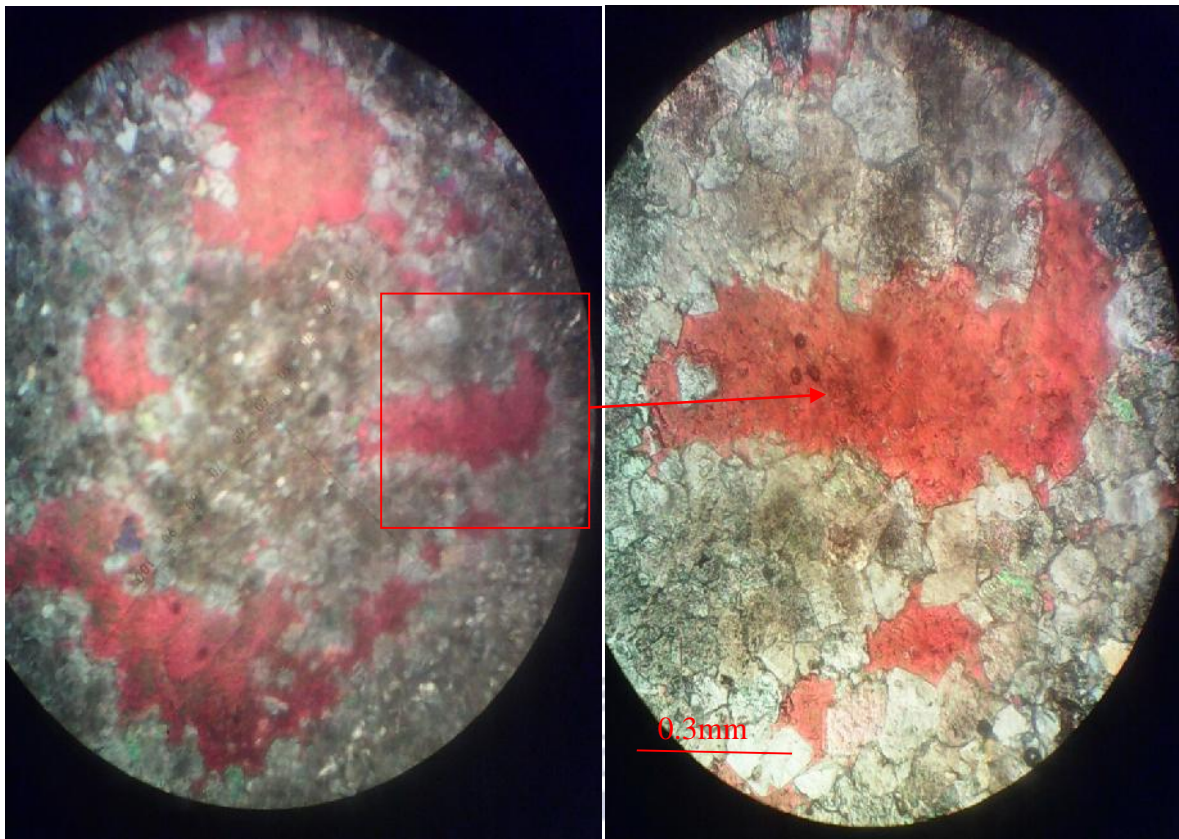


Figure 54: Silty bioclastic dolo-packstone, moldic space filled with calcite

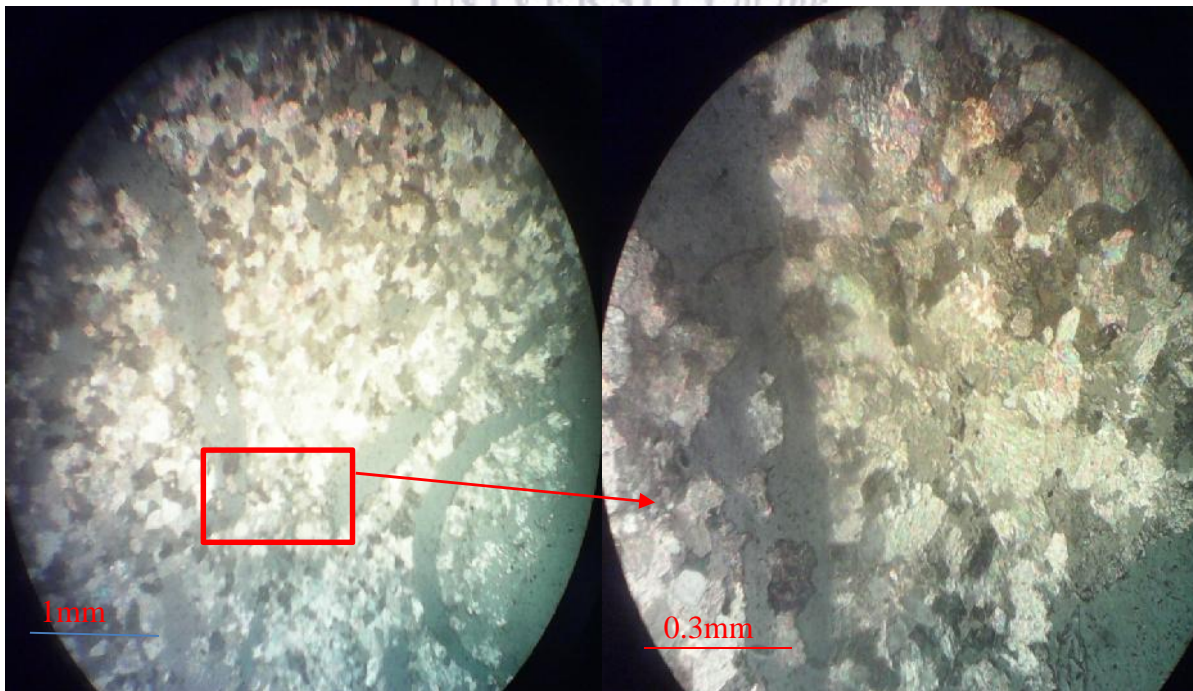


Figure 55: Silty bioclastic dolo-packstone.

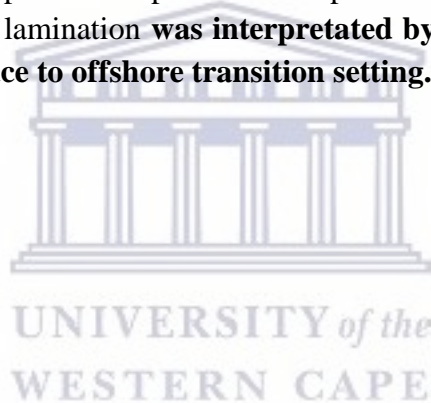
## **Facies 21**

This facies consists of bioclastic calcareous siltstone with argillaceous matrix, bioclasts comprise bivalves and echinoids' whole shells, fragmented skeletal comprising echinoderms and lamellibranches and either recrystallized or dissolved (forming vacuoles). This facies is characterized by lower surface displaying load cast or flame structure.

Observation of thin sections revealed that it consists of siltstone with calcareous -argillaceous matrix with bioclasts, the facies shows either dissolved bioclast with micrite cement around (coating) or micrite coated grain with drusy sparry cement in the inner part of the shells. Some of the shells showed recrystallization of the shells with remnants of the original aragonite or calcite. The matrix also shows blocky cement consisted of rhombohedra of dolomite.

## **Discussion**

Drusy cement has probably developed as result of burial while blocky cement has precipitated as result of dissolution of aragonite cement or grains or as late diagenetic cement filling the remaining pore space; the occurrence of echinoderms was interpreted by Wilson (1975), Lindsay & Kendal (1985) as specific to open sea to slope facies while silt size of the matrix coupled with some horizontal lamination **was interpreted by Reineck & Singh (1980) as characterizing lower shoreface to offshore transition setting.**



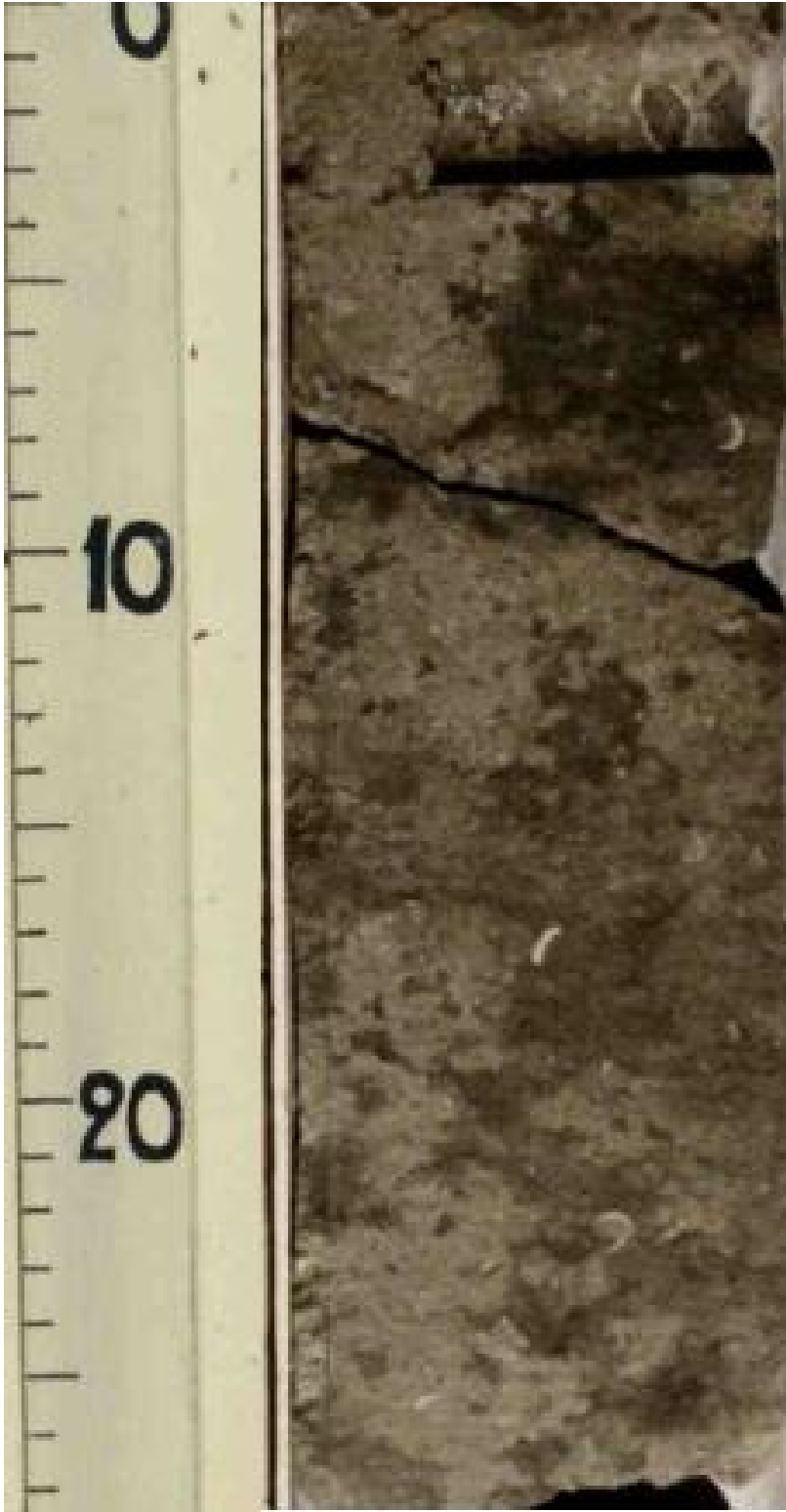


Figure 56: Bioclastic calcareous siltstone (TBEM2 from 549, 50 to 549,77m).

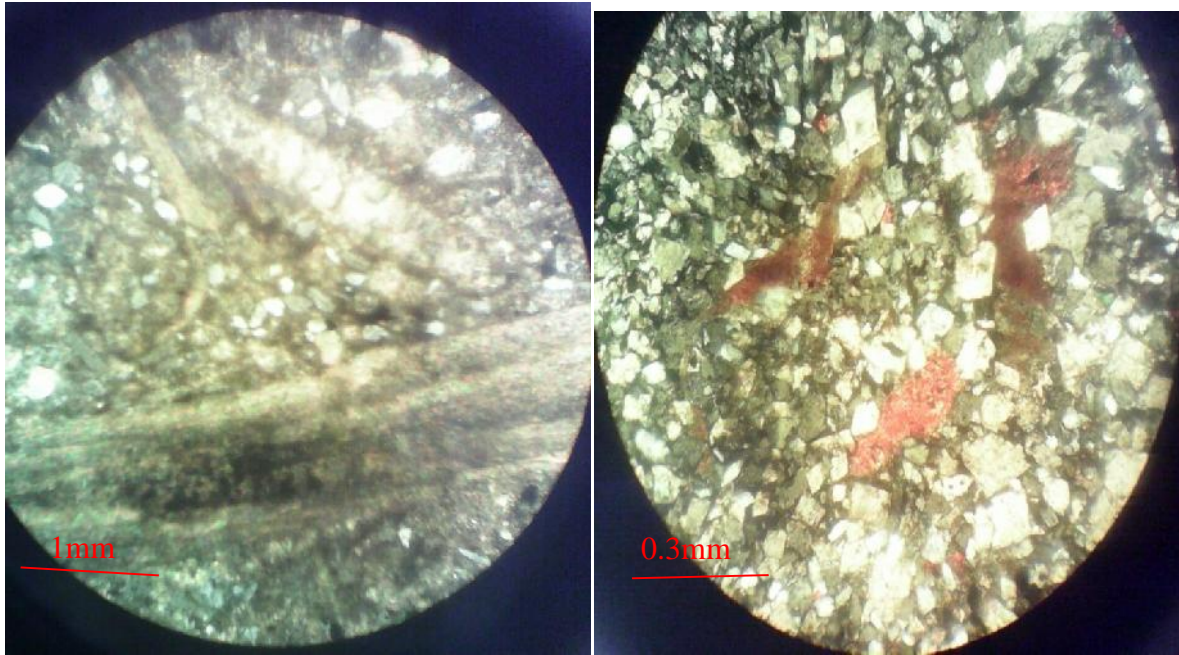
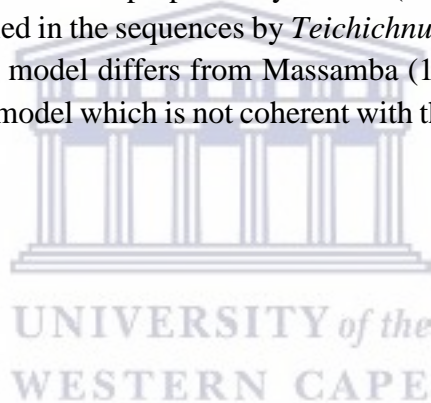


Figure 57: facies thin sections showing echinoids and dolomite rhombs



The analysis of all the above facies shows that the Turonian deposits of The Congolese Coastal Basin distinguish two parasequences: a siliclastic parasequence indicating a development in fluvial to distal bay settings and a carbonate parasequence which indicates development from inner or shallow ramp to offshore. The carbonate parasequences is coherent with carbonates ramp parasequences proposed by Nichols (2009) (appendix 9). This Ramp model suggests an increase of bioclastic facies characterizing high energy shoreline facies as one move from offshore to coastal area. The correlation line (figure 61) from Tchendo field (offshore field) to Tchibouela field (proximal) clearly shows an increased in thickness of the high energy shoreline facies advocating for an increase of energy of the deposition area from offshore to shoreline that is characteristic of ramp setting. **The model shows that Turonian deposit deposited in estuary with bay side or bay ahead with a carbonate ramp or re-combined chenier.**

**Hence, the facies model from cores study corresponds to chenier model from outcrops study (Djeno and Mvassa outcrops)even though they are not of the same age interval. This indicates a diachronism of the series.** This model is coherent to chenier model proposed by Masse (2008); however, the Model proposed by Masse (2008) does not include the bay setting which is clearly identified in the sequences by *Teichichnus* facies versus *Thalassinoides* facies. On the other hand, this model differs from Massamba (1985), Massala (1993), Biondi (1996), (1996a & b) Turonian model which is not coherent with the increase of bioclastic facies from offshore to shoreline.



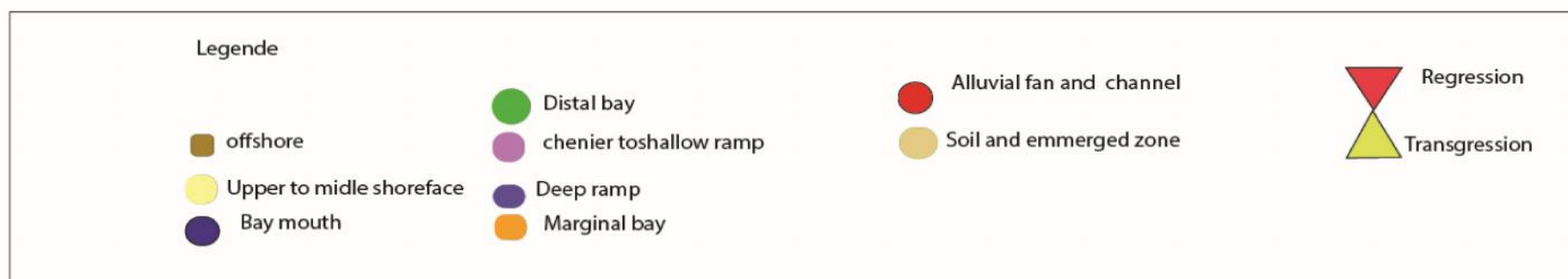
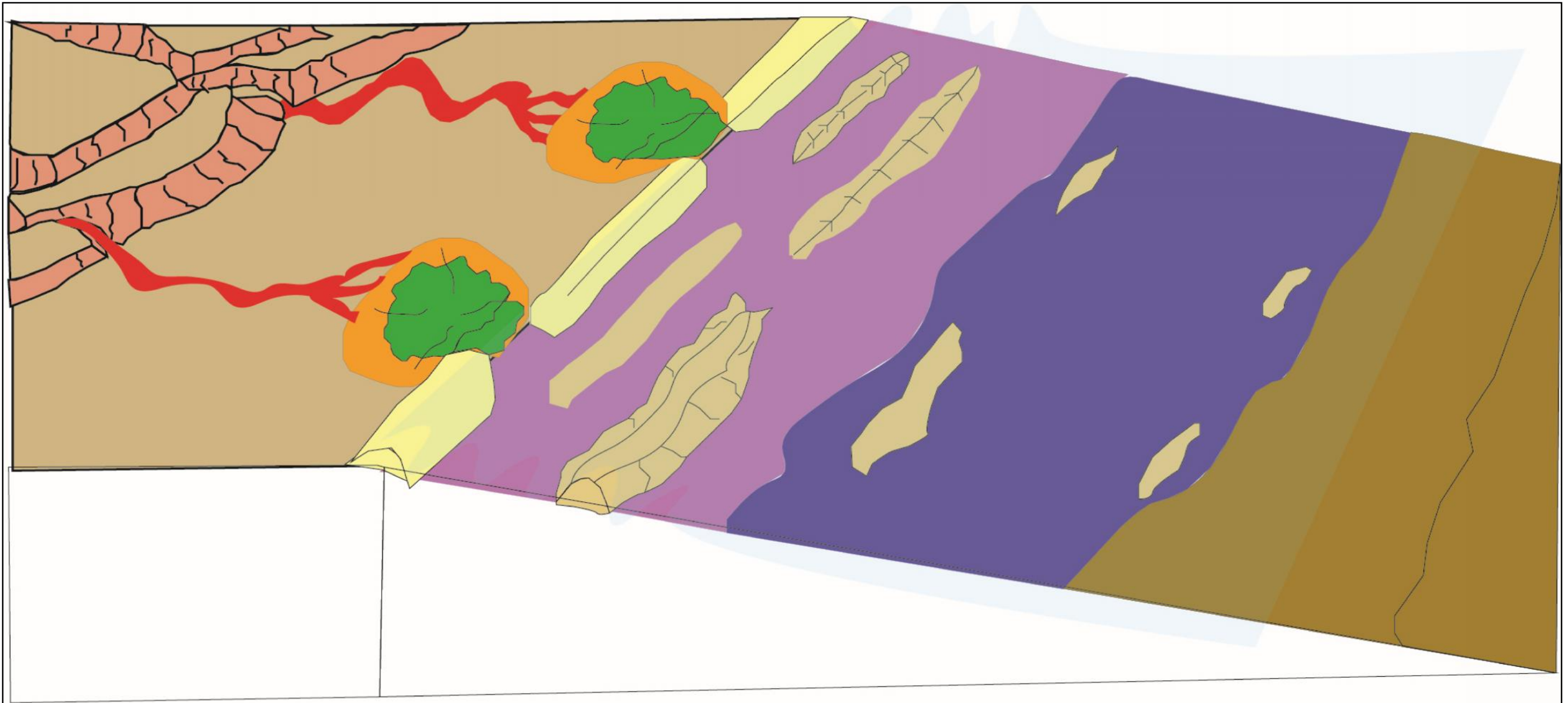


Figure 58: Turonian facies model

### 3.3. Basin framework correlation

Considering the depositional vertical sequence, the Turonian series of the Congolese Coastal Basin show an overall transgressive system as the sediments have deposited from more continental environments (alluvial and fluvial) to bay environments to shelf setting and to open marine setting revealing deepening of the environment (figures 59 and 60).

Four major sequences strikeward and dipward were documented here. However, along the depositional strike second order sequences were identified. Aiming to have a more comprehensive frame of the dynamic context, this study took into account individual sequences. The following table shows the various sequences.

Tableau 2: Summary of sequences boundaries and maximum flooding surfaces

Major sequences	Sequences boundaries	Maximum flooding surface	Strike direction	Dip direction	
4	SB 8	MFS6			
3	SB 7		Yes	Yes	
2			Yes	Yes	
1	SB6	MFS5	Yes	No	
			Yes	yes	
	SB5	MFS4		yes	
				No	
	SB4				
		SB3	MFS3	Yes	No
		SB2	MFS2		
	SB1	MFS1			

Height sequences boundaries (SB) were recognized along depositional strike. The sequences boundaries SB3, SB5 SB6, and SB7 can be correlated strikeward through the basin while dipward SB1, SB2, SB4 cannot be followed along the depositional dip. The latter sequence boundaries correspond either to soil facies especially in silty dolomitic and dolomitic silty deposits or consist of two major lithofacies shift while the others only correspond to lithofacies shift from somewhat shallower to somewhat deeper across the sequences boundaries (In calcareous deposits).

SB1, SB2 and SB4 corresponding to soil (emersion surface) probably formed by allocyclic response to unsteady sea level, creating forcing sea level fall event followed by transgressive –regressive

movement of the shoreline while the sea level was rising. This event was only noted in well along the outermost depositional strike while not observed in innermost offshore wells (such as TCDM3).



UNIVERSITY *of the*  
WESTERN CAPE

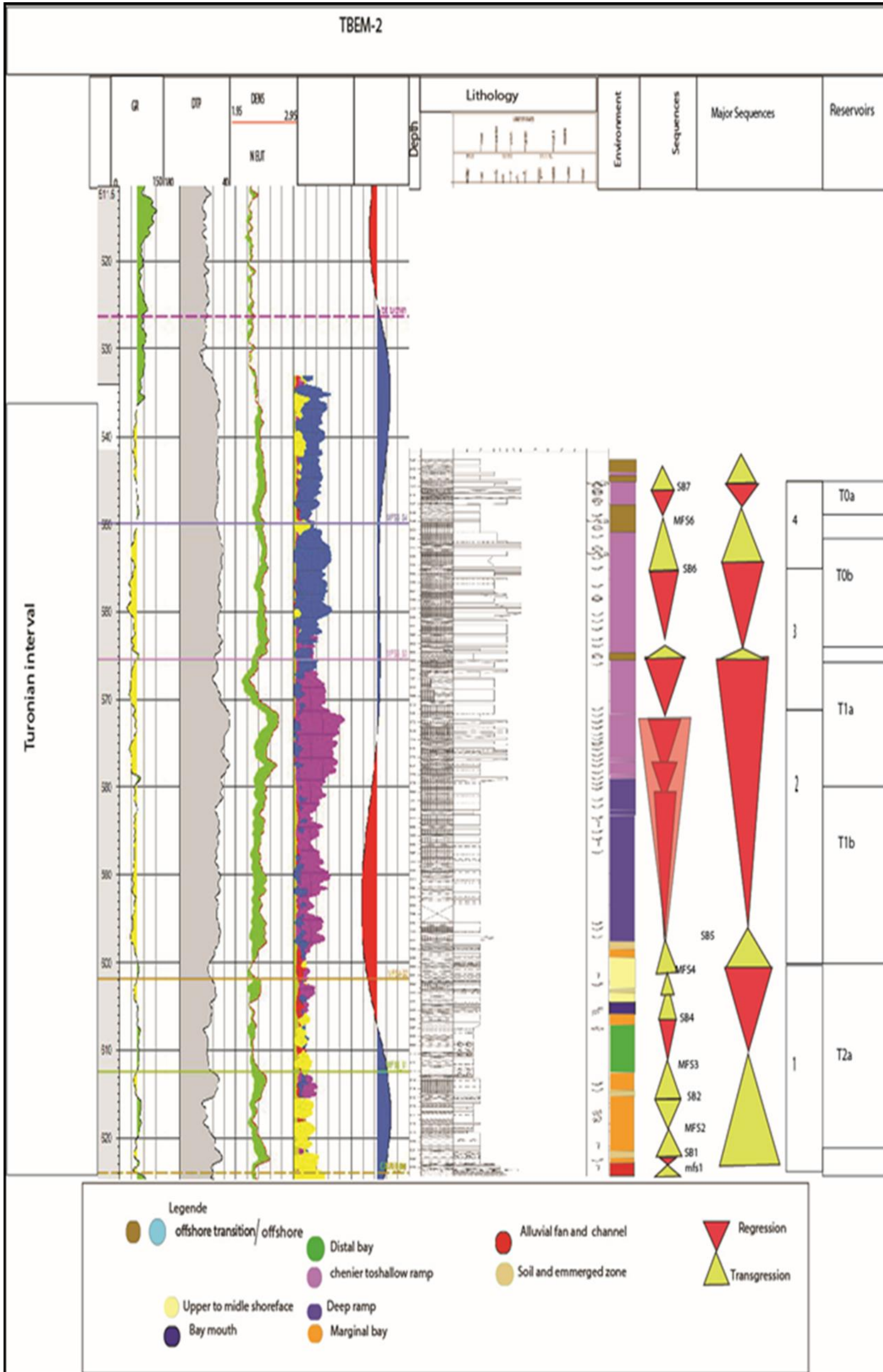


Figure 59: Well TBEM-2 sequential stratigraphy (based on vertical superposition of the environments)

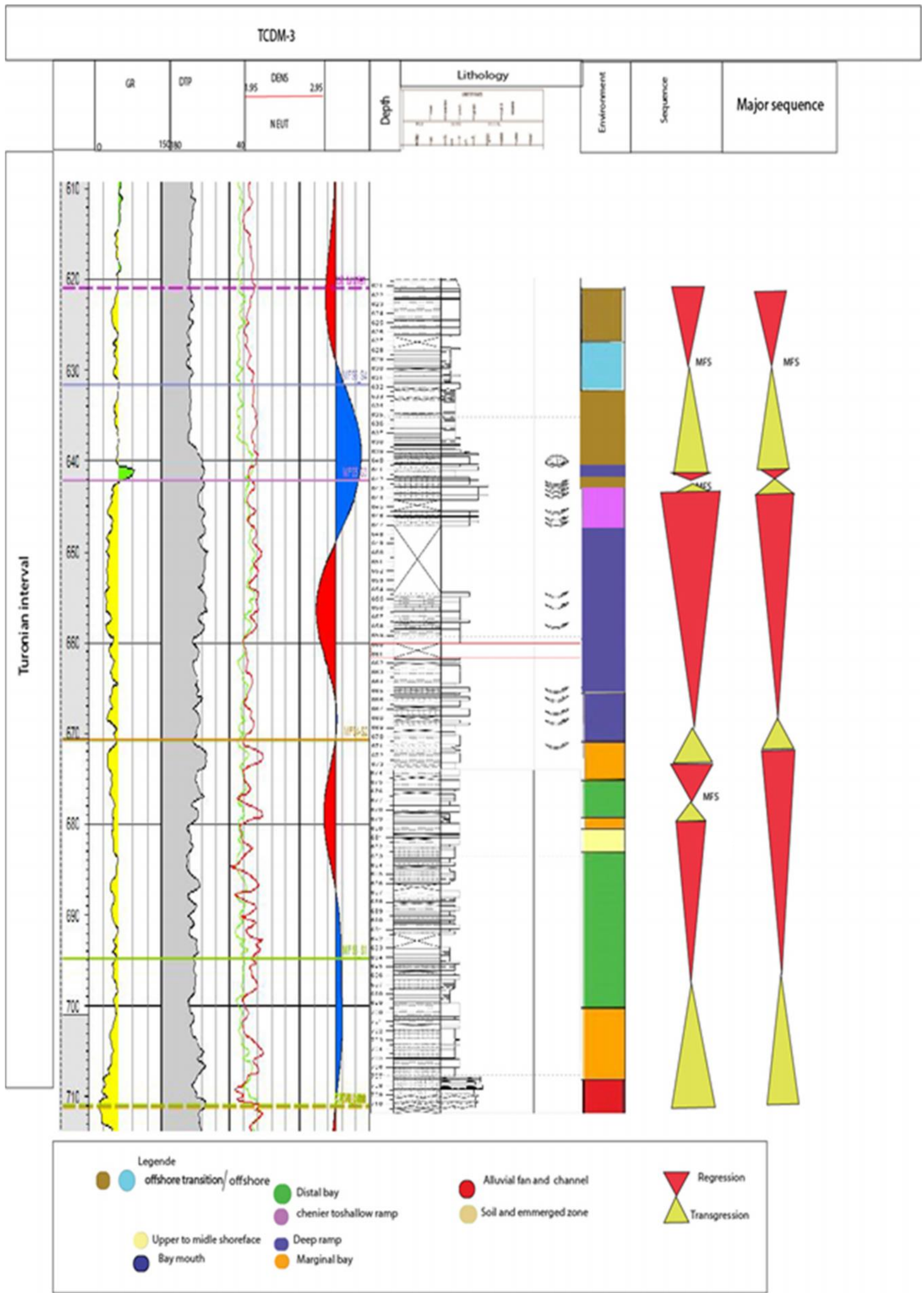


Figure 60: Well TCDM3 sequential stratigraphy (Based on vertical superposition of the environments)

Seismic profile revealed that those SBs are situated near a syndepositional fault. Hence, this fault movement could have triggered movement which led to sea level fall near the fault while in the all basin sea level was rising.

SB3, SB5, SB6 and SB7 consist to a major lithofacies change probably related to autocyclic event which can be correlated throughout the basin strikeward and dipward.

Six maximum flooding surfaces (MFS) are recognizable on outcrops and as for SBs some of the MFs are correlatable throughout the basin and the others are not. Correlatable MFSs (MFS3, MFS5 and MFS6) correspond to maximum flooding surfaces for the three major sequences and they are indicated on Seismic profile by reflectors (figure 61, 62 and 63). Non correlatable MFS represent maximum flooding surface formed by transgressive-regressive movement induced by potential allocyclic event and they do not correspond to any reflector on seismic profile.

The maximum flooding intervals (MFI) are mostly represented by bioturbated argillaceous to silty argillaceous sediment (facies 19, facies 20) with exception for the MFI located between 600 and 602m on well TBEM-2 which is represented by *Ophiomorpha* bioturbated very fine sandstone to siltstone. The MFS 1, 2 and 4 are bounded by SB1, SB2 and SB4 are not correlatable through the entire basin and could be considered as resulting from transgression \_regression movement which followed sea level fall responsible for SB1, SB2 and SB4. Those MFSs do not correspond to seismic horizons while MFS3, MFS5 and MFS6 are correlatable throughout the basin and correspond to major seismic horizons.

Vertically in silty dolomitic interval, we recognized Hardground (*e.g.* TBEM2 between 574 and 565m) corresponding to paleo-soil or emersion surface sea level fall. The hardgrounds correspond to decrease of sediments influx due to relative. They developed by depletion in sediment input to form starvation surface on top of the transgressive surface shelf strata. The hardgrounds mentioned earlier are period of condensed sedimentation in the basin during which fossils were there but sediment influx was brutally reduced leading to biologic detritus increase (observed packstone grainstone facies).

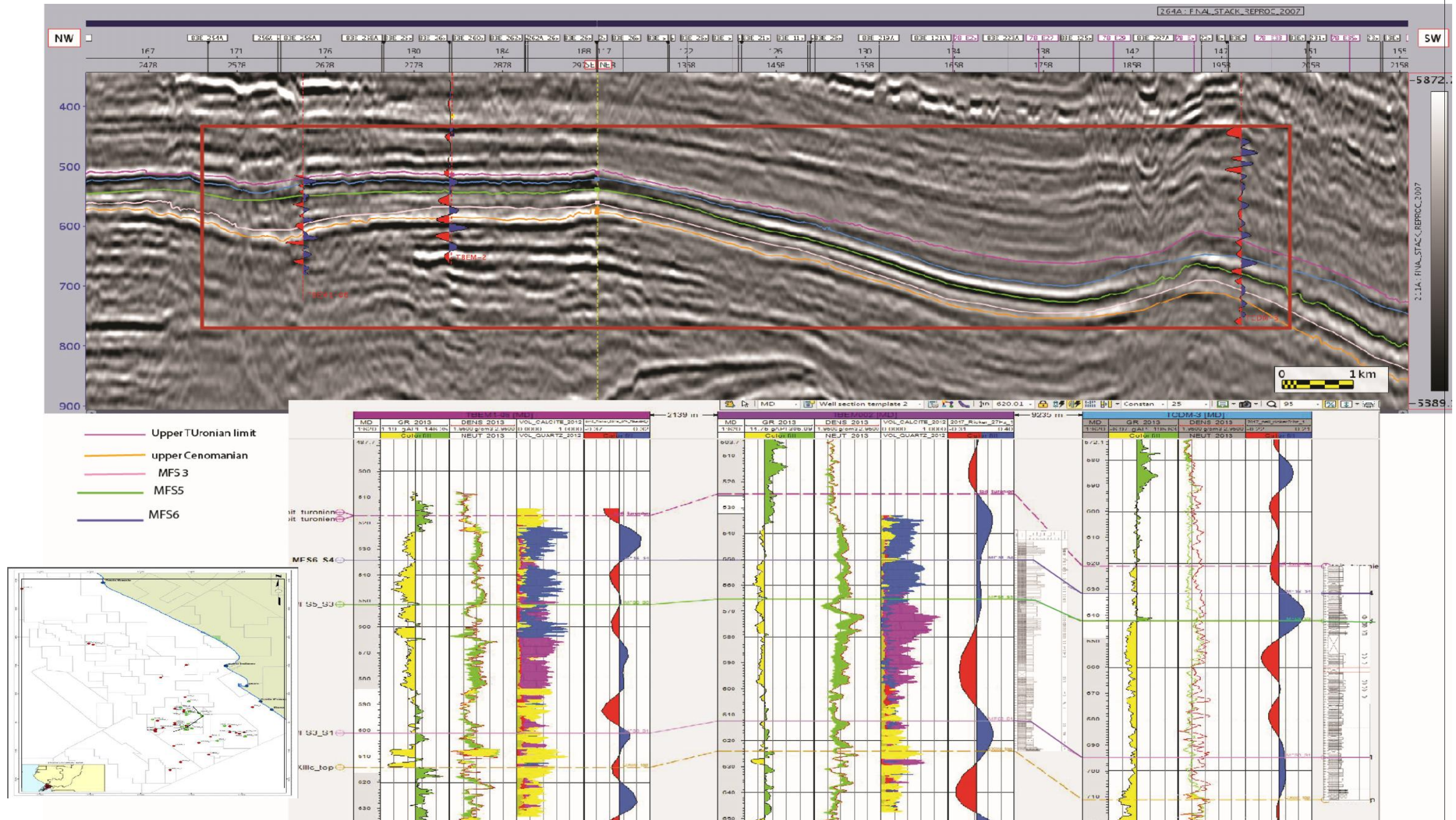


Figure 61: Basin correlation; cross section from TBEM106 to TCDM3 through TBEM2.

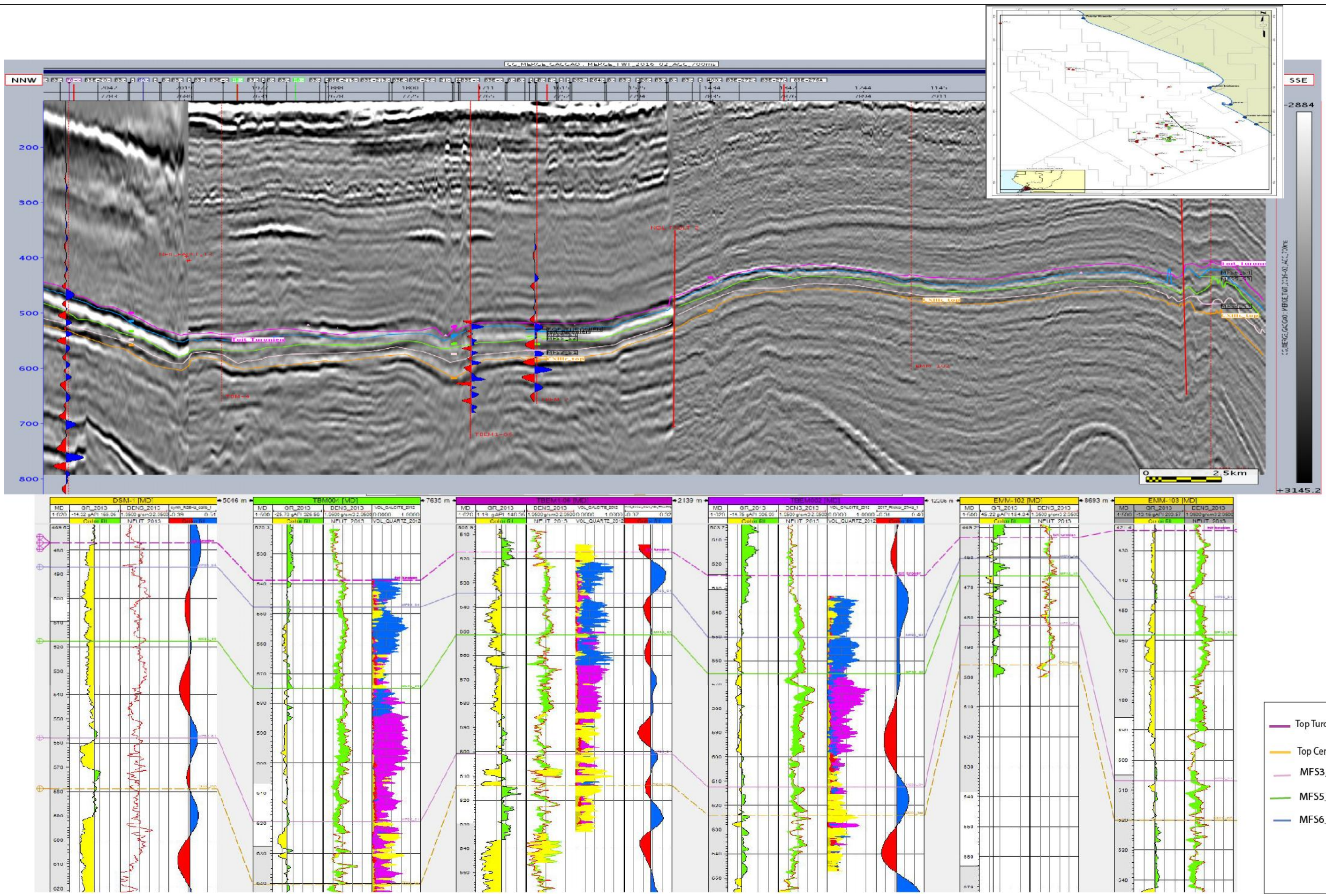


Figure 62: Basin correlation, cross section from DSM1 to EMM103

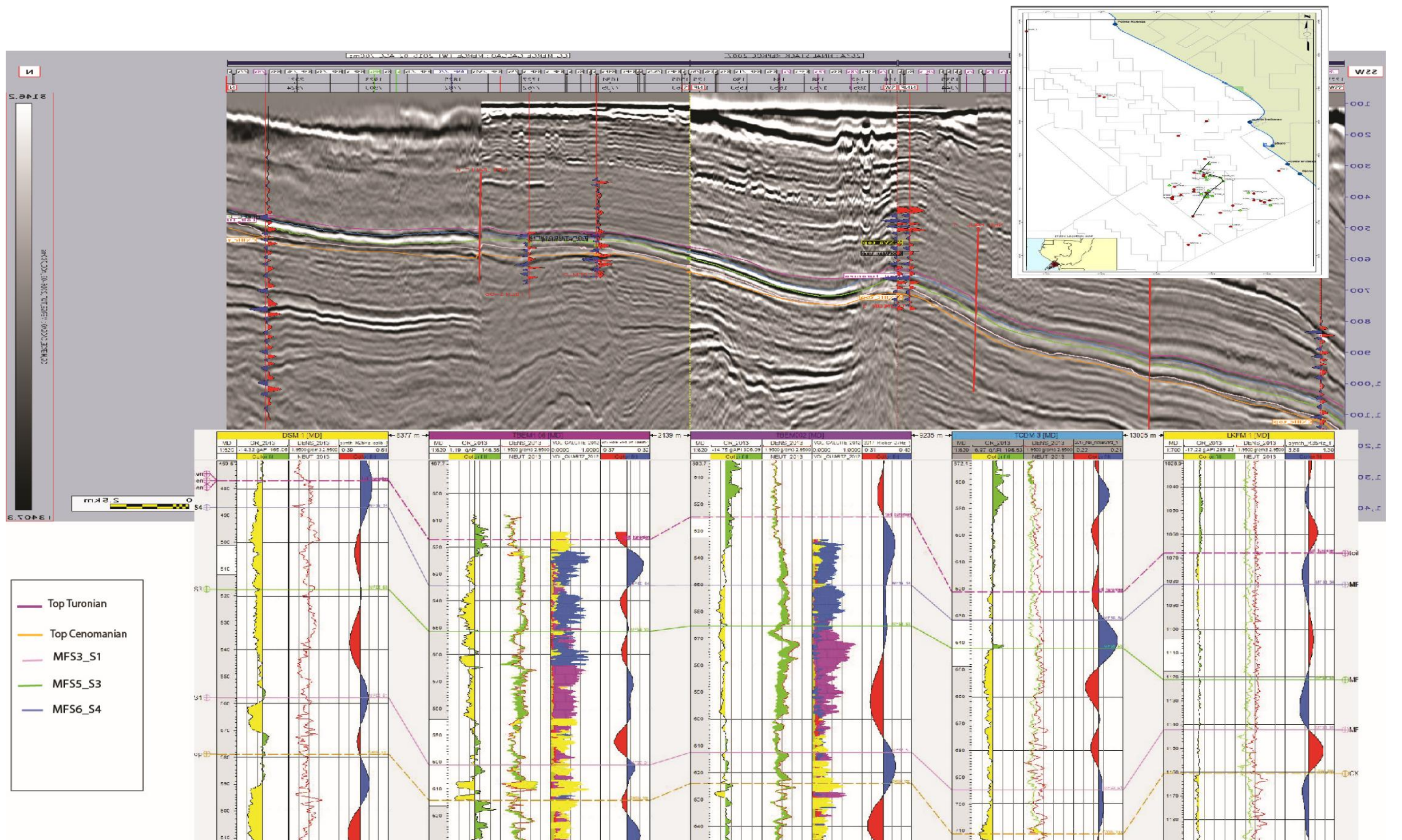


Figure 63: Basin correlation; cross section from DSM to LKFM1

Sequence 1: It is bounded upward by SB5, this sequence indicates deposition from fluvial to bay environments. It has preserved transgressive and regressive tracts.

Transgressive tract shows basinward progression from alluvial deposit to distal bay deposits. This transgressive system tract is marked by second order cycles delineated by soil facies mainly developed in marginal bay environments. As characterized above the sequence boundaries delineating those second order cycles could be related to fault movements which have triggered transgressive-regressive movement of the sea level. The maximum flooding interval consists of *Teichichnus* bioturbated argillaceous facies; its Maximum flooding interval is clearly identifiable on seismic section.

Regressive system tract consists to regular coarsening upward from distal bay to upper shoreface to marginal bay facies. During this sea level fall period, second order cycles were also noticed where basinward progression showed evolution from distal bay setting to shoreface followed by backstepping from upper shoreface to marginal bay setting. This latter backstepping episode was marked by formation of soil facies considered as induced by fault movement which triggered shoreline regression. Soil facies was only observed in well TBEM-2 and TBEM-106 which are situated near the fault while further basinward this facies which acts as emersion surface was not observed. This is consistent with Walter law which indicated deepening of the environment as one move basinward.

Sequence 2:

The major sequence 2: It is bounded by SB5 and SB6. This sequence indicates deposition in ramp setting. Its transgressive tract shows basinward shift from marginal bay to deep ramp setting. The maximum flooding interval for this sequence corresponds to bioturbated (*Thalassinoides*) facies. This interval was observed throughout the basin and recognized on well log. The regressive system tract indicates backstepping from deep ramp setting to shallow ramp (or shoreline Chenier). The tract characterized by bioclastic silty grainstone shows emersion surface or hardground corresponding to the final stage of regression. The maximum flooding surface corresponding to this sequence is not recognizable on seismic section.

Sequence 3:

The major sequence 3 indicates evolution of the sediment from shallow ramp or shoreline chenier to offshore setting. This sequence has preserved transgressive and regressive tracts. It indicates that transgressive tract corresponds to basinward shift from emersion surface to offshore setting. Hence, the sediment deposited from shallow ramp to offshore setting while regressive tract indicates backstepping from offshore to deep ramp setting. Here the flooding interval corresponds to bioturbated argillaceous offshore facies.

Sequence 4:

The major sequence 4 indicates deposition in deep environment below the wave base. It shows transgressive tract characterized by deposition from deep ramp to offshore while regressive tract indicates backstepping from offshore to deep ramp setting.

The above major sequences indicate an overall transgression which is consistent with a major transgression which took place during Turonian and which established the first communication

between Atlantic and Tethyan waters in Guinea golf, West Africa (Reyment, 1980; Brownfiled & Charpentier, 2016). Reyment (1980) had drawn the same evolution of the environments where transgression swamped many marginal areas (environments) moreover in the Turonian of Morocco the same depositional environments and general transgressive sequences were observed.



### 3.4. Diagenetic environment, processes and relationship with sedimentological evolution

From the above facies descriptions, the dominant diagenetic cements are: microsparry to sparry equant, drusy and blocky cements. The filling of moldic space by secondary dolomite shows that dolomitization and deposition are not synchronous and that dolomitization post-dated deposition. Therefore, dolomitization and deposition occurred in two different environments. In addition, facies show that cement post-dated burial (compaction) as no evidence of fractured or broken cements was evidenced.

Well TBEM-2 was selected to evaluate the evolution of the diagenetic environments during Turonian.

The interval between 624.3 and 598m shows facies dominated by silico-clastic sediments with microsparry cementor showing no cement between grains (particularly in sandstone facies); **this indicates development in meteoric environment:**

- Between 624.3 and 610m, the cement shows recrystallization of aragonite to Mg-calcite. This may result from the sediments exposition to meteoric water infiltration which triggered aragonite leaching. Considering that dolomitization post-dated deposition and that Mg-calcite leaching do not produce enough Mg for dolomite formation, and the emersions corresponding to paleo-soil facies in this interval (see fig. 59) may have played important role during dissolution recrystallization through action of organic acid (humic acids). This important leaching led to high intergranular porosity observed in sandstone facies.
- Between 610 and 602m, sea level fall (regression) may have led to exposure to meteoric water which induced dissolution of unstable mineral. Mg could have been introduced by organic matter during low stand.
- Between 602 and 598m, the sediments mostly carbonated are characterized by subhedral and anhedral dolomite mosaic or with a sucrosic aspect at certain depth. This dolomite shows a translucent aureole around, sparry equant cement and moldic porosity which is considered to characterized a meteoric water zone. This zone is although considered as being deposited during transgression period; Moore (1989) explained that during sea-level rise and subsequent high stands, carbonate islands are established along the margins of carbonate platforms and meteoric lens beneath these islands which is function of recharge, islands width, and hydraulic conductivity (Budd & Vacher, 1991; Kindler & Hearty, 1997).

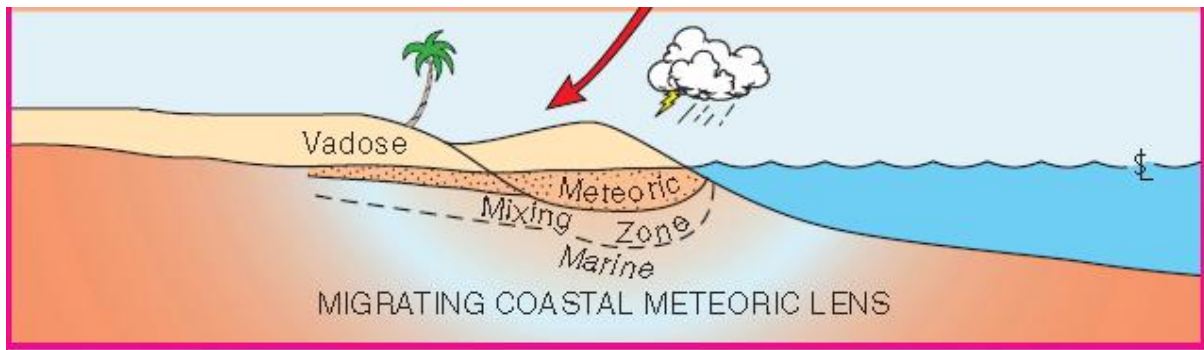


Figure 64: Hydrologic settings of meteoric diagenetic environments as a function of sea level and depositional settings (isolated platform vs. land-tied shelf). (A) During sea-level high stand; (B) during sea-level low stand (Moore, 1989).

The regression phase between 598 and 572m shows diagenetic facies characterized by sparry cement, moldic porosity; these characteristics correspond to development in meteoric zone (Land 1970, Moore, 1989).

Moore (1989) explained that carbonate shelves tend to be steep sided and relatively flat topped and that a relative sea level fall may lead to exposure of the entire shelf or platform to meteoric water and establishment of meteoric aquifer. Hence meteoric water infiltration induced unstable minerals (Mg-calcite and aragonite) dissolution and recrystallization of original aragonite or Mg-calcite into dolomite. This recrystallization occurs by addition of Mg excess through either fluxing of Mg resulting from dedolomitization of dolomite elsewhere or by mixing with Mg rich marine water or through action of organic matter.

According to Budd & Vacher (1991), short period exposure to meteoric lens seems to lead to significant diagenetic overprint, including moldic porosity after aragonite dissolution, cementation by calcite circumgranular crust by conversion of Mg-calcite into calcite (this could explain translucent aureole around the dolomite grain). The excess in calcite from Mg-calcite dissolution and calcite dissolution may have concentrated in moldic space and crystallized. This concentration of calcite could have been induced by development of hardgrounds within this section; the interval between 576 and 570m may have acted as barrier to calcite rich fluid flow and kept it in pore space in which calcite precipitated.

**Hence, this interval developed in meteoric environment. This section has developed in diagenetic meteoric zone.**

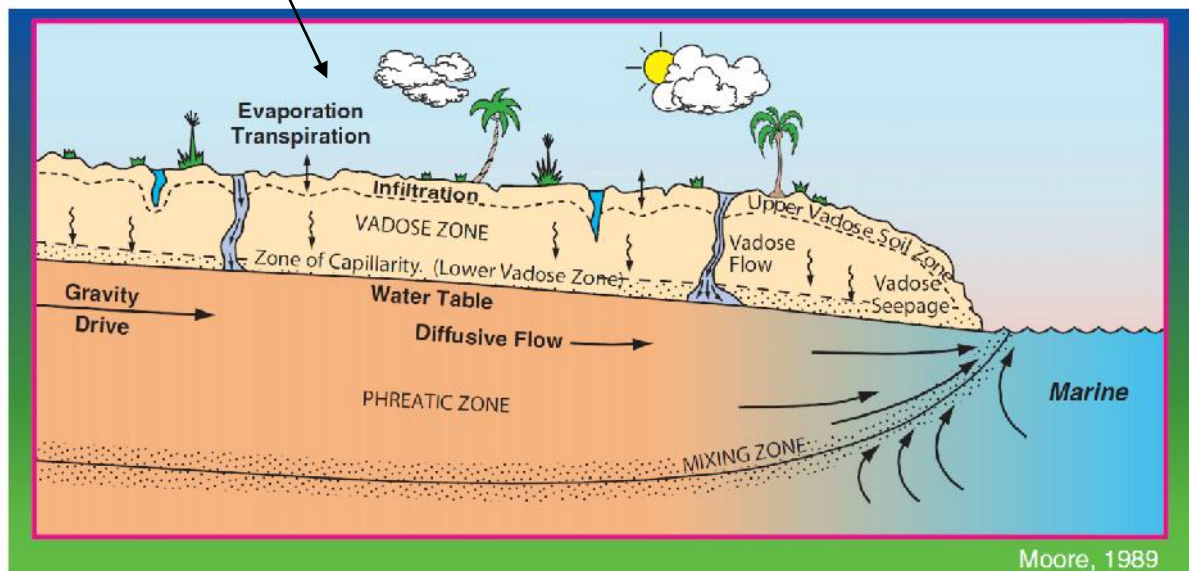
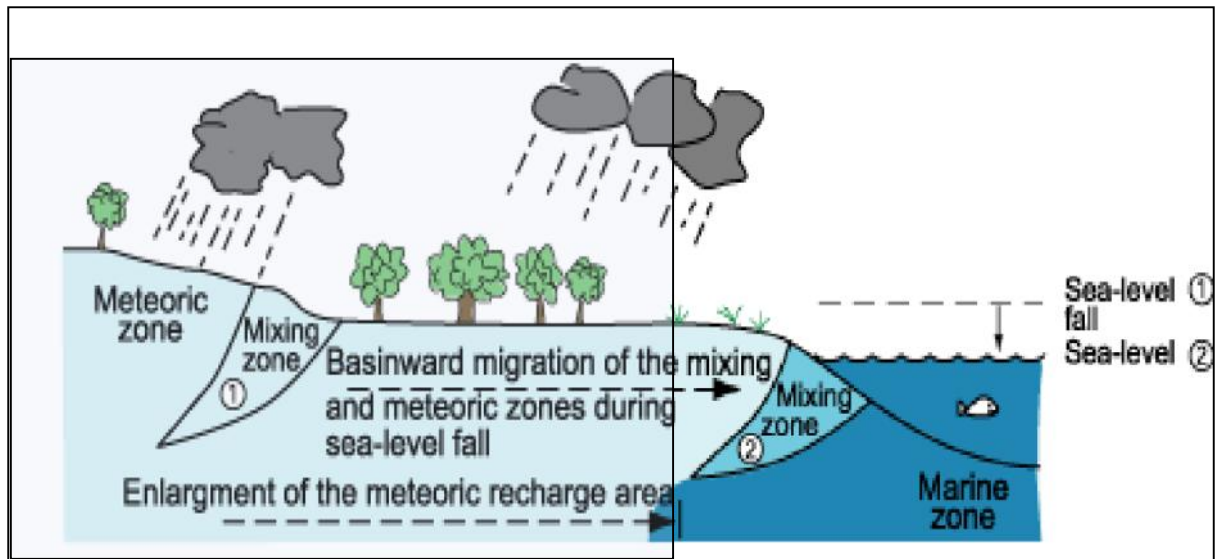


Figure 65: Conceptual model of the major diagenetic environments and hydrologic conditions present in the meteoric realm (From Moore, 1989).

Between 570 and 565m, the sediments show sucrosic dolomite with intercrystalline porosity. The genesis of this diagenetic facies may be explained by integrating Purser's 1985 model where rising marine water brought calcite and which precipitated between flushed dolomite rhombs resulting from early dolomite dissolution by fresh water along landward margin (fig 66).

The emersion surface (hardground) observed in the well TBEM-2 between 573 and 570m, may have played an important role as sedimentological barrier to vertical infiltration of meteoric water and hence induced horizontal diffuse flow which brought dolomite rhombs. The calcite brought by marine water was later dolomitized probably by mixing with meteoric water. Hence, this section underwent diagenesis in mixed meteoric-marine water zone.

Choquette & Pray, 1970; Murray, 1960 and Roehl & Choquette, 1985, related sucrosic facies to Meteoric phreatic environment. This facies may have developed in mixed meteoric phreatic-marine environment. **Purser (1985) defined a development process from dissolution–cementation in meteoric environment, dedolomitization and dolomitization in mixed meteoric-marine environment, which is coherent with this facies.**

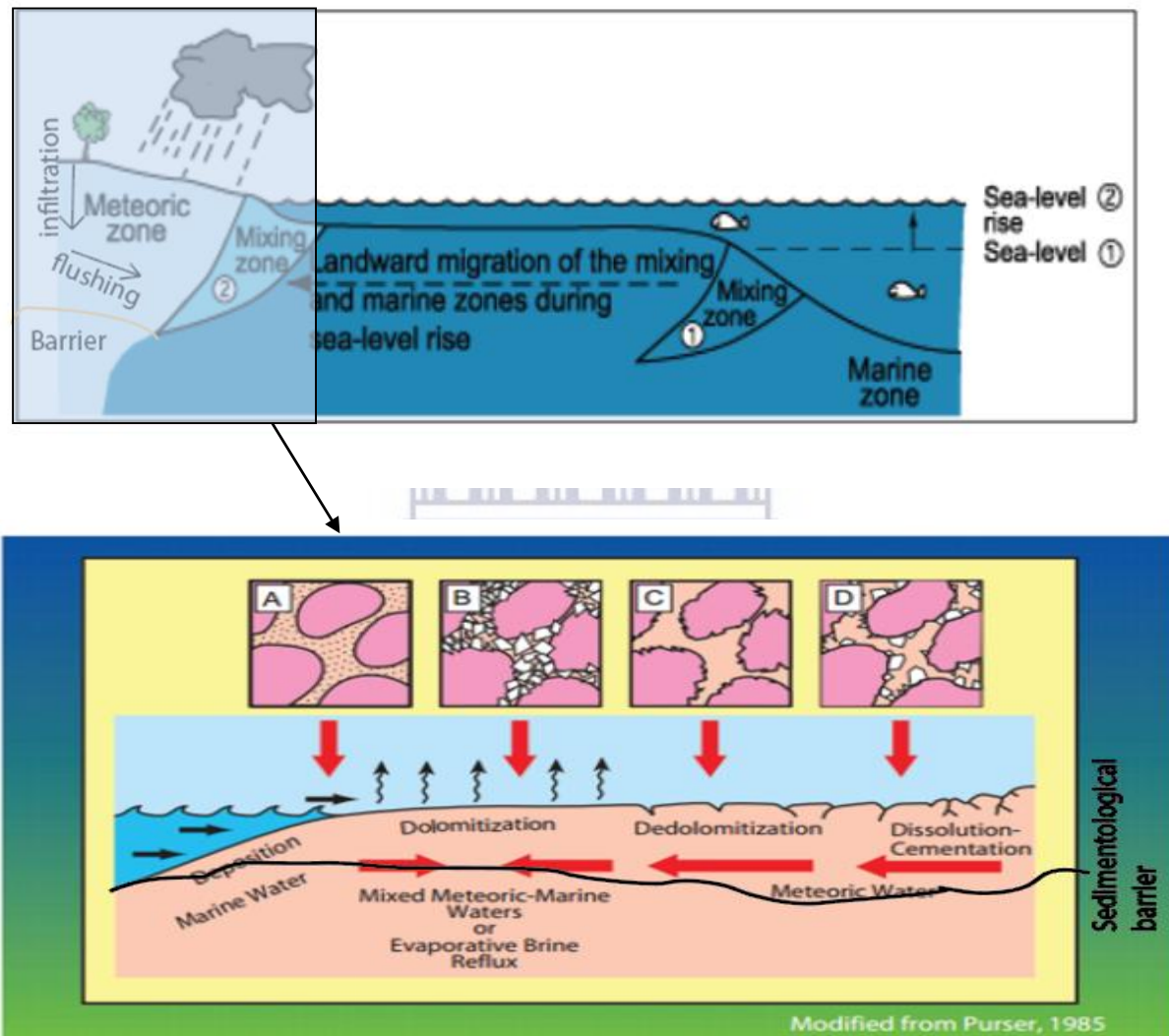


Figure 66: Geologic setting for the dolomitization–dedolomitization of Jurassic ooid packstones from the Paris Basin. Final porosity consists of cement-reduced dolomite crystal-moldic porosity. Used with permission of Springer-Verlag, New York (From Purser, 1985).

The interval between 565 and 542m presents facies characterized by microsparry to sparry cement with a patchy distribution (blocky cement) and both aragonite remnant and shells structures overprint. Land (1970) and Moore (1989) described this diagenetic facies as developed in meteoric-vadose zone.

This interval shows more recrystallization than dissolution. This developed through inversion of former aragonite to calcite or loss of Magnesium by Mg-calcite. Aragonite and Mg-calcite being purely marine minerals this shows existence of marine conditions or environment. This

section displays selective dolomitization of micritic matrix which may have resulted from partial dolomitization of the former unstable minerals by hypersaline marine water. Dissolution coincided with regression phase; the water table lowering induced by regression phase (sea level fall) may have allowed infiltration of meteoric water which in turn induced leaching of Mg from Mg-calcite and precipitation. This may have caused plugging of existing porosity by precipitation of calcite (fig 54).

All the above indicates that **during Turonian, the dissolution was most active only during low stand periods. The different diagenetic environments induced different porosity type as the degree of leaching of the unstable crystals varies from one environment to another; coupled with action of humic acid where soil developed.** Dolomitization resulted mainly from exposure to marine to hypersaline- marine water during stand and mixed marine-meteoric water during intermediate low stand. Dissolution could have resulted only during final phase of low stand.

### 3.5. Petrophysic properties

Considering the two reference wells (appendix 10, 11, 12); it appears that porosity and permeability logs show no relationship with depth; this is consistent with the fact that no compaction effect has been noticed during facies study. However, it appears that each facies displays different porosity and permeability values. Hence, these properties are related with intrinsic characteristic of each facies (figure 67 and 68).

Well TBEM-2 was chosen to study relationship between facies, permeability and porosity values. The values of the petrophysical properties and the nature of the rocks allowed determination of reservoirs and non-reservoirs facies:

Reservoirs facies from the base to the top of the well are:

- ❖ Reservoir 1 (T2a) (624-622m) consists of dolomitic sandstone (facies 9 and 10) and it presents 25% porosity and a permeability of 1113mD. These values are consistent with characteristic of this facies which shows intercrystal porosity, well sorting allowing accumulation of hydrocarbon and pore connectivity also allowing hydrocarbon to flow through the rock. Pore connectivity was increased by high degree of cement leaching.
- ❖ Reservoir 2 (T1b) (598-582m) consists of facies silty dolomite facies 14. It presents 30% porosity and low permeability 1.63 to 34mD. These results could be explained by diagenesis effect on the rock. Study of this facies both from core and thin sections revealed that development of large vacuoles and few molds and vugs (from selective dissolution of the matrix) which could have raised original porosity. However, less connectivity between vacuoles and molds coupled with the matrix which is slightly argillaceous strongly decrease horizontal permeability within this reservoir. Moldic and cavernous (vacuolar) porosities coupled with the observed extensive circumgranular crust cementation in this interval is consistent with porosity development in meteoric phreatic zone.
- ❖ Reservoir 3 (T1a) (581-565m) consists of four different facies, each displaying different petrophysical properties. These facies as observed in well TBEM-2 are:

- Facies 14 as for reservoirs T1b
- Facies 15 consisted of silty dolomitic mudstone shows 20% porosity and 20mD permeability. These values are related to moldic type of porosity coupled with low connectivity between molds which strongly affected permeability.
- Facies 18 made of packstone bioclastic dolomite presents 20% porosity while permeability varies for the same facies from the base to the top within this reservoir. Here the difference in permeability could also be related to the degree of connectivity within the same facies. At depths where only few dissolutions occurred (selective dissolution), connectivity pores or molds connectivity is low and hence permeability will also be lowered while at depths with high degree of dissolution, connectivity is increased and hence permeability is also increased.
- Facies 16 shows both high porosity from 23 to 40% and permeability between 1741 and 5963mD. These measures are related to the observed porosity which combined moldic, sucrosic and intercrystalline porosities. This highly increased porosity and the interconnectivity between pores favored high permeability. Note that the increase of silty and sandy fractions in this facies as compared to other facies may have also played a role in permeability increase. The high initial porosity (intergranular) combined with the solid volume decrease of mole-for-mole replacement during dolomitization could easily lead to the 30–40% porosity exhibited by many sucrosic dolomite reservoirs (Murray, 1960; Choquette & Pray, 1970 and Roehl & Choquette, 1985).

Reservoir 4 (T0b) and reservoirs 5 (T0a) consist of facies 17 with poor permeability 5mD and up to 20% porosity may be due to only partial dolomitization of the facies and the lack of dissolution.

**The above results evidence that porosity and permeability values in Turonian reservoirs are strongly related to the facies. Dolomitization and dissolution strongly affected development of porosity within the reservoirs; this particularly in dolomitic sections where dissolution either increased or decreased porosity by formation of vacuolar, moldic and sucrosic type of porosity. Furthermore, the degree of dissolution of calcite also played a significant role in porosity and permeability. It has been noticed that the reservoirs which underwent different type of diagenesis gave different porosity and permeability measures.**

**Silty and sandy fraction in the reservoirs also played important role in porosity and permeability increase.**

Non reservoirs (seal) facies are mostly argillaceous or silty argillaceous facies such as facies 11, 12, 20, 21 which presents porosity and permeability.

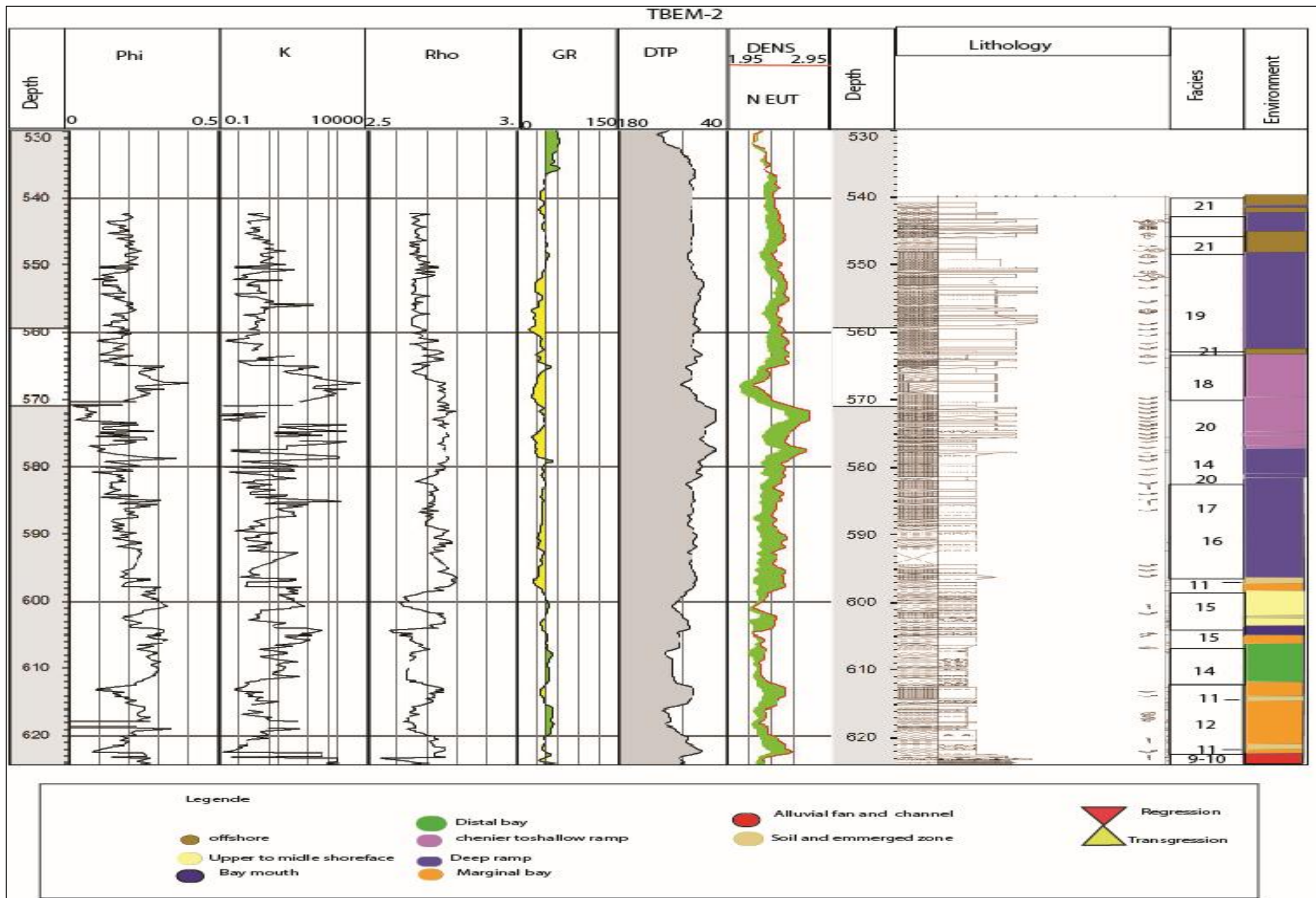


Figure 67: Petrophysical property – sedimentologic logs tied (well TBEM2)

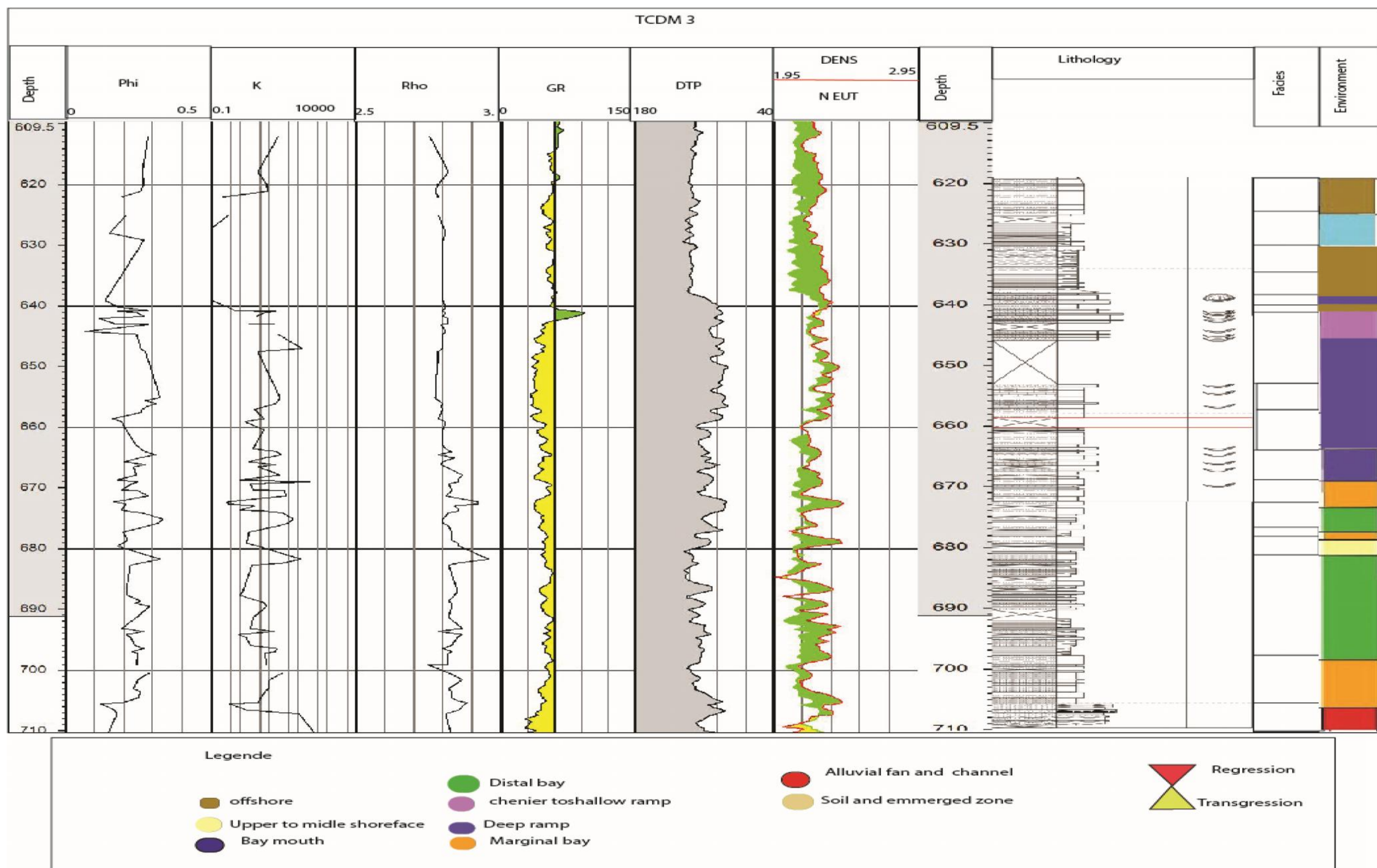


Figure 68: Petrophysical property – sedimentologic logs tied (well TCDM3)

## Chapter 4: Conclusions and recommendations

The Turonian series of the Congolese Coastal Basin have been largely study in this manuscript within the value and quantity of the available data.

Through this study it has been shown that:

- ❖ Onshore of the basin:
  - The previously considered Turonian Djeno and Mvassa outcrops are actually upper Coniacian -Santonian to lower Campanian.
  - Turonian rocks are only observed at the sea port lighthouse and Pointe Indienne.
  - The facies onshore and offshore of the basin are the same even though the sediments are not of the same age; **hence, the Loango dolomite known as characteristics of Turonian is diachronous from Turonian up to Campanian.**
- ❖ Offshore of the basin;
  - The Turonian series are lithologically constituted of dolimitic sandstone, dolomitic siltstone, dolomitic shale, bioclastic dolomite from mudstone to grainstone and dolomitic limestone comprising the Loango dolomite formation overlain by silty calcareous shale and argillaceous calcareous siltstone comprising the Madingo Marl.
  - The available cores were comprehensively analyzed and it appeared that the sediments deposited from fluvial-estuarine environment through bay to shoreline chenier or ramp and to open Marine environment; indicating that the Turonian sediments deposited during an overall **transgressive period characterized by four Major sequences** clearly recognizable on seismic profiles. The Stratigraphic study of the series also that this transgression was marked by low stand period and that syndepositional faults have also played a role in transgressive –regressive movement of the shoreline. Dip direction revealed a variation of the facies from proximal to distal environment marked by an increase of bioclastic facies (reservoirs facies).

Facies	Sedimentary environment	Reservoir /seal	Dolomitization effect on reservoir porosity
Argillaceous siltstone to silty claystone grey to green, very bioturbated ( <i>Teichichnus</i> ) with pyrite nodules	Marginal to Distal bay	Seal facies	
Dolomitic siltstone to very fine sandstone with slightly dipping bedding or HCS	Upper shoreface	Reservoir facies	Low porosity due to dolomitization
Planar cross bedded sandstone with argillaceous clast and plant debris at the base.	Fluvial/estuary	Reservoir facies	Poorly affected by dolomite cementation

Facies	Sedimentary environment	Reservoir /seal	Dolomitization effect on reservoir porosity
Silty Bioclastic Wackestone to grainstone with peloids and echinoderms bioclastic	Deep ramp	Reservoir	Porosity reduced by calcite recrystallization
Silty bioclastic dolomudstone to wackestone with <i>Thalassinoides</i>	Deep ramp	Reservoir facies	Porosity highly influenced by dissolution of the shells and silty fraction.
Silty bioclastic packstone to grainstone (limestone or dolomite) with Bivalves and Gastropods, bioturbated ( <i>Thalassinoides</i> ). shells are dismembered and dissolved	Shallow ramp to shoreline chenier	Reservoir facies	
Argillaceous calcareous siltstone (marl) to silty calcareous claystone with horizontal lamination or echinoids debris	Deep ramp	Seal	

- Diagenetic ally the present study evidenced that Turonian series were affected by secondary dolomitization which mainly affected precursor rocks during low stands through action of both meteoric water and paleo-soils. **The degree of exposure to meteoric to meteoric –vadose water, the initial lithology of the rocks has strongly affected porosity and permeability of the reservoirs.**

- Turonian series are constituted of reservoirs of various lithologies, from Sandy silty reservoirs to bioclastic reservoirs dolomite and limestone. These reservoirs porosity and permeability strongly depend on dissolution, lithology (sandy to silty fraction) and diagenesis. The latter either increased or decreased porosity and permeability.



UNIVERSITY *of the*  
WESTERN CAPE

## Chapter 5: References

- Abbott, R.T. & Morris, P.A., 1995. *A Field Guide to Shells: Atlantic and Gulf Coasts and the West Indies*. New York: Houghton Mifflin, p. 34
- Adams, J.E., Rhodes, M.L., 1961. Dolomitization by seepage refluxion. AAPG Bull. 44, 1912–1920
- Aigner, Th. & Futterer, E. 1978: Kolk-Töpfe und-Rinnen (pot and gutter casts) im Muschelkalk — Anzeiger für Wattenmeer? — N. Jb. Geol. Paläont. Abh., 156(3), 285–304.
- Aigner, T., 1982. Calcareous tempestites: storm-dominated stratification in Upper Muschelkalk limestones (Middle Trias, SW-Germany). Cyclic and event stratification, p.181-195.
- Antunes, M. T. & Cappetta, H., 2002. Sélaciens du Crétacé (Albien-Maastrichtien) d'Angola. *Palaeontographica, Abt. A*, 264 (5-6): 85-146, 3 fig., pl. 1-12.
- Augustinus, P., 1989. Cheniers and chenier plains: a general introduction. *Marine Geology*, 90, 219–229.
- Baudouy, S., and Legorjus, C., 1991. Sendji field, Republic of Congo, Congo Basin, in Foster, N.H, and Beaumont E.A., eds., *Treatise of petroleum geology , Atlas of oil and gas fields structural traps , Tulsa , Okla , AAPG*, p.121-144.
- Bengtson, P., 1996. The Turonian stage and substage boundaries. *Bulletin de l'Institut royal des Sciences naturelles de Belgique, Sciences de la Terre*, 66, 69-79.
- Biondi, P., 1996. Congo offshore, Upper Cenomanian-Turonian Sedimentological model of TCHIBOUELA/TCHIBOUELA EST MARINE fields; stratigraphic correlation between TCDM3, TCDM1-01, TBM-3, TBM-213 and TBEM-2, Elf Aquitaine report. Page 9 (unpublished).
- Blissenbach, E., 1954. Geology of alluvial fans in semi-arid regions. *Geol. Soc. Am. Bull.* 65, 175-190.
- Boltenhagen, E., 1967. Spores and pollen of the Upper Cretaceous of Gabon. [Spores et pollen du Crétacé Supérieur du Gabon.] *Pollen et Spores* Vol. 9 # 2 P. 335- 339.
- Boltenhagen, E. (1976) Senonian microflora of Gabon. [La microflore Senonienne du Gabon. ] *Revue de Micropaléontologie* Vol. 18 # 4 P. 191- 199
- Brice, S.E., Cochran, M.D., Pardo, Georges, and Edwards, A.D., 1982. Tectonics and sedimentation of the South Atlantic rift sequence, Cabinda, Angola, in Watkins, J.S., and Drake, C.L., eds., *Studies in continental margin geology: American Association of Petroleum Geologists Memoir* 34, p. 5–18.

Bromley, R.G., 1990. Trace Fossils. Biology and Taphonomy. Unwin & Hyman, London, P. 280.

Bromley, R. G. 1996. Trace fossils, biology, taphonomy and applications. 2nd ed. Chapman and Hall, London.

Brownfield, M. E. & CHARPENTIER R., 2006. Geology and total petroleum system of the West-Central coastal province (7203) West Africa; U.S. Geological Survey Bulletin 2007-B, p. 1-25.

Buatois, L. A., & Mángano, M. G., 2004. Animal-substrate interactions in freshwater environments: applications of ichnology in facies and sequence stratigraphic analysis of fluvio-lacustrine successions. Geological Society, London, Special Publications, 228(1), p. 311-333.

Buatois, L.A. & Mángano, M.G. 2001: Ichnology, sedimentology and sequence stratigraphy of the Cambrian Mesón Group in northwest Argentina. In Buatois, L.A. & Mángano, M.G. (eds): Ichnology, Sedimentology and Sequence Stratigraphy of Selected Lower Paleozoic, Mesozoic and Cenozoic Units of Northwest Argentina, 8–16. Fourth Argentinian Ichnologic Meeting and Second Ichnologic Meeting of Mercosur. Field Guide

Buatois, L. A., & Mángano, M. G., 2011. Ichnology: Organism-substrate interactions in space and time. Cambridge University Press.

Budd, D.A., Vacher, H.L., 1991. Predicting the thickness of fresh-water lenses in carbonate paleo-islands. J. Sediment. Petrol. 61, p. 43–53.

Callec Y., Fullgrof, T., Lasseur, E., Gouin J., Paquet, F., Thiebelmont, D., Maloungula, D., Makolobongo, B. and Obambi, U., 2014. Carte géologique au 1/200.000, Pointe Noire.

CASIER, E., 1957. Les faunes ichthyologiques du Crétacé et Cénozoïques de l'Angola et de l'enclave du Cabinda. Leurs affinités paléontologiques. Communicações dos Serviços Geológicos de Portugal, 38(2): p. 269-290.

Chen, A.; Chong, J.; Zhanghua, L., 2013 Salt tectonics and basin evolution of the Gabonese coastal basin, West Africa, Journal of Earth sciences , Vol.24.Nº6, page 903-917.

Choquette, P.W., Pray, L.C., 1970. Geologic nomenclature and classification of porosity in sedimentary carbonates. AAPG Bull. 54, 207–250.

Clifton, H.E., 1971. Orientation of empty pelecypod shells and shell fragments in quiet water. Journal of Sedimentary Research, 41(3), pp.671-682.

Collignon, M., 1961. Ammonites néocrétacées du Menabe (Madagascar). VII, Les Desmoceratidae. *Annales Géologiques du Service des Mines de Madagascar* 31: p.115.

COLLIGNON, M. 1966. Atlas des fossiles caractéristiques de Madagascar (Ammonites). XIV, Santonien. x + 1–134. Tananarive: Service Géologique

Cooper, M.R., 1998. Stratigraphy and paleontology of the Upper Cretaceous (Santonian) Baba Formation at São Nicolau. *Annals of the South African Museum*, volume 110, Issue 3, Pages 147-170.

Da Costa, J. L., Schorner, T.W. and Laws, B.R., 2001. Lower Congo Basin, Deep Water exploration province, offshore West Africa, AAPG Memoir 74, p.517-530.

Darteville, E., 1949. Les Poissons fossiles du Bas-Congo et des régions voisines par Darteville E. & Casier. E Musée

Darteville E., Freneix, S. & Sornay J., 1957. Mollusques du Crétacé de la cote occidentale d'Afrique du Cameroun à l'Angola. III. Conclusions stratigraphiques et paléontologiques; *Annales du musée royal du Congo belge, Tervuren (Belgique)*. Sciences géologiques, volume 24, page 35-48.

Darteville, E. & Casier, E., 1959. Les poissons fossiles du Bas-Congo et des régions voisines. *Annales du Musée du Congo Belge, Sér. A (Minéralogie Géologie, Paléontologie)*, 3, 2 (3): 257-568, fig. 77-98, pl. 23-39.

Deaf, A. S., Harding, I. C., & Marshall, J. E., 2014. Cretaceous (Albian—? Early Santonian) Palynology and Stratigraphy of the Abu Tunis 1x Borehole, Northern Western Desert, Egypt. *Palynology*, 38(1), 51-77.

Dickson, W. G., Fryklund, R. E., Odegard, M. E., 2003. Constraints for plate reconstruction using gravity data: Implication for source and reservoir distribution in Brazilian and West African margin basins: *Marine and Petroleum geology*, 20, p. 309-323.

Dixon, N. A., 2007. Experimental and theoretical hydrodynamic analysis of *Mercenaria* valves from the Florida Pinecrest beds.

Dorenkamp, A., 1973. Etude palynologique de 12 échantillons provenant d'affleurements de la Pointe Konda à la Pointe Mayumba. Société Elf pour la recherche pétrolière et l'exploitation des hydrocarbures, département géologiques central laboratoire, Elf Congo, archives exploration NDA N° RF 10356. p. 1-4.

Dorenkamp, A. & Jardine, S., 1973. Biostratigraphic study: Palynology and Micropaleontology of Congo basin post-salt series, ELF Congo report 2035n°3/ 816 R/md, page 12-14 (unpublished).

Duval, B., Cramez, C. & Jackson, M.P.A., 1992. Raft tectonic in Kwanza basin Angola; *Marine and Petroleum geology*, V.9, n°4, page 389-404.

El-Hedeny, M. M., Abdel Aal, A. A., Maree, M. and Seeling, J., 2001. Plicatulid bivalves from the Coniacian- Santonian Matulla Formation, Wadi Sudr, western Sinai, Egypt.- *Cretaceous Research* 22: 295- 308, London.

Emery, K.O., 1968. Positions of empty pelecypod valves on the continental shelf. *Journal of Sedimentary Research*, 38(4).

Emilianoff, 1934. Notes sur la région de Pointe Kounda, Moyen Congo ; Elf Congo, département exploration, Archives Elf Congo, NDA N°RF 12372; p. 1-4.

Flügel, E., 2009. *Microfacies of Carbonate Rocks, Analysis, Interpretation and Application*. Second edition Springer-Verlag, New York, p.681-715.

Fort, X., Brun J-P, Chauvel and Al, 2004. Salt tectonic on Angolan margin, syn-sedimentary deformation processes, *AAPG*, 88(8); p.1163-1184.

Fraaye, R.H.B. and Werver, O.P., 1990. Trace fossils and their environmental significance in Dinantian carbonates of Belgium. *Palaöntologische Zeitschrift*, 64, p. 367–377.

Frey, R. W., 1972. Paleocology and depositional environment of Fort Hays Limestone Member, Niobrara Chalk (Upper Cretaceous), west-central Kansas.

Fürsich, F.T., 1998. Environmental distribution of trace fossils in the Jurassic of Kachchh (Western India). *Facies*, 39(1), pp.243-272.

Fursich, F.T. and Pandey, D.K. 1999. Genesis and environmental significants of Upper Cretaceous shell concentrations from the Cauvery Basin, southern India. *Palaeogeography, Palaeoclimatology, Palaeoecology* 145, 119-139.

Futterer, E., 1978. Untersuchungen ueber die Sink- und Transportgeschwindigkeit biogener Hartteile. Investigations on the settling and transport of biogenic particles: *Neues Jahrbuch fuer Geologie und Palaeontologie. Abhandlungen*, v. 155, no. 3, p. 318-359.

Futterer, E., 1982. Experiments on the distinction of wave and current influenced shell accumulations. In *Cyclic and event stratification*, pp. 175-179. Springer, Berlin, Heidelberg.

Harris, N.B., 2000. Toca Carbonate, Congo Basin, Response to an evolving rift lake, in Mello, M.R. and Katz, B.J.; eds. *Petroleum systems of South Atlantic margin*, AAPG Memoir 73, p.341-360.

Haas, J.O., 1934. Etude géologique de la Pointe M'Vassa, Elf Congo/explo, archives Elf Congo NDA N° RF 1376. Page 1-4.

Hancock, J. M., & Gale, A. S., 1996. The Campanian Stage. *Bulletin de l'Institut royal des Sciences naturelles de Belgique, Sciences de la Terre*, 66, 103-109.

Haq, B.U., Hardenbol, J. and Vail, P.R., 1987. Chronology of fluctuating sea levels since the Triassic. *Science*, 235(4793), p.1156-1167.

Hirtz, P., 1951. Mission du Moyen Congo, rapport de fin de campagne, Société des pétroles d'Afrique Equatoriale Française; Elf Congo; département exploration; archives NDA N° 12366, p. 25-34.

Jackson, M.P.A., Cranez, C. and Fonck J.P., 2000, Role of Subaerial volcanic rocks and mantle plume in creation of South Atlantic margin, Implication for Salt tectonic and source rocks, Marine and Petroleum geology, 17, p. 477-498.

Jain, K.P. and Millepied, P., 1973: Cretaceous microplankton from Senegal Basin, NW Africa. 1. Some new genera, species and combinations of dinoflagellates. The Palaeobotanist, v.20, p.22-32, pl.1-

James, N.P., Bone, Y., Borch, C.C. and Gostin, V.A., 1992. Modern carbonate and terrigenous clastic sediments on cool water, high energy, mid latitude shelf: Lapepede, southern Australia. Sedimentology, 39(5), p.877-903.

James, N. P., & Dalrymple, R. W. 2010. Facies Models 4: GEOtext 6, Geological Association of Canada, St. John's, Newfoundland

Jardine, S., 1972. The genus *Hexaporotricolpites* Boltenhagen, 1967, morphology, systematics, stratigraphy, and geographic extension. [Le genre *Hexaporotricolpites* Boltenhagen 1967 Morphologie, Systematique, stratigraphie et Extension Geographique.] African Micropaleontological Colloquium, Proceedings, Actes 5<sup>th</sup>, p. 175- 190

Johnson, R.G., 1957. Experiments on the burial of shells. The Journal of Geology, 65(5), p.527-535.

Karner, G.D. & Discroll, N.W., 1999. Tectonic and stratigraphic development of the West African, and Eastern Brazilian margin; insight from quantitative basin modelling. In: N.R. Cameron, R.H., Bate and V.S., Clure (edition), the oil and gas habitats of South Atlantic. Geological society, London, Page 11-40.

Karner, G.D. & Discroll, N.W. and Barker, D.H., 2003. Syn-rift subsidence across the West African continental margin: the role of lower plate extension. In: T.J. Arthur, D.S., McGregor and Cameron, N.R. (editors), Petroleum geology of Africa: New themes and developing technologies. The geological society, London; p. 105-129.

Kauffman, E.G., Kennedy, W.J., Wood, C.J., Dhondt, A.V., Hancock, J.M., Kopaeovich, L.F. and Walaszczyk, I., 1996. The Coniacian stage and substage boundaries. Bulletin de l'Institut Royal des Sciences Naturelles de Belgique, Sciences de la Terre, 66(SUPPL.), p.81-84.

Kennedy, W. J. & Klinger, H., C.; 2014 Cretaceous faunas from Zuland and Natal South Africa. Valdedorsella, Pseudohaploceras, Puzosia, Bhimates, Pachydesmoceras, Parapuzosia (Austiniceras) and P.(Parapuzosia) of the ammonite subfamily Puzosinaespat. 1992

Kennedy, W. J. & Klinger, H. C., 1975. Cretaceous faunas from Zululand and Natal, South Africa. Introduction, stratigraphy. Bulletin of the British Museum of Natural History (Geology) 25 (4), p. 263-315.

Kindler, P. & Hearty, P.J., 1997. Geology of the Bahamas: architecture of Bahamian islands. In: Vacher, H.L., Quinn, T.M. (Eds.), *Geology and Hydrogeology of Carbonate Islands*. Elsevier Science B.V, Amsterdam, Netherlands, p. 141–160.

Kossmat, F., 1895-1898. Untersuchungen über die Südindische Kreideformation. *Beiträge zur Paläontologie Österreich-Ungarns und des Orients*. 9 (1895): 97-203; 11 (1897): 1-46 (108-153); 11 (1898): 89-152 (154-217).

Lombard & Schneegans, 1930. Etudes des echantillons de la pointe Mvassa. (Unpublished)

Lamolda, M.A. and Hancock, J.M., 1996. The Santonian stage and substages. *Bulletin de l'Institut royal des Sciences naturelles de Belgique, Sciences de la Terre*, 66(Supplement), p. 95-102.

Land, L.S., 1970. Phreatic versus vadose meteoric diagenesis of limestones: evidence from a fossil water table. *Sedimentology*, 14(3-4), p.175-185.

Le fournier J. & Mathieu M., 1972. Cretaceous lithofacies of Congo offshore exploration for Aptian-Cretaceous interval: Sedimentological description interpretation, ELF report 2035n°3/736R/CA, p.1-7 (unpublished).

Lindsay, R. F., & Kendall, C. G. S. C., 1985. Depositional facies, diagenesis, and reservoir character of Mississippian cyclic carbonates in the Mission Canyon Formation, Little Knife field, Williston basin, North Dakota. In *Carbonate Petroleum Reservoirs*, p.175-190. Springer New York.

Louango-Tchikaya, 1972. Etude géologique du port de Pointe Noire, Elf Congo, département exploration, archives Elf Congo, NDA N°10708.

Lui J., Pan X., Ma J., Tian Z., Chn Y., Man L., 2008. Petroleum geology and ressources of Western Africa, An Overview, *Petroleum Exploration and development* volume35, issue 3, p. 378-384.

Lindsay, R.F. & Kendall, C.G.S.C., 1985. Depositional facies, diagenesis, and reservoir character of Mississippian cyclic carbonates in the Mission Canyon Formation, Little Knife field, Williston basin, North Dakota. In *Carbonate Petroleum Reservoirs*, p. 175-190. Springer New York.

MacEachern, J. A., & Gingras, M. K. 2007. *SEPM Special Publications*. Special Publications, 88, p.149-193.

McHargue, T.R., 1990,.Stratigraphic development of protosouth Atlantic rifting in Cabinda, Angola–A petroliferous lake basin, in Katz, B.J., ed., *Lacustrine basin exploration case studies and modern analogs: American Association of Petroleum Geologists Memoir* 50, p. 307–326.

Mangano, M.G. & Buatois, L.A. (1994). Trazas fosiles e icnofabricas en depósitos carbonaticos cretácicos, Las Cuevas, Alta Cordillera de Mendoza. *Ameghiniana*, 31, p. 55–66.

Mantell, G.A., 1850. A Pictorial Atlas of Fossil Remains Consisting of Coloured Illustrations Selected from Parkinson's "Organic Remains of a Former World", and Artis's "Antediluvian Phytology". xii+207 p., 74 pl.; Henry G. Bohn, London, U.K.

Maples, C.G. and Archer, A. A., 1986. Shoaling-upward sequences and facies-dependent trace fossils in the Monteagle Limestone (Mississippian) of Alabama. *Southeastern Geology*, 27, p. 35–43.

Massala A., 1993. Le Crétacé supérieur et Tertiaire du bassin côtier congolais; Biochronologie et stratigraphie séquentielle. Université de Bourgogne, Centre des sciences de la Terre, p. 21.

Massala, A; Bellier, J-P; Magniez-Jannin, F. and Laurin, B., 1996. Biostratigraphy (Planktonic Foraminifera) and Environments of the Upper Cretaceous from two wells in the offshore Congo Basin; *Géologie de l'Afrique et de l'Atlantique Sud: Actes Colloques Angers 1994m*, p. 29-38.

Massamba L., 1984. Tchendo Marine 3, sedimentological and lithological study of cored reservoir zone (Cenomanian-Turonian-Senonian, (449-739m)); ELF report 2634 (unpublished).

Massamba L., 1985. Congolese Atlantic Basin, Sedimentologic study of Loango dolomite Formation and Madingo marl, ELF Congo report ref .PN>85/05, page 8-19 (unpublished).

Masse P., 2008. Revision of facies model and of sedimentary scheme of calcareous Turonian deposit of TCHIBOUELA MARINE, comparison with modern depositional environment and facies distribution at field scale, Total E&P Congo report, (unpublished).

Masters, C.D., 1965. Sedimentology of the Mesaverde Group and of the upper part of the Mancos formation, Northwestern Colorado. Dissertation. Yale University, U.S.A. p.88.

Matsumoto, T. 1954. Family Puzosiidae from Hokkaido and Saghalien. *Memoirs of the Faculty of Science, Kyushu University*, Series D, Geology 5, p.69-118.

Mboro, R., Anglada, R. and Brun, L., 1981. Le Bassin de Pointe-Noire (Congo), du Sénonien Supérieur au Néogène (stratigraphie-paléogéographie). *Cahiers de micropaléontologie* 4, p. 73-102.

Mbani, J. N., 2008. Micropaléontologie et géochimie organique du bassin côtier congolais au Crétacé supérieur: paléoécologie des foraminifères, espèces et associations indicatrices des paléoenvironnements des roches mères pétrolières (Doctoral dissertation, Université Pierre et Marie Curie-Paris VI).

Menard, L., 1996. Congo offshore, EMMERAUDE MARINE stratigraphical synthesis of upper Cenomanian-Turonian (Loango dolomite), Elf Aquitaine report 1177, p. 10-11 (unpublished).

Mc Hargue, T.R., 1990. Stratigraphic development of proto-south Atlantic rifting in Cabinda, Angola Petroliferous lake basin, in Katz, B.J., ed., lacustrine basin exploration, case studies and modern analogs; AAPG, Memoir 50, p. 307-326.

Middleton, G. V., 1967. The orientation of concavo-convex particles deposited from experimental turbidity currents. *Journal of Sedimentary Research*, 37(1).

Monsaingeon, A., 1983. Cenomanian-Turonian in the Congolese Coastal Basin, ELF Congo, report PN 83/60, p. 7-13 (unpublished).

Moore, C.H., Bebout, D.G., 1989. Carbonate Rock Sequences from the Cretaceous of Texas. 28th Int. Geol. Cong. Field Trip Guidebook T376, American Geophysical Union, Washington, DC, p.47.

Moore, C.H. & Wade, W.J., 2013. Carbonate Reservoirs: Chapter 7. Evaporative Marine Diagenetic Environment (Vol. 67). Elsevier Inc. Chapters.

Musial G., Reynaud, Gingras M. K., Féliès H., Labourdette R. and Parize O.; Subsurface and outcrop characterization of large tidally influenced point bars of the Cretaceous McMurray Formation (Alberta, Canada). *Sedimentary Geology* 279 (2012) 156–172

Murray, R.C., 1960. Origin of porosity in carbonate rocks. *J. Sediment. Petrol.* 30, 59–84.

Narbonne, G.M. (1984). Trace fossils in Upper Silurian tidal flat to basin slope carbonates of Arctic Canada. *Journal of Paleontology*, 58, 398–415.

Ngastsé L.R. & Guernet C., 1989; Les ostracodes du post-salifère congolais du Crétacé inférieur au Miocène: Systematique, Stratigraphie, Biogeographie. Université Pierre et Marie Curie (Paris).

Nichols, G., 2009. *Sedimentary and stratigraphy* (2<sup>nd</sup> edition) West Sussex:United Kingdom

Nombo-Makaya, N. and Han C. H., 2009; Pre-salt petroleum system of VAndji-Conkouati structure (Lower Congo Basin), Republic of Congo, *Research journal of Applied sciences* 9,101-107.

Numberg, D. & Muller, R.D., 1991. The tectonic evolution of the South Atlantic from late Jurassic to present. *Tectonophysics*, 199, p. 27-53.

Otvos, E.G., and Howat, W.E., 1996, South Texas Ingleside barrier, coastal sediment cycles and vertebrate fauna. *Late Pleistocene stratigraphy revised: Gulf Coast Association of Geological Societies Transactions*, v. 46, p. 333-344.

Potonie, R.,1970. Synopsis of the genera of the spora dispersae. Part 5. Supplement to all Groups (Turmae). [Synopsis der gattungen der spora Dispersae.5. Teil.Nachtrage Zu Allen gruppen. (Turmae)] Beihefte zum Geologischen Jahrbuch Vol. 87 # 5 P. 1- 172

Price, W.A., 1933, Role of diastrophism in topography of Corpus Christi area, south Texas: *American Association of Petroleum Geologists Bulletin*, v. 17, p. 907-962.

Purser, B. H., (Ed.) 1973. The Persian Gulf. Holocene Carbonate Sedimentation and Diagenesis in a Shallow Epicontinental Sea. 471 p., 250 figs, 7 pls, 3 maps. Springer-Verlag, Berlin, Heidelberg, New York

Purser, B.H. 1985. Dedolomite porosity and reservoir properties of Middle Jurassic carbonates in the Paris Basin, France. In, P.O. Roehl and P.W. Choquette (Eds.), Carbonate Petroleum Reservoirs. Springer-Verlag, New York, p. 341-355

Purvis, K., Wright, V.P., 1991. Calcretes related to phreatophytic vegetation from the middle Triassic Otter sandstone of south west England. *Sedimentology* 38, 539–551.

Read, J.F., 1985. Carbonate platform facies models. *AAPG bulletin*, 69(1), p.1-21.

Reineck, H.E., Singh, I. B. and Wunderlich, F., 1971: Einteilung der Rippeln und anderer mariner Sandkorper. *Senckenbergiana Marit.* 3, 93-101.

Reineck, H.E. & Singh, I.B., 1973. Depositional sedimentary structures.

Reineck, H.E. & Singh, I.B., 1980. Depositional sedimentary environments, with reference to terrigenous clastics, 2nd revised and updated ed.

Reyment, R.A., 1980. Biogeography of the Saharan Cretaceous and Paleocene epicontinental transgressions. *Cretaceous Research*, 1(4), pp.299-327.

Roehl, P.O., Choquette, P.W. (Eds.), 1985. Carbonate Petroleum Reservoirs. Springer-Verlag, New York, 622 pp.

Salazar-Jimenez, A., Frey, R.W. and Howard, J.D., 1982. Concavity orientations of bivalve shells in estuarine and nearshore shelf sediments, Georgia. *Journal of Sedimentary Research*, 52(2).

Sarjeant, W. A. S., 1970. The genus *Spiniferites* Mantell, 1850 (Dinophyceae). *Grana*, 10(1), 74-78.

Savoye, B., Babonneau N., Dennielou B. and Bez M., 2009; Geological overview of Angolan -Congo margin, the Congo deep-sea fan and its submarine valleys; Deep sea research: DOI 10.1016/j.dsr2.2009.04.001.

Schneegans, 1932. Etudes palynologiques des echantillons de la Pointe Mvassa. (Unpublished)

Schneegans, 1954. Etudes palynologique des echantillons du port de Pointe Noire. Unpublished

Schrank, E., 1992. Nonmarine Cretaceous correlations in Egypt and northern Sudan; palynological and palaeobotanical evidence. *Cretaceous Res.* 13:351–368.

Standlee, L. A., Brumbaugh, W. D., & Cameron, N. R. (1992). Controlling factors in the initiation of the South Atlantic rift system. *Eologie Africaine-Compte Rendus des colloques de Géologie de Libreville* (eds Curnelle R), Elf-Aquitaine, 13, 141-52.

Tomašových A. 2004. Effect of extrinsic factors on biofabric and brachiopod alteration in a shallow intraplatform carbonate setting (Upper Triassic, West Carpathians). *Palaios*, 19:349-371.

Toshimitsu, S., 1988. Biostratigraphy of the Upper Cretaceous Santonian Stage in northwestern Hokkaido. *Memoirs of the Faculty of Science, Kyushu University (D, Geology)* 26 (2): p.125-192.

Tröger, K.A. (compiler) & Kennedy, W.J. 1996. The Cenomanian Stage. *Bulletin de l'Institut Royal des Sciences Naturelles de Belgique. Sciences de la Terre* 66 (Supplément), 57-68.

Tucker, M.E. & Wright, V.P. (1990) *Carbonate Sedimentology*. Blackwell Scientific Publications, Oxford, pp 482.

Van Wagoner J.C, Posamentier H.W., and Mitchum R.M.J.R., 1988. An overview of the fundamentals of sequence stratigraphy and key definition. In: Wilgus CK, Hastings BS, Kendall CGStC, Posamentier HW, Ross CA, Van Wagoner JC (eds) *Sea level changes, an approach*. SEPM Spec Publ 42: pp 39–45

Walls, R. A., & Burrowes, G. (1985). The role of cementation in the diagenetic history of Devonian reefs, western Canada.

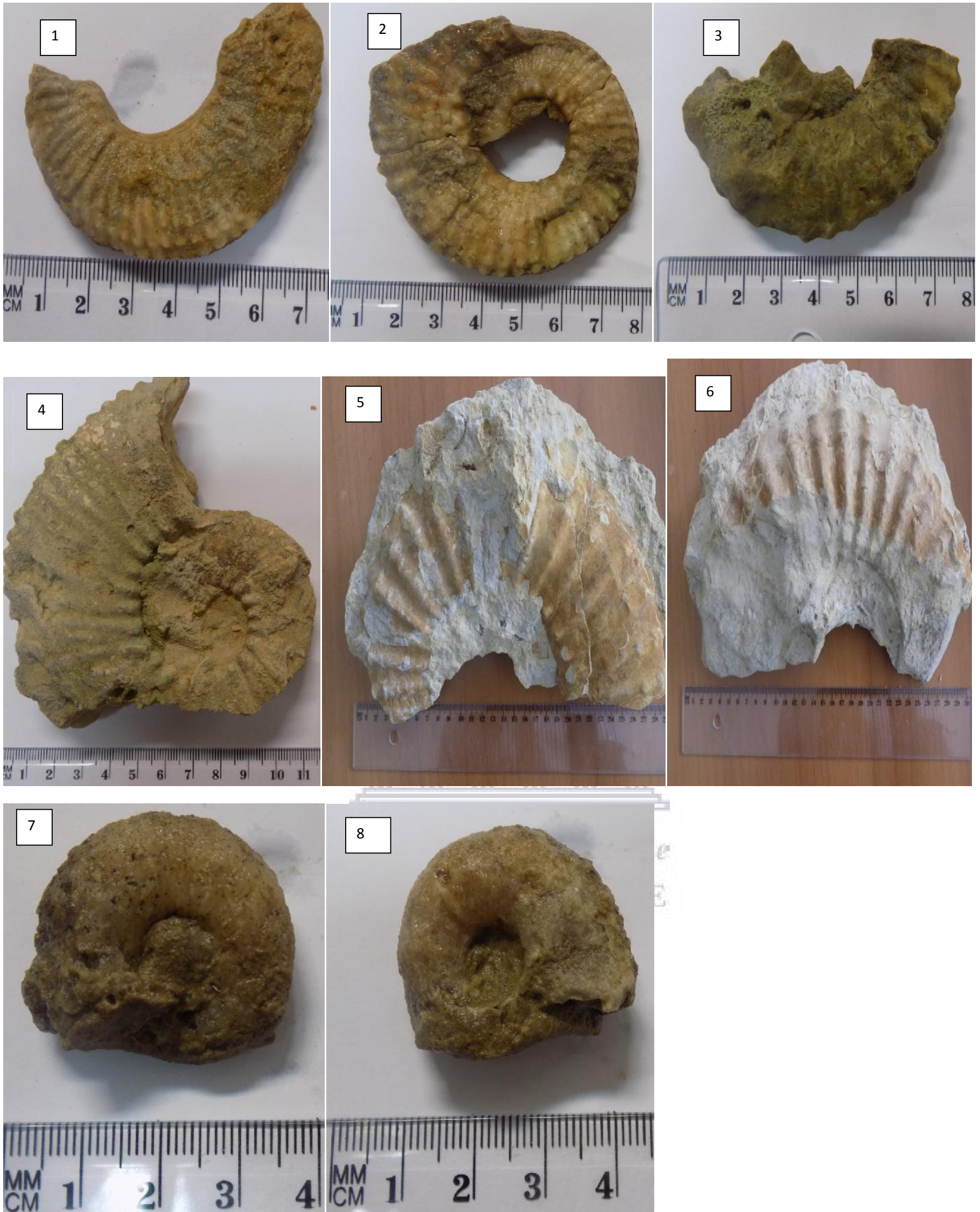
Wilson, J.L., 1975. *Carbonate facies in geological history*. 471 pp. Google Scholar.

Wright, C. W. 1957. Cretaceous ammonites. In: MOORE, R. C. ed. *Treatise of invertebrate gy. Part L. Mollusca 4*. New York and Lawrence: Geological Society of America and University of Kansas Press.

Wright, V.P., 1991. Paleokarst: types, recognition, controls and associations. In: Wright, V.P., Esteban, M., Smart, P.L. (Eds.), *Paleokarsts and Paleokarstic Reservoirs*. Univ. Reading, Postgrad. Inst. Sedimentol., Contr. 152, pp. 56–88 (Chapter 2)

Wright, C. W., Calloman, J. H. and Hozarth, M. K., 1996. *Treatise on Invertebrate Paleontology. Part L. Mollusca 4. Revised*. Boulder: The Geological Society of America Inc. and Lawrence: The University of Kansas.

## Appendix



Appendix 1: Figures 1, 2, 4: *Texanites venustus* Collignon, figure 3: *Prototexanites* sp., figures 5-6: *Texanites soutoni*, figures 7-8: *Menuites* sp.



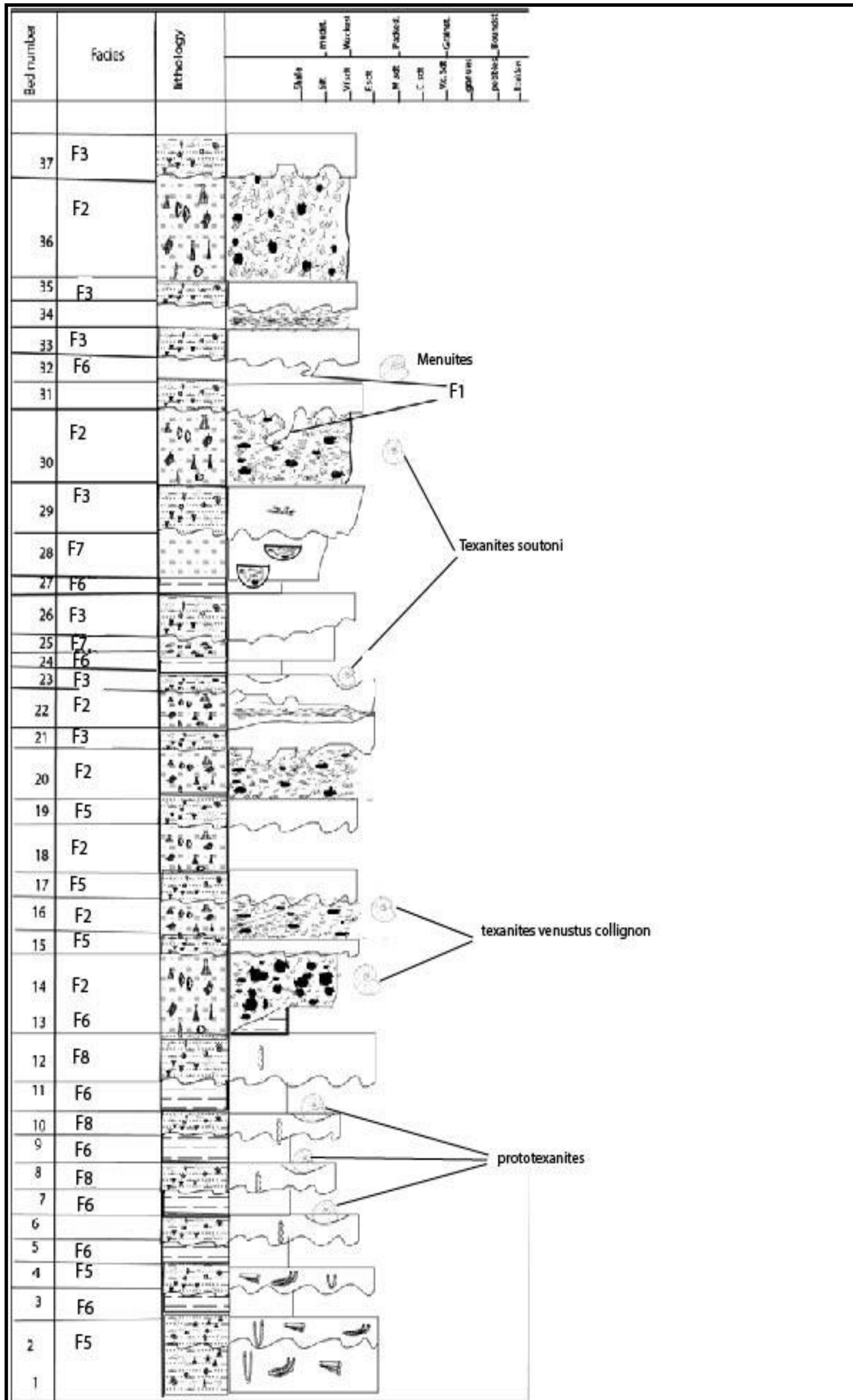
Appendix 2: Figures 9-11: *Lopha aucapitanei* (COQUAND), figures 12-13: *Lopha Lombardi* nov. Sp, figures 14-16: *Plicatula hirsuta*,



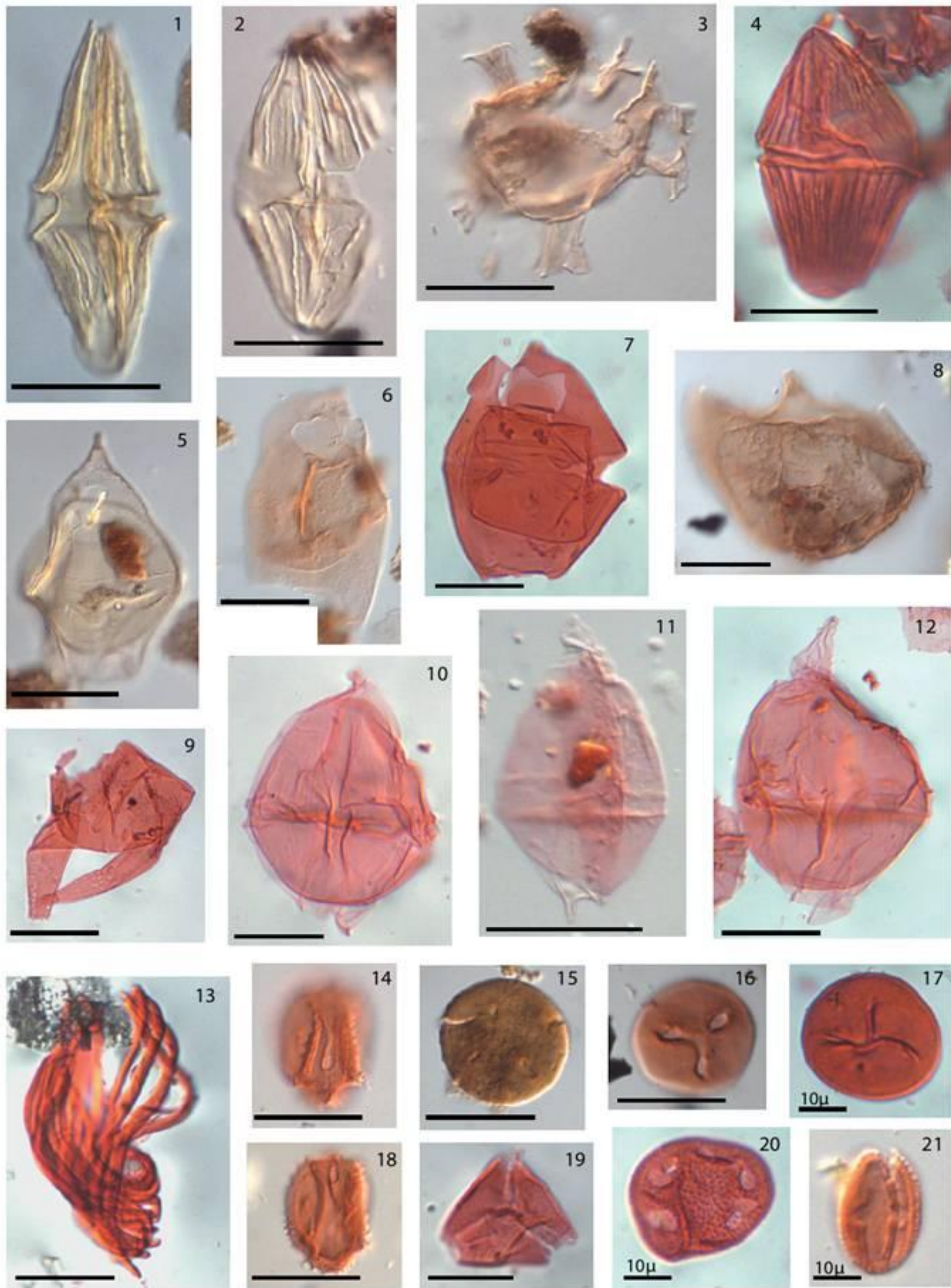
Appendix 3: 18-20 *Plicatula ferryi* Coquand, 21 *Fusus* sp., *Anchura* (*Dicroloma*) Sp., *Tibia* (*Calyptophorus*) *pallata* (forbes).



Appendix 4: Figures 24 and 27: *Trigonarca curvadonta*; figure 25: *Anofia aro* Reyment, figure 26: *Agelasina pledonta*; figures: 28-29: *Enchodus crenulatus*, figure 30: *Anacorax kaupi*, figures 31-34: fishbones.



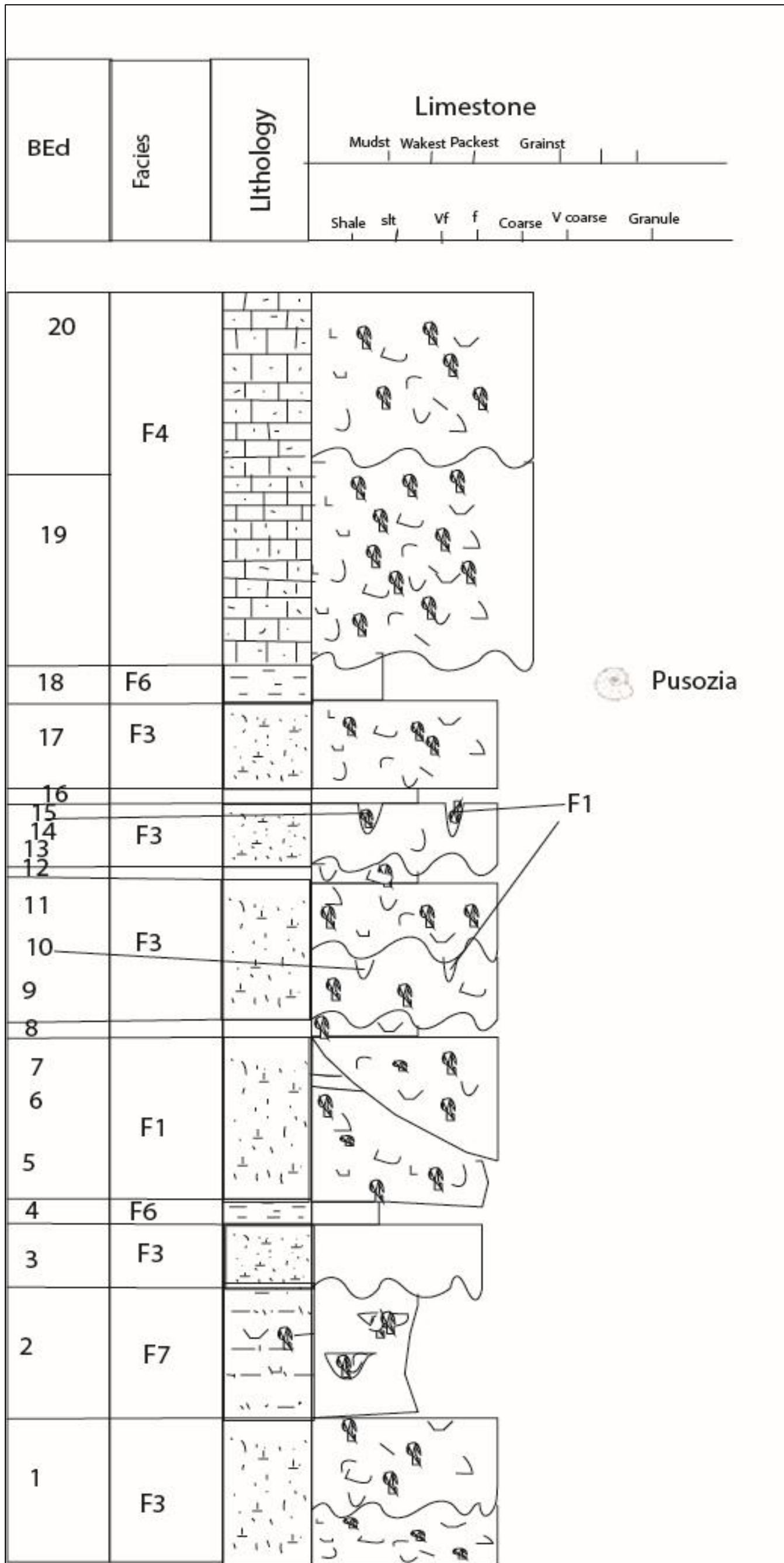
Appendix 5: Mvassa section



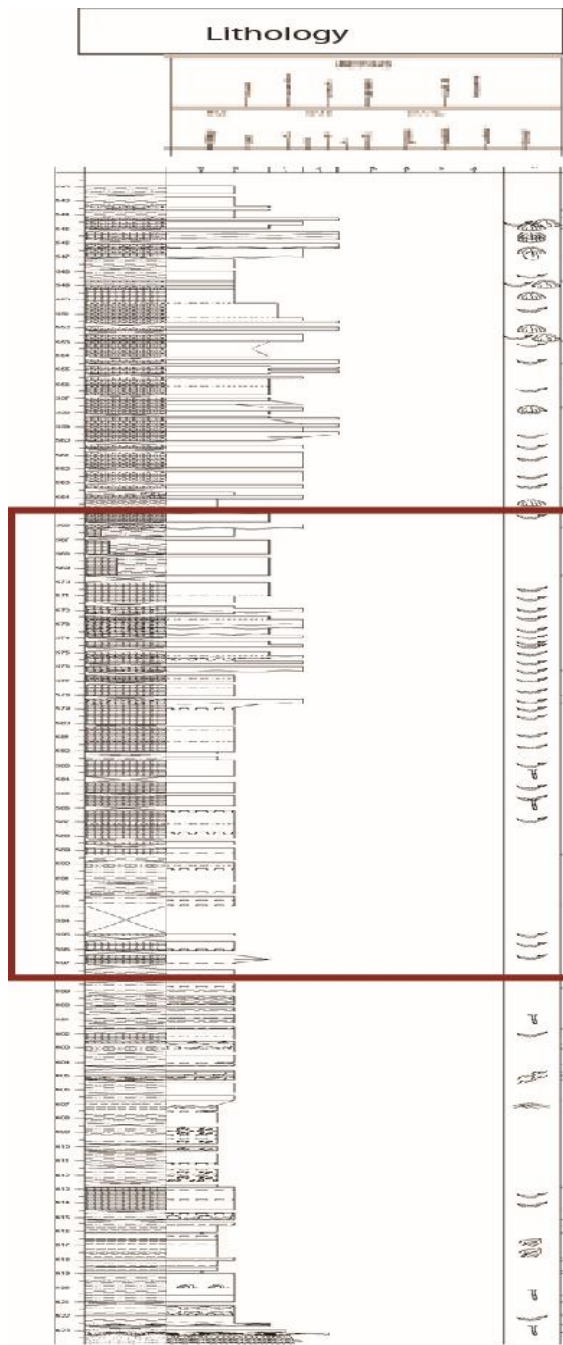
Appendix 6: A selection of CXIVb palynomorph index species is shown in this table. The material comes from both the Pointe M'Vassa and Djeno outcrops. The scale bar is 30µ long, except where otherwise stated. Figs. 1,2,4) *Dinogymnium* spp.; Fig. 3) *Oligosphaeridium* sp.; Figs. 5-7) *Isabelidium* spp.; Fig. 8) *Cribopteridinium* sp. ; Fig. 9) *Odontochitina costata* ; Figs. 10-12) *Senegalinium* spp. ; Fig. 13) *Ephedripites jansonii*; Figs. 14,18) *Hexaporotricolpites emelianovi*; Figs. 15-17) *Constantinisorites* spp.; Fig. 19) *Myrtacidites* sp.; Fig. 20) *Cretacaeiporites* cf. *infrabaculatus*; Fig. 21) *Tricolporites* sp. 164.



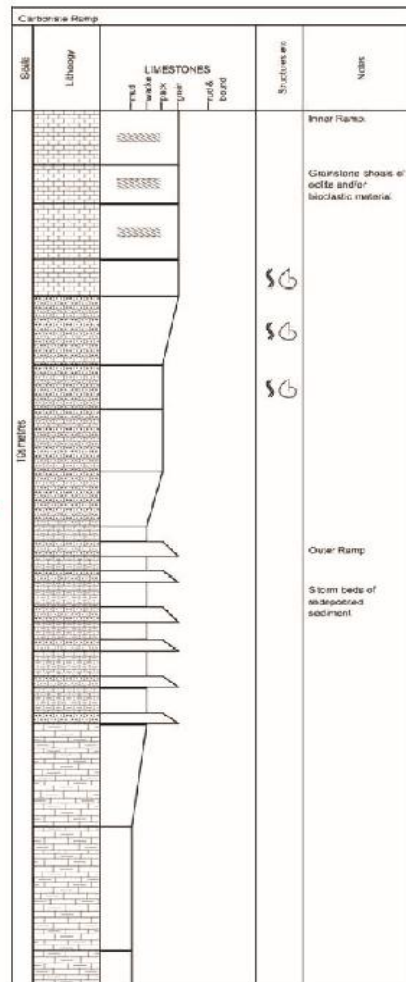
Appendix 7: 1 *Puzosia* Sp, 2 *Trigonarca curvadonta*, 3 *Plicatula ferryi* COQUAND, 4 *Trigonarca curvadonta*



Appendix 8: Djeno section.

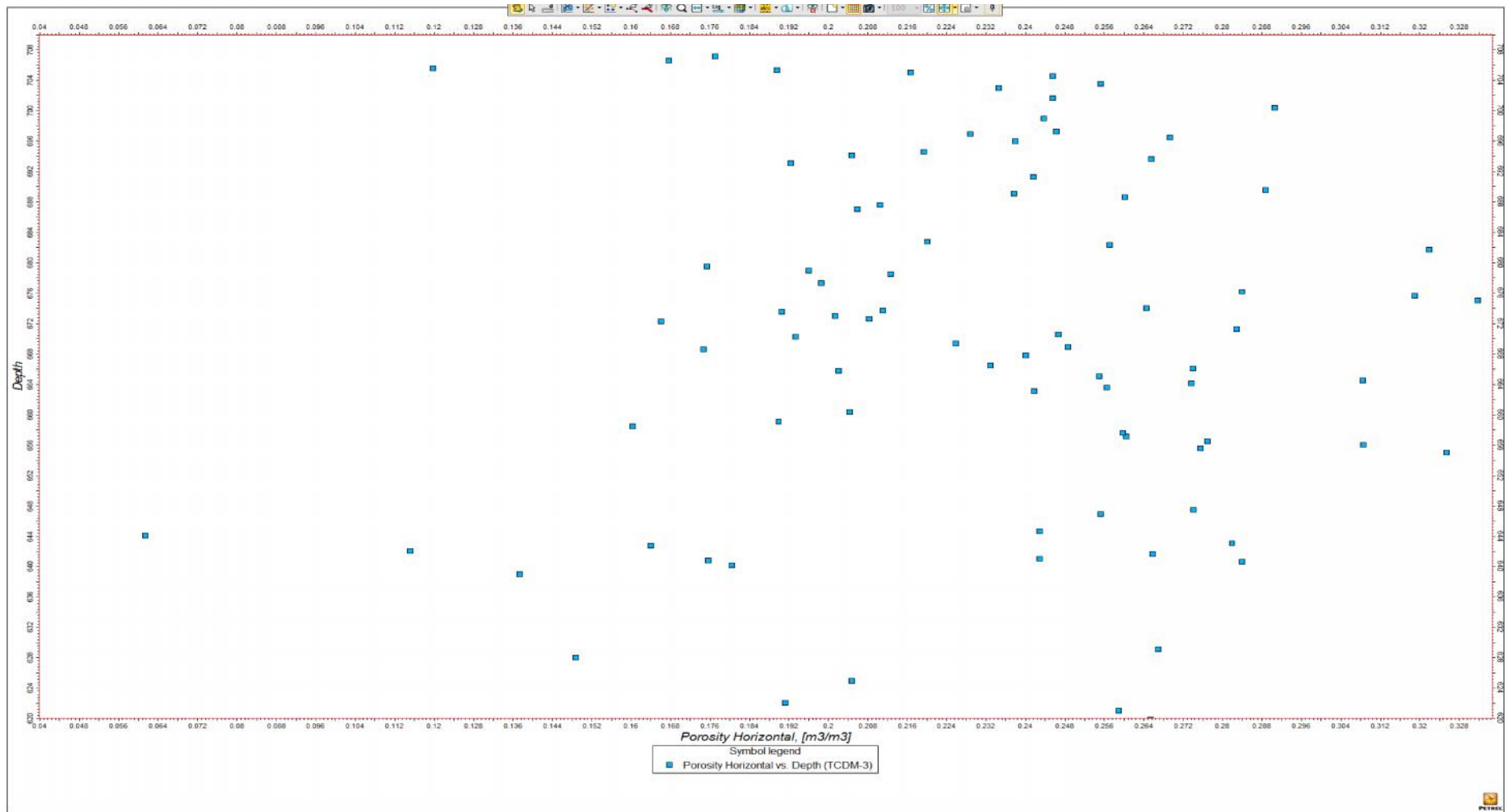


Well TBEM-2 sedimentological sequence (in red box carbonate parasequence)

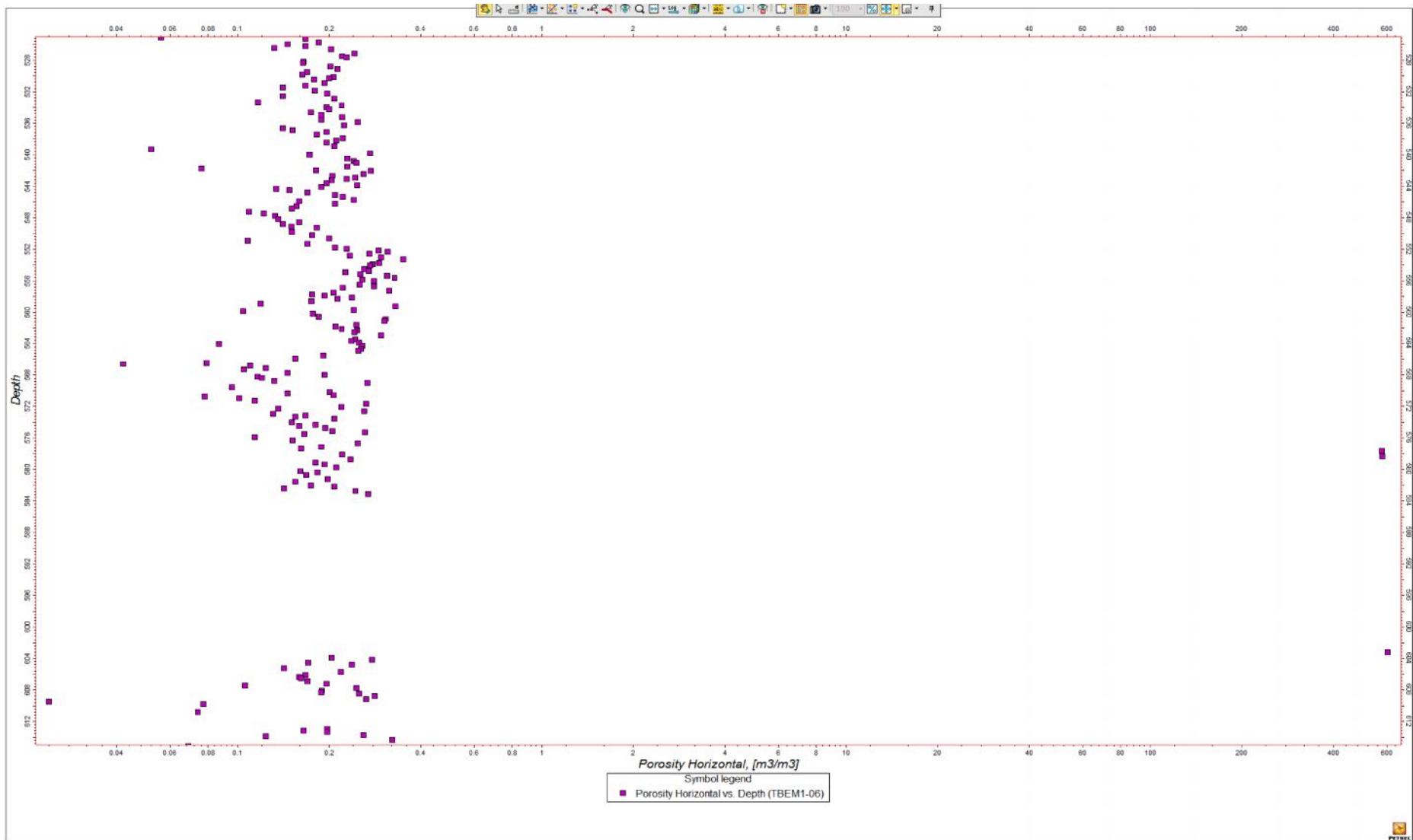


Carbonate ramp virtual sequence ( Nichols ,2009)

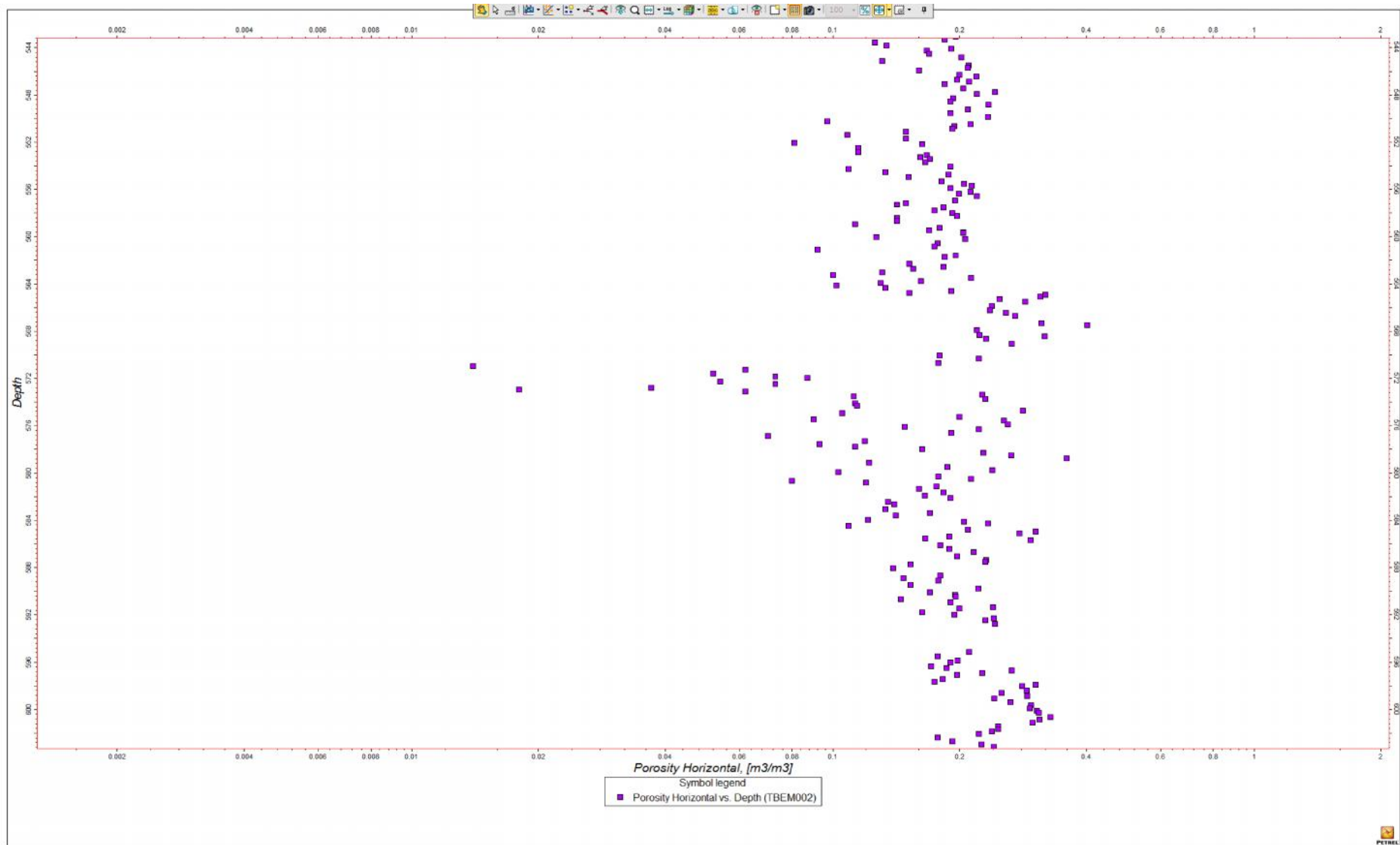
Appendix 9: similarity between sequence within well TBEM2 and carbonate ramp by Nichols (2009)



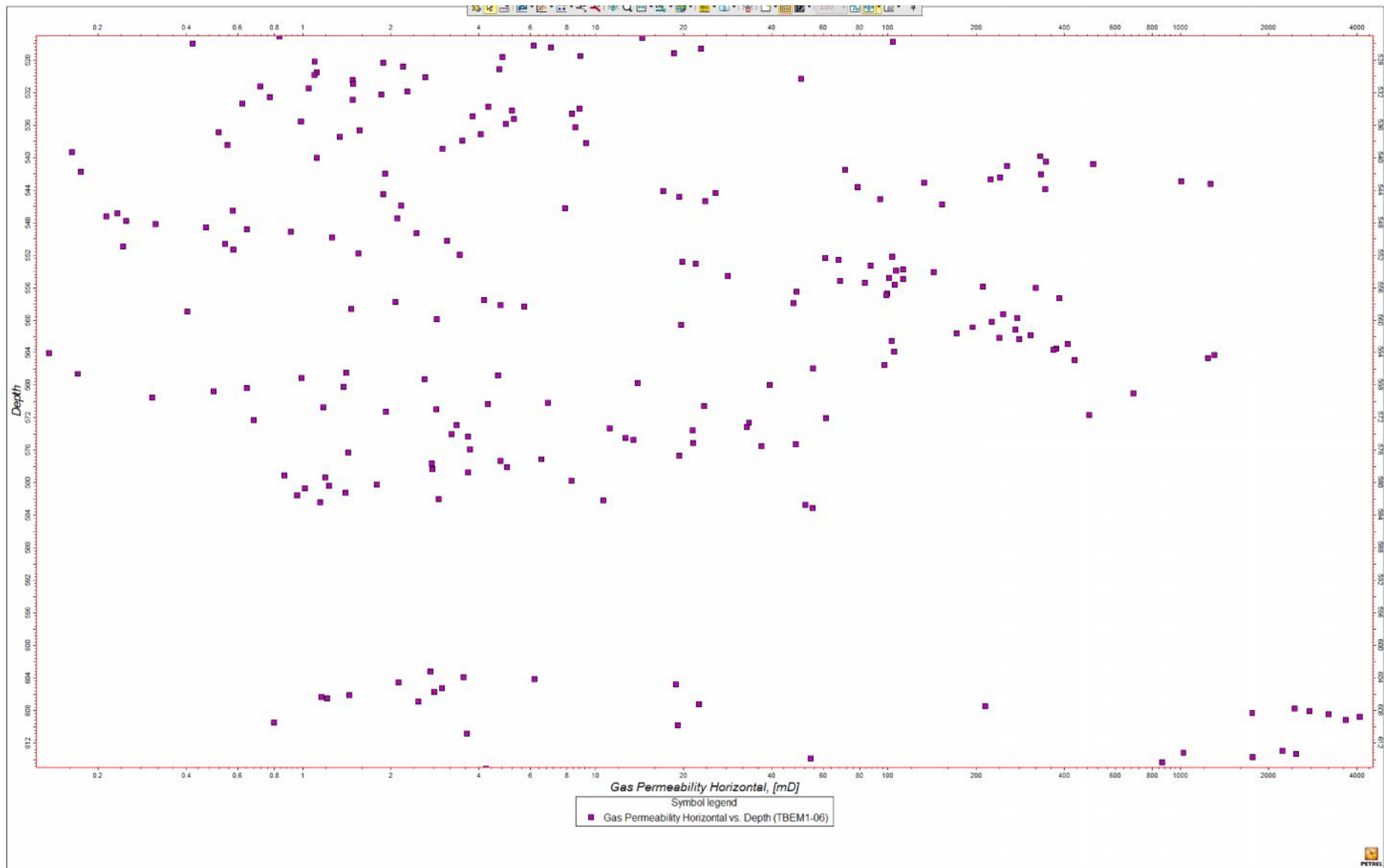
Appendix 10: Depth versus porosity graph (well TCDM3)

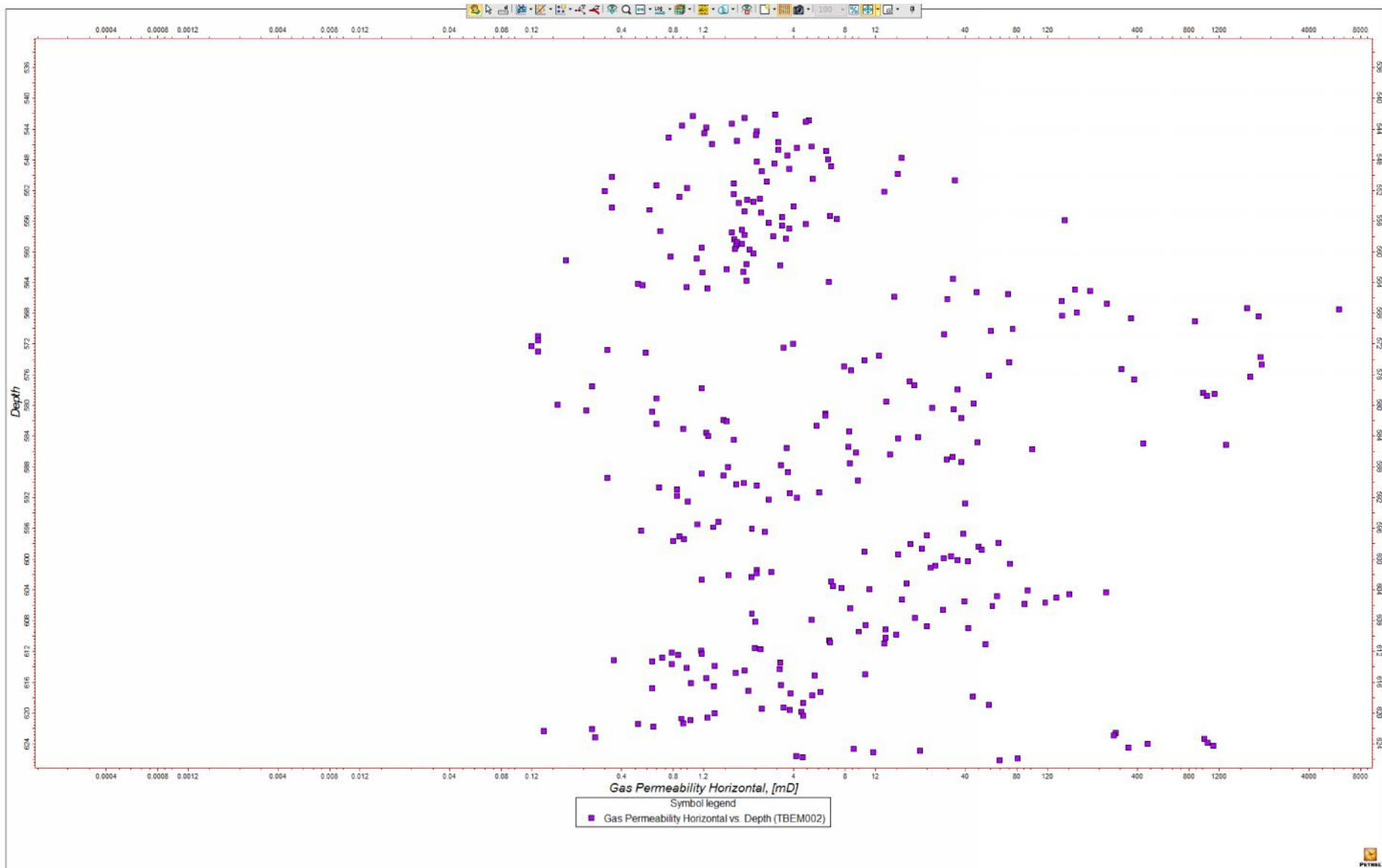


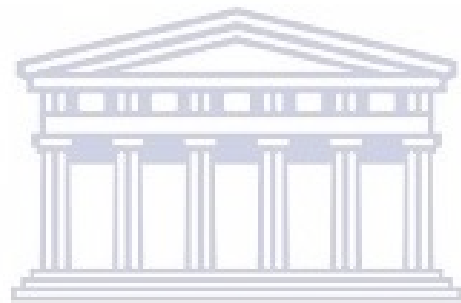
Appendix 11: Porosity versus Depth graph (well TBEM 106)



Appendix 12: porosity versus depth (well TBEM2)







UNIVERSITY *of the*  
WESTERN CAPE